SEVENTH FRAMEWORK PROGRAMME

Project Acronym:	GRASP
Project Type:	IP
Project Title:	Emergence of Cognitive Grasping through Introspection, Emulation and Surprise
Contract Number:	215821
Starting Date:	01-03-2008
Ending Date:	28-02-2012

GRASP

Emergence of Cognitive Grasping through Introspection, Emulation and Surprise

Deliverable Number:	D30
Deliverable Title :	Modelling and simulator integration of the human hand and a grasp reasoning engine
Type:	PU/PP
Authors	B. León, G. Puche, H. Martí , S. Rodríguez, J. Felip, and A. Morales,
Contributing Partners	UJI

Contractual Date of Delivery to the EC: 29-02-2012

Actual Date of Delivery to the EC: 29-02-2012

Contents

Chapter 1

Executive Summary

Deliverable D30 describes fourth year work within work-package WP6 "Introspection and Prediction through Simulation". Previous Deliverables (D9 and D16) from WP6 were focused on the development of the simulation environment. D23 accounted for fewer developments, but focused on applications of the simulator with predictive purposes. According to the Technical Annex, D30 presents activities connected to Tasks 6.2, 6.3, 6.4. The objectives of these are defined as:

- **[Task 6.2]: Development of the basic modules.** The different modules of the simulator will be developed following the next sequence, though some of them can be developed simultaneously: Core modules (internal data management, communication, etc), and basic visualisation; robot oriented plug-ins: sensor simulation, advanced hand models, etc; object collision detection; static modelling (friction, contacts); dynamic modelling.
- **[Task 6.3]: Implementation of the reasoning/prediction engine**. The simulator developed in task 6.2 will be the base to make hypothesis and predictions about the world. This task will be responsible of implementing an engine that performs such operations. It will keep the representation and modelling of the objects involved in the interactions and will also produce predictions of the sensor perceptions (tactile, force and visual) to be obtained when the tasks are executed by real hardware. This engine is critical to the arousing of surprise since the difference between the predicted perceptions and real outputs is the first level of it.
- **[Task 6.4]: Validation of the software environment**. This validation addresses the three main aspects of the simulator: the static and dynamic engines, the contact and friction models, and the robot and sensors models. The means used to validate these components range from computer simulation of benchmarking models common in the physics simulation literature, to experimental validation against real hardware

The work in this Deliverable is related to **Milestone 11:** "Integration and evaluation of scenarios on multiple experimental platforms, demonstration of cognitive capabilities of robots."

The progress in WP6 regarding this deliverable is presented briefly below, and in more detail in the appendix containing attached scientific publications and reports.

- Attachment A reports the biomechanical principles and methodology behind the model of the human hand to be integrated as part of the simulator. The main purpose of this model is not only having a model human hand which is physiologically and biomechanically realistic, but having it integrated on a tool which allows to compute its interactions with simulated objects.
- Attachment B goes a step further and extends the model by including computational tools to generate and analyse grasps performed by the human hand model. It applies well known grasp planning algorithms and principles from the robotic field and validates the feasibility of such approach using real data obtained from human subjects .
- Attachment C focuses on the evaluation of human prehension. The purpose is to apply to human model grasps that has been generated from human subjects, typical robot grasp quality metrics.

The purpose is to determine which of them can robustly assess the goodness of a given human hand grasping posture. In addition, a biomechanical inspired grasp metric is also proposed.

- Attachment D develops a case of the use of the simulator as an integral part of a grasp reasoning process in which a set of grasp hypotheses are analysed and filtered out taking in to account the likelihood of directly perceived parts of the recognized object model. The scientific foundations of this work are developed on deliverable 28. It is only reported here as a paradigmatic example of the use of the simulator as a reasoning tool.

Appendix A

Attached papers

A J.L. Sancho-Bru, A. Pérez-González, M. Mora, B. León, M. Vergara, J.L. Iserte, P.J. Rodríguez-Cervantes and A. Morales, (2011), Towards a Realistic and Self-Contained Biomechanical Model of the Hand, Theoretical Biomechanics, Vaclav Klika (Ed.), pp. 212-240, ISBN: 978-953-307-851-9,

B J.L. Sancho-Bru, M. Mora, B. León, A. Pérez-González, J.L. Iserte, A. Morales. Grasp modelling with a biomechanical model of the hand. In Computer Methods in Biomechanics and Biomedical Engineering. Submitted on July 2011

C B. León, J.L. Sancho-Bru, S. Rodriguez, M.A. Roa, and A. Morales. Evaluation of Human Prehension Using Grasp Quality Measures. IEEE International Conference on Biomedical Robotics and Biomechatronics (BIOROB 2012). Submitted on January 2012.

D A. Aldoma, J. Felip, B. León, W. Wohlkinger, A. Morales, and M. Vincze. Constrained Model-Driven Using the Modes-Object Overlap Metric (MOOM). IEEE International Conference on Robotics and Automation, Submitted on September 2011.

10

Towards a Realistic and Self-Contained Biomechanical Model of the Hand

Joaquín L. Sancho-Bru et al.*
Universitat Jaume I
Spain

1. Introduction

Most of human mechanical interactions with the surrounding world are performed by the hands. They allow us to perform very different tasks; from exerting high forces (e.g. using a hammer) to executing very precise movements (e.g. cutting with a surgical tool). This versatility is possible because of a very complex constitution: a great number of bones connected through different joints, a complicated musculature and a dense nervous system. This complexity is already evident from the kinematics point of view, with more than 20 degrees of freedom (DOF) controlled by muscles, tendons and ligaments.

Mathematical representations are used in order to perform qualitative or quantitative analyses on this complex reality. These representations are known as biomechanical models of the hand. In biomechanics, their use allows studying problems that cannot be analysed directly on humans or that have an experimental cost that is too high; e.g., the study of new alternatives for restoring hand pathologies. Biomechanical models are a description of the hand as a mechanical device: the different elements of the hand are defined in terms of rigid bodies, joints and actuators, and the mechanical laws are applied. As they are simplified mathematical models of the reality, their use and validity depends on the simplifications considered.

The first biomechanical models of the hand were developed to explain and clarify the functionality of different anatomical elements. In this regard, we can find many works that studied the function of the intrinsic muscles (Leijnse & Kalker, 1995; Spoor, 1983; Spoor & Landsmeer, 1976; Storace & Wolf, 1979, 1982; Thomas et al., 1968) and many others that tried to give an insight into the movement coordination of the interphalangeal joints (Buchner et al., 1988; Lee & Rim, 1990). Models for studying the causes and effects of different pathologies of the hand also appeared early on, such as the swan neck and boutonnière deformities or the rupture of the triangular ligament or the volar displacement of the extensor tendon (Smith et al., 1964; Storace & Wolf, 1979, 1982). All these models were, though, very limited, two-dimensional models allowing only the study of flexion-extension movements, they modelled only one finger, and they included important simplifications. By the year 2000, few three-dimensional models had been developed (Biryukova & Yourovskaya, 1994; Casolo & Lorenzi,

* Antonio Pérez-González, Marta C. Mora, Beatriz E. León, Margarita Vergara, José L. Iserte,Pablo J. Rodríguez-Cervantes and Antonio Morales
Universitat Jaume I, Spain

1994; Chao et al., 1976; Chao & An, 1978; Esteki & Mansour, 1997; Mansour et al., 1994; Valero-Cuevas et al., 1998), and none of them modelled the complete hand.

Since 2000, many three-dimensional biomechanical models can be found in literature, having been developed for very different purposes (Fok & Chou, 2010; Kamper et al., 2006; Kurita et al., 2009; Lee et al., 2008a, 2008b; Qiu et al., 2009; Roloff et al., 2006; Sancho-Bru et al., 2001, 2003a, 2003b, 2008; Valero-Cuevas, 2000; Valero-Cuevas et al., 2000, 2005; Vigouroux et al., 2006, 2008; Wu et al., 2010): to understand the role of the different anatomical elements, to understand the causes and effects of pathologies, to simulate neuromuscular abnormalities, to plan rehabilitation, to simulate tendon transfer and joint replacement surgeries, to analyse the energetics of human movement and athletic performance, to design prosthetics and biomedical implants, to design functional electric stimulation controllers, to name a few. These models, however, do not differ much from the ones developed before 2000, and many limitations are still evident. For example, contact forces and zones need to be measured experimentally and input to the model.

In contrast, much research has been carried out on animation techniques over the past years, mainly for use in developing computer games. Lately, these advances have been cleverly used by some ergonomics researchers to develop improved graphical and kinematics hand models for evaluating the use of products (Endo et al., 2007, 2009; Goussous, 2007; Kawaguchi, 2009), with good results.

On the other hand, robot hand grasps have been extensively studied for years. Although until 2000 little attention was paid to human hand grasping, this too has become a hot topic in robotics. The experience in modelling the robot hand grasps has been used to reach a better understanding of human grasping (Miller & Allen, 2004; Peña-Pitarch, 2007). The hand is considered as the end-effector for humans. These models, however, are not appropriate for studying many of the above-mentioned objectives, as their interest is different. The focus in robotics research is on planning the grasp and finding an optimum grasp, and quality grasp measures that have been developed for robots are used. These models do not include muscles and tendons in the formulation.

The latest developments in ergonomic hand models and human hand grasp models can be used to improve the existing biomechanical models of the hand and extend their functionality. A promising research area lies ahead with scientist, aiming to obtain a more comprehensive model of the hand, integrating knowledge and developments from the fields of biomechanics, ergonomics, robotics, and computer animation.

In this chapter, a review of the literature regarding biomechanical models of the hand, ergonomics hand models and human hand grasp models is presented. The three approaches are used to draw out the rules for developing an improved biomechanical model, able to tackle any of the above-mentioned objectives in a virtual environment, without external experimental data.

2. Literature review

2.1 Biomechanical models of the hand

Over the years, biomechanical models of the hand have been developed for different purposes. Some of them tried to study the functionality of different anatomical elements with the aim of gaining a deeper understanding of the causes and effects of many hand pathologies. These are usually very simplified (mostly two-dimensional) kinematic models (sometimes dynamic) that are used to perform qualitative analyses (Leijnse et al., 1992;

Storace & Wolf, 1979). Others were developed to help in medical planning and surgery for patients; they are usually dynamic models and are used to perform quantitative analyses, such as the study of the tendon excursions in the medical planning of tendon transfers (Giurintano & Hollister, 1991) or to study the nervous stimulation required to restore the grasping ability in muscular dysfunction patients (Esteki & Mansour, 1997). Yet others studied the hand while performing specific tasks with different aims, so as to have approximate values for the articular forces for testing prosthetic designs (Weightman & Amis, 1982). These too are quantitative analyses performed on dynamic models.

Recent models do not differ much from the ones developed before 2000 (Fok & Chou, 2010; Kamper et al., 2006; Kurita et al., 2009; Lee et al., 2008a, 2008b; Qiu et al., 2009; Roloff et al., 2006; Sancho-Bru et al., 2001, 2003a, 2003b, 2008; Valero-Cuevas, 2000; Valero-Cuevas et al., 2000, 2005; Vigouroux et al., 2006, 2008; Wu et al., 2010). All models present a similar configuration. The kinematics are modelled without considering the restraining structure, just the resultant physiological articular movement. The concept of instantaneous centre of rotation has been used to define an axis of rotation in joints with a single predominant DOF. Much effort has also been spent on finding the rotation axes of joints with two DOF (Brand & Hollister, 1992), through the consideration of a virtual link connecting the axes (Giurintano et al., 1995). Thus, all works use fixed axes of rotation; depending on the joint, one or two axes of rotation are considered. This approximation has been found to be good enough for most of the cases, particularly if there is no interest in analysing the role of the articular soft tissue or the articular stresses (Youm et al., 1978).

All works in the literature consider the ideal case of a non-friction belt around a pulley to model the tendons on a joint. Therefore, the tensional force on a tendon is the same along its pathway if no split or connection to other tendon exists. Two different approaches have been used to model tendon action on the joints. The first one considers the tendon freely running when crossing the joint between two points attached one to the proximal segment of the joint and the other to the distal segment. This approach is the basis of the first serious attempt to develop a 3D normative model of the hand (An et al., 1979), in which the position of the tendons with respect the bone segments were obtained from the measurement on 10 fresh cadaveric specimens. The second approach comes from the application of the virtual work principle and considers the moment arm created by the tendon as the first derivative of the tendon excursion with respect to the rotated angle about the rotation axis under study (Storace & Wolf, 1979). This second approach is not strictly correct (Casolo & Lorenzi, 1994), as it does not take into account the work due to the deformation of the sheaths and other structures that constrain the tendon's trajectory along its pathway. Although both approaches present advantages and disadvantages, the second one is difficult to implement in 3D modelling, mainly because of the complexity in the tendon excursion calculation at joints with more than one DOF.

Most of the works in the literature use Hill's model to account for the muscles' mathematical modelling. This simple model allows the consideration of the three main parameters, i.e., muscle activation level and variation of the maximum deliverable muscle force with muscle length and muscle contraction velocity.

Finally, the dynamic equilibrium equations lead to an indeterminate system of equations, with more unknowns (muscle forces) than available equations. Inequality constraints taking into account the maximal forces that may be delivered by each muscle and that tendons cannot support compressive forces have to be considered as well. The problem is usually solved by minimising some cost function. Different functions have been investigated, most of them without any physiological basis. The most often used criterion is the minimisation of the sum of the squared muscle stresses, which has been related to the maximisation of fatigue resistance (Crowninshield & Brand, 1981).

All the effort in biomechanics has been focused on appropriately modelling the different hand components (kinematics, muscles, tendons, etc.). Little effort has been spent on the formulation of the grasping problem when using a biomechanical model. In this sense, many limitations persist. Current models do not allow the estimation of the contact information required to use biomechanical models for simulating the grasping of objects. Forces and zones of contact still need to be measured experimentally and input to the model.

2.2 Hand models in ergonomics

Ergonomics, according to the International Ergonomics Association, is 'the scientific discipline concerned with the understanding of interactions among humans and other elements of a system, and the profession that applies theory, principles, data and methods to design in order to optimise human well-being and overall system performance'. Hand models in Ergonomics are used to simulate postures adopted while grasping objects with different purposes. One of the main goals of physical ergonomics is the study of the size and shape of objects according to the anthropometry of the different people that have to interact with them. Thus, the main feature of a model for Ergonomics is that it has to allow representing different populations and percentiles. People having hands of different sizes and proportions will adopt different postures in grasping the same object for the same functions. For example, pressing a button of a phone with the thumb while holding it with the same hand can be easily achieved for a specific hand size while keeping the grasp. However, other people with different size of hand will need to change the grasping posture to achieve pressing the button. This is a typical problem of reach that needs to be solved in ergonomic assessment.

In recent years, virtual humans have been incorporated into the design process for ergonomic assessment of different types of products, mainly in the aerospace and automotive industry but also in others like product design, tasks simulation, personnel training or simulation of other worker environments (Colombo & Cugini, 2005; Yang et al., 2007). Several commercial software programs such as Jack, RAMSIS, HumanCAD, Safework and SantosHuman are available and other studies have been conducted on digital human models such as SAMMIE (Case et al. 1990) or the Boeing Human Modeling System for the same purposes. A virtual human in these packages is defined as a kinematic chain composed of a number of rigid links connected by joints. These joints have the DOF and allowable motion limits corresponding to the anatomical joint of the human being. Direct and inverse kinematics is incorporated into the models so they can replicate human body movements and also evaluate forces acting in joints. Moreover, different population and percentiles may be selected for the size of the model, usually from known anthropometric databases. With these capabilities the problems of reach and clearance usual in ergonomics may be solved easily. Other useful capabilities of these models are the simulation of the sense of sight with virtual cameras located in the eyes or the possibility to change any particular data of the model, like dimensions of limbs or motion limits of some joints, in order to simulate a particular person or disability. However, the majority of these models focuses on the whole body and does not pay attention to the accuracy of the hand model. Most of them just incorporate a list of hand postures (grasping or others) to be chosen, i.e.

direct kinematics, but do not allow for example inverse kinematics for the joints of the hand, even when it is incorporated for the other joints of the body. In recent developments some attempts to improve the hand model incorporated into some programs have been done (Peña-Pitarch, 2007, Yang et al., 2007).

Early models of the hand (Davidoff & Freivalds, 1993) were actually kinematic models that simulated roughly the external geometry of the hand and its movements. The geometry of the hand has been modelled mainly by jointed cylinders (Fig. 1) and cones (Armstrong, 2009; Sancho-Bru et al., 2003a, 2003b). However, if the geometry of the hand model is not very accurate, the algorithms for inverse kinematics are not precise enough. Recently, some efforts have been made in accurately modelling the surface of real hands to be incorporated into 3D hand models. Rhee et al. (2006) presented an automated method to make a specific human hand model from an image of the palm of the hand. Different algorithms were used in the process: principal creases are extracted, joint locations are estimated from them and the skin geometry of a generic hand model deformed based on hand contours. Rogers et al (2008) made a scalable 3-D geometric model of the hand based on 66 landmarks of the palm surface from 100 subjects in four functional postures. The purpose was to analyse the deformation of the palm surface during the grasp of an object. Recent models incorporate the surface of the hand as a mesh object with more or less realism, obtained from the location of a number of landmarks of the hand or from digital 3D-scanning of the hand (Endo et al., 2007; Peña-Pitarch, 2007, van Nierop et al., 2008). The mesh is linked to a skeleton whose movement controls the deformation of the mesh with different types of algorithms.

Fig. 1. Different views of the geometric model used in Sancho-Bru et al. (2003a) simulating a hand gripping two cylinders of different diameters.

Other important aspect of hand models for ergonomics is associated with the study of musculoskeletal disorders. Early epidemiological studies (Mital and Kilbom, 1992) showed that the use of hand tools with an improper design for the worker or the task could lead to a high risk of developing cumulative hand trauma disorders (CHTD). The factors influencing the development of CHTD have been reported in different works (Keyserling, 2000; Kong et al., 2006; Muggleton et al., 1999; Schoenmarklin et al., 1994; Spielholz et al., 2001) and different methods have been used in these studies: epidemiological studies, physiological measurements (electromyography activity, pressure in tissues, posture of hand and wrist, tactile sensitivity), biomechanical models of hand and wrist structures and psychophysical assessments. These studies report that CHTD are associated with repetitive tasks, high forces, extreme or awkward postures of hand and wrist, velocity and acceleration of wrist motions and exposure time, among others. Different theories of injury development have been proposed (Kumar, 2001). All of them assume that CHTD and other musculoskeletal disorders are of biomechanical nature.

Therefore, biomechanical hand models able to predict movements, postures and internal forces of hand and wrist structures can be used to assess the risk of developing CHTD. Tendon excursions or maximum gripping strength have been used as index in different works to assess gripping posture for health (Armstrong et al., 2009, Sancho-Bru et al., 2003b).

None of the reported biomechanical models of the hand for ergonomics accounts for all the above-mentioned requirements, although some attempts have been made. Armstrong et al (2009) have developed a scalable kinematic model of the hand with simple geometry (cones and cylinders). The model includes a posture prediction algorithm for fingers that reproduces in a high percentage the observed postures and is able to compute tendon excursions and wrist movements. The model is used to assess how much space is required for hands in an assembly task and to calculate the risk of CHTD from tendon forces and hand strength. Other group of researchers (Endo et al 2007, 2009; Kawaguchi et al., 2009) have developed a scalable digital hand model with an accurate shape of the hand that includes a semiautomatic grasp planning function with robotics indexes of quality (see next section). The model incorporates a 'comfort database' obtained from experimental measurements to assess comfort of postures and is used in the assessment of physical interaction with electronic appliances.

2.3 Grasping in robotics

For many years the robotics community has been studying the autonomous handling of objects by robots. A robot should be able to locate the object and then grasp it, and possibly transport it to a specified destination. The purpose of a grasp is to constrain the potential movements of the object in the event of external disturbances. For a specific robotic hand, different grasp types are planned and analysed in order to decide which one to execute.

A grasp is commonly defined as a set of contacts on the surface of the object. A contact model should be defined to determine the forces or torques that the robot manipulator must exert on the contact areas. Most of the work in robotics assumes point contacts, and larger areas of contact are usually discretised to follow this assumption (Bicchi & Kumar, 2000).

Two main problems can be distinguished in robotic grasping: analysis and synthesis (Mason, 2001). Grasp analysis consists on finding whether the grasp is stable using common closure properties, given an object and a set of contacts. Then, a quality measure can be evaluated in order to enable the robot to select the best grasp to execute. On the other hand,

grasp synthesis is the problem of finding a suitable set of contacts given an object and some constrains on the allowable contacts.
In the following sections, a detailed description of the contact models and the most common approaches for grasp analysis and synthesis is presented.

2.3.1 Grasp contact models

A contact can be defined as a joint between the finger and the object. Their shape, stiffness and frictional characteristics define the nature of this joint (Mason, 2001). The force applied by a finger at a contact point generates a *wrench* on the object with force and torque components. The contact model maps the wrench at some reference point of the object, usually the centre of mass. Salisbury (1982) proposed a taxonomy of eight contact models. Among these, the more common contact models used in robotic grasping (Fig. 2) are the point contacts with and without friction and the soft-finger contacts (Roa Garzón, 2009). Point contact models, also named rigid-body contact models, assume rigid-body models for the hand and the grasped object while the soft-finger contact models, also called compliant or regularised models, assume that the hand is a deformable element grasping a rigid body (Kao et al., 2008). The former models assume the collision to be an instantaneous and discontinuous phenomenon (discrete event) and the equations of motion are derived by balancing the system's momenta before and after the impact. In contrast, compliant models describe the normal and tangential compliance relations over time.
A *point contact without friction* can only transmit forces along the normal to the object surface at the contact point. No deformations are allowed at the points of contact between the two bodies and, instead, contact forces arise from the constraint of incompressibility and impenetrability between the rigid bodies. These models do not represent the real contact situations that appear in robotic manufacturing operations (Cutkosky, 1989; Lin et al., 2000) and, when used, the machine accuracy is negatively affected. Moreover, they are not capable of predicting the individual contact forces of a multiple-contact fixture (Bicchi, 1994; Harada et al., 2000).
A *point contact with friction* can also transmit forces in the tangential directions to the surface at the contact point. If Coulomb's friction model is used, all the forces that lie within the friction cone with an angle $atan(\mu)$ can be applied, where μ is the friction coefficient of the contacting materials. Here, contact forces arise from two sources: the rigid-body model assumption for both the hand and the object, and the frictional forces. The use of this contact model in the manipulation planning problem has led to some interesting conclusions. There may be multiple solutions to a particular problem (ambiguity) or there may be no solutions (inconsistency) (Erdmann, 1994).
Finally, the soft contact model is used to model the contact between a soft finger and a rigid object allowing the finger to apply an additional torsional moment with respect to the normal at the contact point (Ciocarlie et al., 2005, 2007; Howe et al., 1988; Howe & Cutkosky, 1996; Kao & Cutkosky, 1992; Kao & Yang, 2004). A typical contact between a soft finger and a contact surface can be modelled by the Hertzian contact model (Hertz, 1882; Johnson, 1985). However, robotic fingertips are made of nonlinear elastic materials. For that reason, the Hertzian contact model does not accurately represent this contact. In Xydas & Kao (1999) and Xydas et al. (2000) a power-law theory is presented for modelling nonlinear elastic contacts present in robotic fingers. It subsumes the Hertzian contact theory. More realistic, and complicated, models have been developed in the last few years that better represent the

contact mechanics for soft fingers (Ciocarlie et al., 2005, 2007; Gonthier, 2007). However, it is the hard finger contacts with friction that are used more often in robotics.

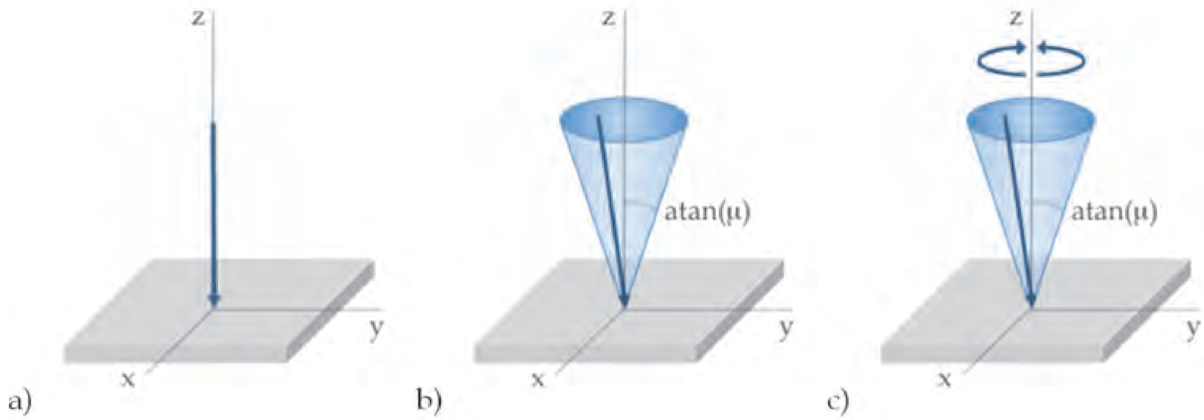

Fig. 2. Contact models commonly used in robotics: a) Point contact without friction; b) Point contact with friction; c) Soft-finger contact

2.3.2 Grasp analysis

After establishing the contact model, the set of contacts defining each grasp can be analysed in order to test its ability to resist disturbances and its dexterity properties. As it is presented afterwards, a grasp can resist disturbances in any direction if it fulfils one of the two closure conditions. However, there is usually more than one grasp that fulfils them. That is why many metrics and approaches have been proposed to evaluate the dexterity of the selected grasps and determine which one is the best to be executed.

Disturbance resistance

The first test for evaluating a grasp consists of determining its ability to constrain the motions of the manipulated object and to apply arbitrary contact forces on the object without violating friction constraints at the contacts (Bicchi, 1995). Two commonly used properties have been proposed to ensure this condition: force and form closure. A grasp is in *force-closure* if the fingers can apply, through the set of contacts, arbitrary wrenches on the object, which means that any motion of the object is resisted by the contact forces (Nguyen, 1988). On the other hand, a grasp is in *form-closure* if the location of the contact points on the object ensures its immobility (Bicchi, 1995).

Form closure is a stronger condition than force closure and it is mostly used when executing power grasps (Siciliano & Khatib, 2008). Force closure is possible with fewer contacts, making it suitable for executing precision grasps, but it requires the ability to control internal forces.

In order to verify the form or force closure property of a grasp, many tests have been proposed (see Liu et al. (2004b) and Roa Garzón (2009) for a review). Most of them define conditions to be satisfied by the grasp wrenches in the wrench space. A *grasp wrench space (GWS)* is the space of wrenches that can be applied to the object at each contact point. The boundary of the wrench space can be calculated as a convex hull. Force-closure then can be determined verifying if the origin of the wrench space lies inside this convex hull (Mishra et al., 1987). Several tests have been proposed to verify this condition, with the one developed by Ferrari & Canny (1992) being the most widely-used. They proposed to calculate the radius of the largest ball inscribed in the convex hull centred in the origin. Force-closure grasps are the ones where the sphere's radius is larger than zero.

Measures of grasp performance

Many approaches have been proposed to measure the quality of a grasp. Some of the measures focus on evaluating the ability to resist external disturbances, others on evaluating the dexterity. These measures can be classified into two groups depending on whether they consider the location of the contact points on the object or the configuration of the end-effector. There are also some that are a combination of these two approaches (see Roa Garzón (2009) for a thorough review).

Measures from the first group take into account the geometric properties of the objects, their materials and closure properties to evaluate the grasp. For example, Li & Sastry (1998) proposed to calculate the smallest singular value of the grasp matrix, which indicates how far the grasp configuration is from losing the capability of withstanding external wrenches. Others have proposed to favour the grasps whose contact points are distributed in a uniform way on the object surface, which improves their stability (Mirtich & Canny, 1994; Park & Starr, 1992). This can be done by measuring either the angles or the area of the polygon whose vertices are the contact points. The centroid of this polygon is also used to calculate its distance to the object centre of mass (Ding et al., 2001; Ponce et al., 1997). The smaller this distance the better the grasp can resist the effect of external forces. In addition, some other measures take into account the uncertainty in the position of the fingers; therefore instead of contact points they calculate contact regions in which force closure grasps are assured (Nguyen, 1988; Roa Garzón, 2009). The quality of the grasp is measured by the size of these regions.

The previous approaches do not consider any limitation on the finger forces, so that in some cases the fingers have to apply very large forces to resist small perturbations. Other measures do consider limitations on the magnitudes of the finger forces. They can limit the force on each finger or the sum of forces applied by all fingers. Ferrari & Canny (1992) used the largest ball not only to evaluate grasp closure but also to measure the grasp quality. This is a geometric representation of the smallest perturbation wrench that breaks the grasp, independently of its direction. It has been widely used by the robotics community (Borst et al., 2003; Miller & Allen, 1999; Roa Garzón, 2009). The volume of the ball is also considered as a quality measure with the advantage that it remains constant independently of the used torque reference system (Miller & Allen, 1999).

When a task is specified to be performed after the object is grasped, the quality of the grasp can be measured with its ability to counteract the expected disturbances during the task execution. The set of all wrenches that are expected to be applied on the object defines the *task wrench space (TWS)* and can be approximated as an ellipsoid (Li & Sastry, 1988) or as a convex polytope (Haschke et al., 2005; Zhu at al., 2001). The problem with these approaches is that modelling the TWS can be quite complicated (Borst et al., 2004). Pollard (2004) introduced the concept of an *object wrench space (OWS)*, which is the set of wrenches generated by applying a distribution of disturbance forces on the surface of the object. Borst et al. (2004) proposed the use of the largest factor by which the OWS can fit the GWS as the measure of the grasp quality.

On the other hand, there are measures that consider the configuration of the end-effector, requiring the hand-object Jacobian for their calculation (Roa Garzón, 2009). An example of this group is a measure that favours a grasp that, given certain velocities in the finger joints, produces the largest velocities on the grasped object, calculated with the volume of the manipulability ellipsoid (Yoshikawa, 1985). There is another measure that penalises the joints of the hand being in their maximum limits, calculating the deviation of the joint angles from their centres (Liegeois, 1977). Additionally, there are other measures in this group that also consider the task, giving higher quality indexes to the grasps which ensure the maximum transformation ratio along the direction wrenches more likely to be applied on the object when executing it (Chiu, 1988).

2.3.3 Grasp synthesis

Given an object, grasp synthesis algorithms should provide a suitable set of contacts on the object surface and determine an appropriate hand configuration. Usually they take the geometry of the object as an input to select optimal force-closure contact locations. These contacts are the starting point for grasp analysis and dexterous manipulation methods.

Some approaches give only information about the finger contact locations on the object without considering the hand constraints. They can result in stable grasps that are not reachable in practice by the robot hand. Moreover, even if they are reachable, it is difficult to position the fingers precisely on the contact points because there will be always unavoidable errors locating the end-effector (Morales et al., 2006).

Alternative approaches, called knowledge-based approaches, have considered the configuration of the hand by generating the grasp with a predefined set of hand postures. The idea of hand preshapes started with studies of the human prehension capabilities (Napier, 1956) that introduced the distinction between power and precision grasps. Following this work, Cutkosky (1989) created a taxonomy in which details of the task and the object geometry are taken into account. Since then, several papers have adopted this approach for grasping (Morales et al., 2006; Stansfield, 1991; Wren, 1995). Miller et al. (2003) used a simulator called GraspIt! to test the set of hand preshapes on a 3D model of the object. Using a simulator has many advantages, including the ability to plan grasps in complex environments involving obstacles and also to check the reachability constraints of the robot arm. More recently OpenRAVE, a planning architecture that has a more flexible design, has been proposed to automate this process (Diankov, 2010).

Despite many years of research and all the advances we have reviewed, the robotics community is still not able to build a manipulator with similar capabilities to the human hand. The robot hands constructed until now are only simplifications (Fig. 3), given the complexities not only at the sensor and actuator level, but also at the control level. They vary from the easiest to control, such as 2-jaw grippers, to more anthropomorphic hands like the Salisbury Hand, the Utah-MIT Hand, the Barrett Hand, the ARMAR III Hand or the DLR Hand II (see Biagiotti et al. (2002) and Parada et al. (2008) for a review).

3. Hand biomechanical model proposal

In this section, the current knowledge on biomechanical, ergonomics and robotics hand models is used to draw out the rules for developing a realistic and self-contained biomechanical model of the hand.

Based on the literature review, current hand biomechanical models allow estimating the muscular patterns required to perform a movement while counteracting a system of external forces. But their use for studying object grasping is limited. On the one hand, biomechanical

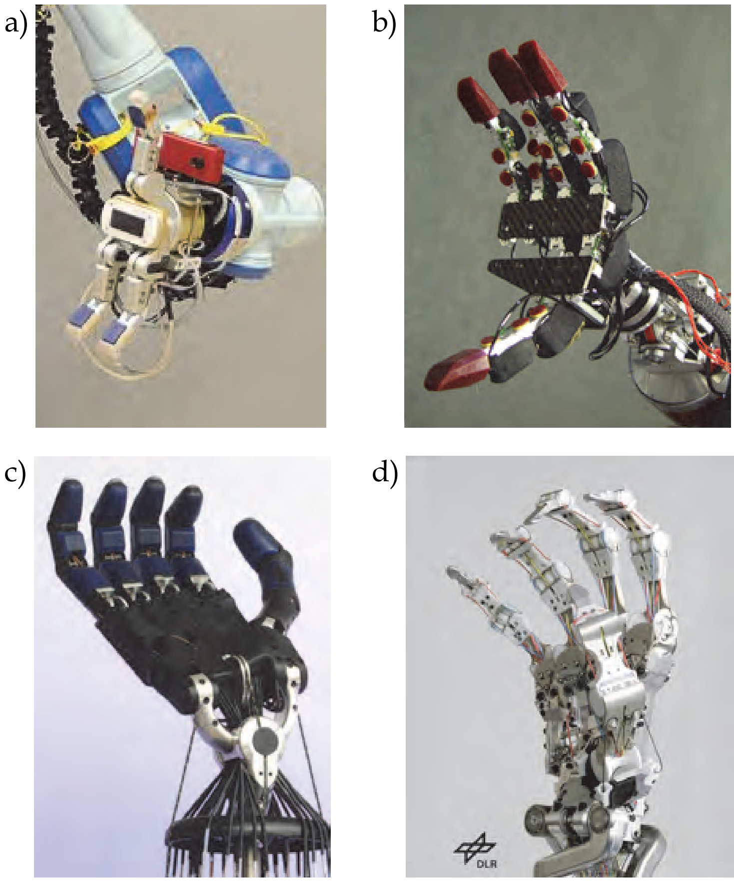

Fig. 3. Anthropomorphic robot hands: a) Barrett Hand (courtesy of the UJI Robotics Intelligent Lab); b) ARMAR III Hand (courtesy of the Institute for Anthropomatics at KIT); c) Shadow Hand C5 (courtesy of Shadow Robot Company); d) Anthropomorphic DLR Hand Arm System (courtesy of DLR Robotics and Mechatronics Center)

models lack realism for assessing the use of handheld products from an ergonomics point of view. Hand models in ergonomics have reached a high level of realism but do not allow for mechanical analyses. On the other hand, biomechanical models are not self-contained, as they need contact information to be input to the model. Current models do not allow predicting grasping postures nor evaluating contact forces and zones, much less predicting the movements while grasp planning. Quality grasp measures in robotics allow comparing different robotic grasping postures and could be adapted to human grasping.

A detailed proposal for modelling the different components of the hand is provided below: joints-kinematics, muscles, ligaments and passive tissues, skin, contact with objects and neuromuscular control. The features that we require in order to create a model are:

- The model has to simulate the complete hand in order to allow the study of any grasp.
- The model has to be scalable to allow the simulation of different population groups.
- The model has to simulate and show the grasping of an object in a realistic way.
- The model has to estimate the muscular patterns required to perform a movement while counteracting the system of external forces that define the object manipulation. Furthermore, the model has to estimate the articular forces at the hand joints.
- The model has to be dynamic in order to allow the study of any grasping task (slow or fast) during the object manipulation.

- The model has to predict feasible grasping postures for a given object and provide the contact information required for evaluating the grasp
- The model has to incorporate quality grasping measures for evaluating the grasp.

The model proposed in this section has been developed in a scalable way, choosing two very well known anthropometric parameters of the hand that are easy to measure and representative of the hand size. The parameters are the hand length (HL) and hand breadth (HB) and are shown in Fig. 4.

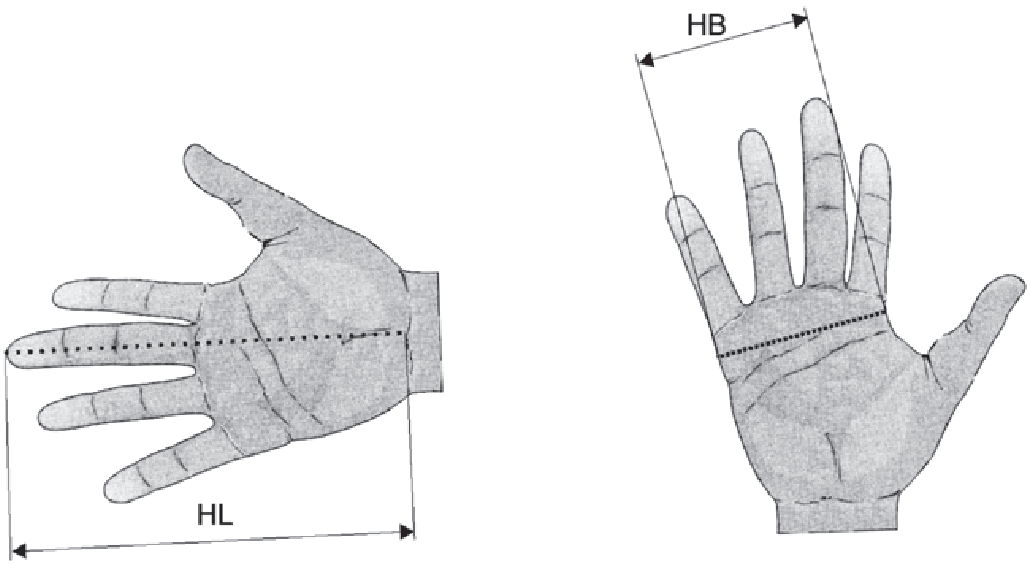

Fig. 4. Parameters used to scale the model: HL (hand length) and HB (hand breadth)

3.1 Kinematics

In order to achieve realistic grasping postures, care has to be taken when selecting the appropriate DOF among the different hand bones. The DOF have to allow the hand model to reach the hand posture for any grasping task. In this sense, it is important that the model considers not only the thumb and finger movements but also the palm arching.

The hand has been considered as five skeletal open chains of rigid bodies connected to the carpus through different joints which characterise the kinematic behaviour of the chains.

Distal and proximal interphalangeal (DIP and PIP) joints of the fingers as well as the interphalangeal (IP) joint of the thumb are trochlear joints, capable only of flexion/extension movements (Brand & Hollister, 1992). These joints are modelled as one DOF joints by means of defining a rotation axis connecting the adjacent phalanxes (hinge joint).

Thumb and fingers metacarpophalangeal (MCP) joints are condylar joints, capable of flexion/extension and abduction/adduction movements (Brand & Hollister, 1992). The thumb carpometacarpal (CMC) joint is a saddle joint, capable also of flexion/extension and abduction/adduction movements (Brand & Hollister, 1992). All these joints are modelled as two DOF joints by defining two axes of rotation connecting the adjacent segments. The axes are neither intersecting nor orthogonal (Brand & Hollister, 1992), so that a virtual link is used to connect both axes (Giurintano et al., 1995).

Finally, the hand model allows the arching of the palm by modelling the CMC joints of the little and ring fingers. These joints are arthrodial joints, with a very limited range of movement (Kapandji, 1998). They have been modelled as one DOF joints by means of

defining a flexion/extension axis of rotation connecting the carpus to each metacarpal. The orientation of the axes is defined oblique in order to appropriately simulate the arching of the palm (Kapandji, 1998). Due to the important role that the shape of the palm plays in grasping, this model is considered more suitable for grasping simulation than others in the literature.
The data for the location and orientation of the rotation axes comes from An et al. (1979), Buchholz et al. (1992) and Hollister et al. (1995). Axes data and link lengths are fully scaled with respect to the hand length and hand breadth (Sancho-Bru, 2000). Limits for the joints have been obtained from Tubiana (1981) and Tubiana et al. (1996).
In order to study the forward and inverse kinematics of the hand, the Denavit- Hartenberg method from the robotics field (Denavit and Hartenberg, 1955) was adapted to define the position of any segment point.

3.2 Musculo-tendon action

Muscles and tendons control the movement of the skeletal chains. Muscles have been considered using a simple Hill three-component model (Hill, 1938) that takes into account the muscle activation level (α) and the force-length and force-velocity relationships, as well as the different index of architecture of muscles. The model considers a contractile element (CE), which is the basic component that generates force, a parallel elastic element (PEE), which is responsible for the passive force generated by the muscle when it is stretched, and a series elastic element (SEE), the muscle tendon unit, which has been considered to be inextensible (Fig. 5).

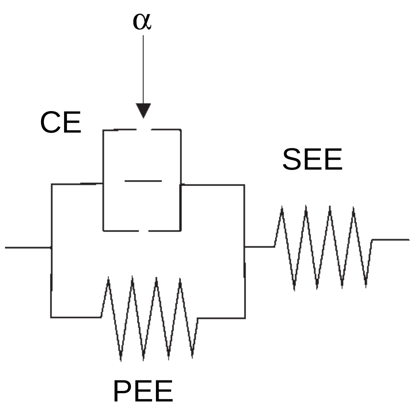

Fig. 5. Hill's three-component model for the muscles

The force a muscle can exert depends on the actual muscle length and contraction velocity. It is widely accepted (An et al., 1991) that the maximum force a muscle can exert in optimal conditions is proportional to its physiological cross-sectional area (PCSA):

$$F_{\max} = PCSA \cdot S_{\max}\,, \tag{1}$$

where S_{max} is the maximum stress the muscle can bear, which has been considered the same for each muscle (An et al., 1991).
The strain of tendons is insignificant for the magnitude of forces developed by the muscles (Goldstein et al., 1987). Under this consideration, the SEE has been considered to inextensible, so that the force the muscle exerts (*F*) can be written as:

$$F = F_{\max}(F_{CE} + F_{PEE}) \,, \tag{2}$$

where F_{CE} and F_{PEE} are the normalised forces delivered by the CE and PEE, respectively.
The force exerted by the muscle can be decomposed into an active force and a passive force corresponding to the forces delivered by the CE and PEE, respectively. The force delivered by the CE is related to the muscle architecture and is a function of the muscle length l_{CE}, the contraction velocity v_{CE}, and the muscle activation level α (from 0 to 1), which is controlled by the central nervous system (Kaufman et al., 1991):

$$F_{CE} = \alpha \cdot F_l(l_{CE}) \cdot F_v(v_{CE}) \tag{3}$$

where F_l and F_v are the non-dimensional force-length and force-velocity relationships.
A characteristic bell-shaped curve exists between force and length of the muscle. To model this dependence, the expression proposed by Kaufman et al. (1991) has been used:

$$F_l(\varepsilon, i_a) = e^{-\left[\frac{(\varepsilon+1)^{0.96343\cdot\left(1-\frac{1}{i_a}\right)}-1.0}{0.35327\cdot(1-i_a)}\right]^2} \quad \text{for } i_a < 1 \tag{4.a}$$

$$F_l(\varepsilon, i_a) = e^{-[2.727277\cdot\ln(\varepsilon+1)]^2} \quad \text{for } i_a = 1 \tag{4.b}$$

where i_a is the muscle architecture index, defined as the ratio between the muscle fibre length and the muscle belly length, and ε is the muscle strain due to its lengthening from l_o, the muscle length for the optimal conditions.
The force a muscle can exert decreases when the contraction velocity of the muscle fibres increases. To model this dependence the expression proposed by Hatze (1981) has been used

$$F_v(\dot{\eta}) = \frac{0.1433}{0.1074 + e^{-1.409\cdot\sinh(3.2\cdot\dot{\eta}+1.6)}} \tag{6}$$

where $\dot{\eta}$ is the normalised contractile element velocity, given by the ratio between the lengthening velocity of the muscle ($\dot{\varepsilon}$), and its maximal value ($\dot{\varepsilon}_{\max}$).
The force generated by the PEE is a function only of its length. An exponential relationship has been considered in this case (Lee & Rim, 1990; Kaufman et al., 1991), with b_1 and b_2 muscle dependent constants:

$$F_{PEE} = b_1 \cdot e^{b_2\cdot\varepsilon} - b_1 \,, \tag{7}$$

The scalability of the muscular action is achieved by scaling the PCSA of the muscles with respect to the product of hand length and hand breadth parameters (Sancho-Bru et al., 2008) from its value for $\overline{HL}$ = 18.22 cm and $\overline{HB}$ = 8.00 cm.

$$\frac{PCSA(HL, HB)}{PCSA(\overline{HL}, \overline{HB})} = 1 + 0.01333 \cdot (HB \cdot HL - \overline{HB} \cdot \overline{HL}) \tag{8}$$

The muscles considered on each skeletal chain are listed in Table 1. PCSA data for index finger muscles have been taken from Valero-Cuevas et al. (1998); data for the remaining muscles have been obtained from Brand & Hollister (1992). Muscle stress limit (S_{max}) has been obtained from Zajac (1989). Fibre and muscle lengths and the constants b_1, b_2 for index finger muscles have been taken from Lee & Rim (1990); data for the remaining extrinsic muscles have been obtained from Lemay & Crago (1996) and for the remaining intrinsic muscles from Jacobson et al. (1992). The muscle maximal lengthening velocity ($\dot{\varepsilon}_{\max}$) has been taken to be 2.5 s^{-1} (Kaufman et al., 1991).

Index	Medial	Ring	Little	Thumb
1st FP	2nd FP	3rd FP	4th FP	APB
1st FS	2nd FS	3rd FS	4th FS	FPB
1st EDC+EI	2nd EDC	3rd EDC	EDQ	OPP
1st LU	2nd LU	3rd LU	4th LU	ADD
1st DI	2nd DI	4th DI	3rd VI	1st DI
1st VI	3rd DI	2nd VI	FDQ	APL
			ADQ	EPB
				FPL
				EPL

Table 1. Muscles modelled on each skeletal chain (acronyms in the nomenclature section)

Most of the muscles do not act directly on the bones, but transmit the force to the tendons, which finally insert into the bones. To model the tendon action crossing the joints, straight lines connecting 2 points have been considered, one fixed with respect to the proximal bone and the other one with respect to the distal bone (Fig. 6a). This approximation has been found to be close enough to the behaviour of all tendons with the exception of extensors (An et al., 1979), for which Landsmeer's model I has been considered (Fig. 6b). The data for the points defining the tendon actions have been obtained from An et al. (1979).

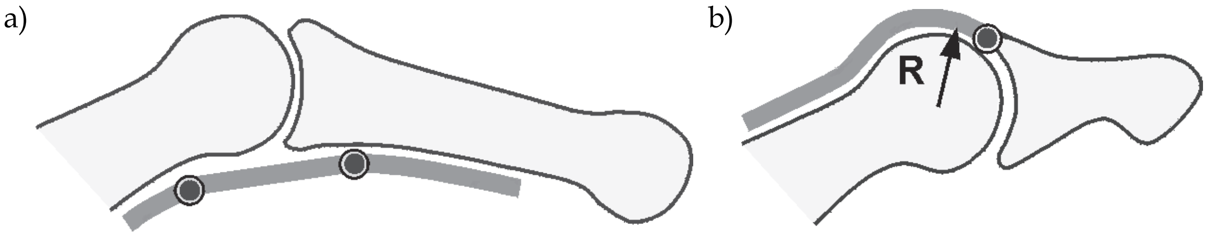

Fig. 6. Models for the tendons crossing the joints: a) Straight lines; b) Landsmeer's model I

The extensor hood mechanisms of the fingers are modelled as a tendon net. The net allows for the connection and division of the tendon paths. The insertions and connection points considered for the tendon nets on each skeletal chain are shown in Fig. 7. Appropriate force balances have been considered in the connecting points of this deformable tendon net. Second DI, fourth DI and ADQ tendons do present a double insertion into the proximal phalanxes and into the extensor aponeuroses. A force distribution proportional to the amount of fibres of each branch (Eyler & Markee, 1954) has been considered.

The muscle force-length and force-velocity relationships presented above require the calculation of the lengthening of the muscles from l_o as a function of time. Having considered the tendons inextensible, the muscle lengthening coincides with the tendon excursion. To calculate the length of the tendon path crossing each joint (l_i), straight lines connecting the points have been considered, except for the extensor tendons, for which a circular path has been considered.

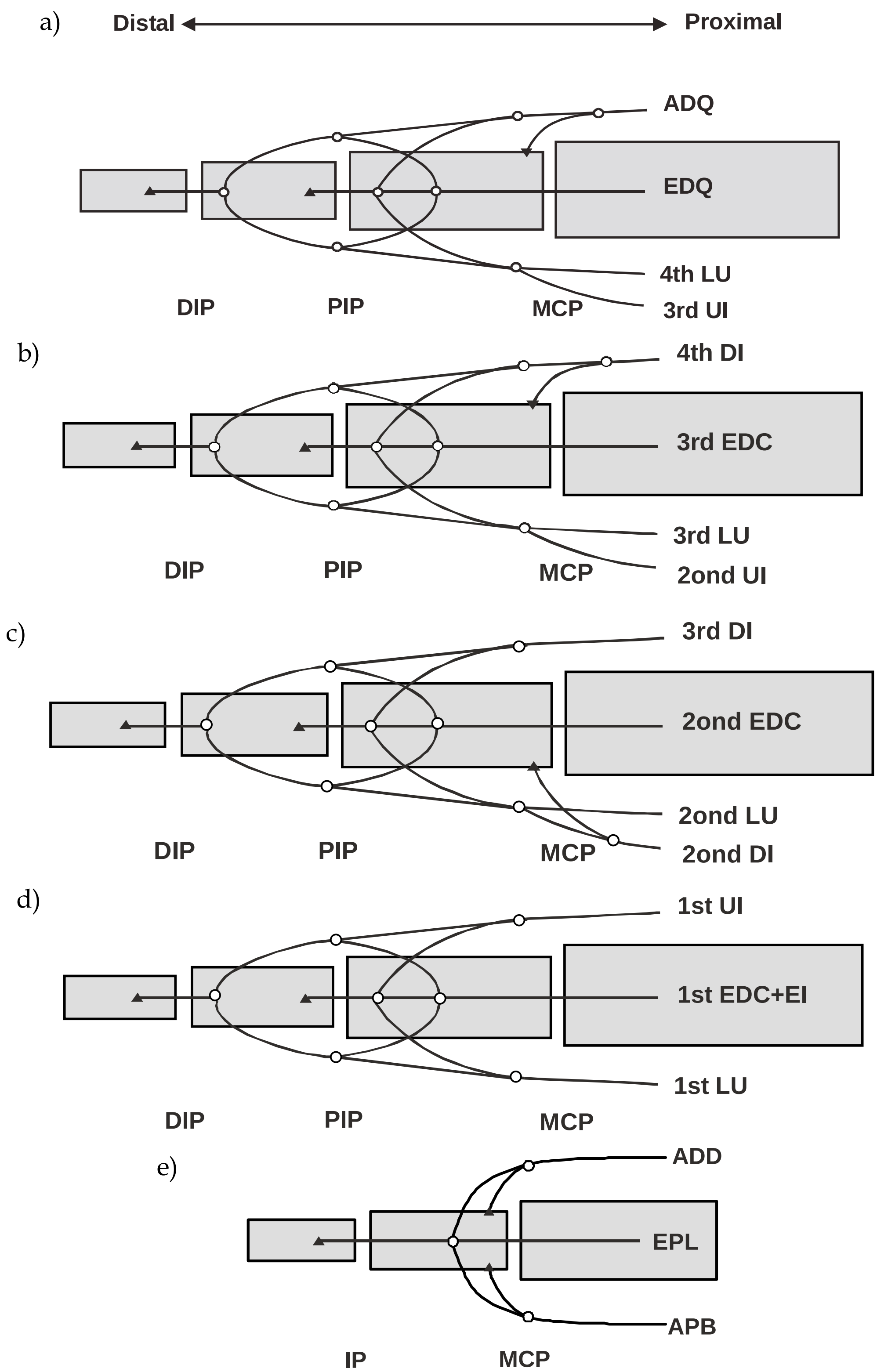

Fig. 7. Sketch of the extensor mechanisms of the fingers and thumb (dorsal view) showing the insertions into the bones (▲) and the connections and splittings considered (○): a) little finger; b) ring finger; c) medial finger; d) index finger; e) thumb.

The data for the location of the points defining the tendon paths comes from An et al. (1979) and Buchholz et al. (1992), and are also scaled with respect to the hand length and hand breadth (Sancho-Bru, 2000).

3.3 Ligaments

In previous work, we showed the importance of modelling the effect of ligaments for studying free finger movements. In the case of grasping, their consideration is not so relevant. Their effect can be neglected for studying power grasps, but they can play an important role in the case of some precision grasps, particularly those involving fast movements.

In the case of DIP and PIP joints of fingers and thumb, the insertion of the collateral ligaments on the proximal segment of the joint corresponds to the flexion-extension axis (Dubousset, 1981). Therefore, they do not develop any flexion-extension moment over the joint and they do not need to be modelled. In the case of MCP joints, the proximal insertion of the lateral ligament on the metacarpal head remains dorsal to the center of the articular curvature (Fig. 8), so that collateral ligaments are lax in extension, but they become taut in flexion, decreasing significantly the range of lateral movement (Craig, 1992; Dubousset, 1981; Kapandji, 1998). Tension on the radial and ulnar ligaments increases with adduction and abduction of the MCP joint, respectively. Furthermore, the line of action of the ligaments remains dorsal to the flexion- extension axis of the joint (Craig, 1992), developing an extension moment over the joint, in addition to the abduction-adduction moment.

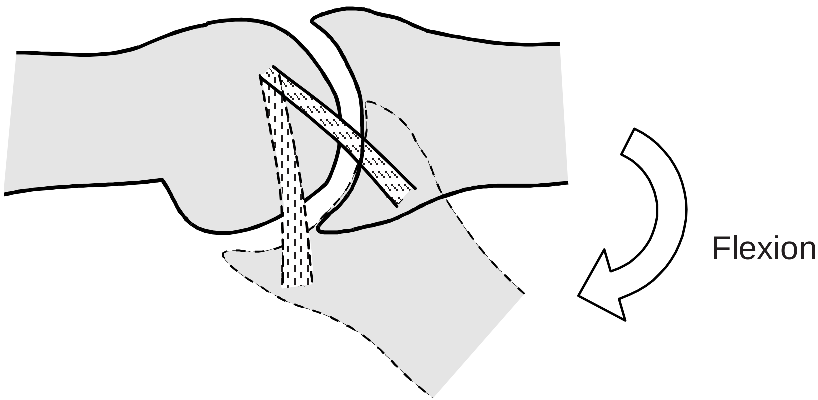

Fig. 8. Collateral ligament over MCP joints becomes taut with flexion.

Both ulnar and radial ligaments over MCP joints have been considered. A unique fibre for each ligament has been considered, joining two points representing the insertions into the bones. One point is fixed with respect to the metacarpal, and the other one with respect to the proximal phalanx. No interaction between bone and ligament has been considered; therefore the ligament path is a straight line between the insertion points. Its non-linear behaviour has been taken into account considering a quadratic relationship between the force developed by the ligament (F_{lig}) and its elongation (Mommersteeg et al., 1996)

$$F_{lig} = K \cdot \left(L_{lig} - L_{lig,o}\right)^2 , \tag{10}$$

where K is the characteristic constant of the ligament, L_{lig} the length of the fibre representing the ligament, and $L_{lig,o}$ the unstrained length of the ligament.

The data for the ligament insertion points have been obtained from the geometric model presented in Youm et al. (1978), and the stiffness constant has been estimated to be 750 N/cm^2 from Minami et al. (1985).

3.4 Skin and contact with objects

One of the applications of the biomechanical model is its use in assessing the use of handheld products from an ergonomics point of view. To accomplish that goal, the model has to incorporate a realistic model of the skin from the visual point of view. The advances in computer animation have made possible the development of a number of convincing surface skin models.

We propose to use a surface skin model similar to that of Endo et al. (2007) or Goussous (2007). The surface skin model is a 3-dimensional polygonal mesh for the hand surface generated from CT images. The geometry of the skin model is defined at only one opened posture. A surface skin deformation algorithm defines the deformed geometry of the surface skin model when the posture of the kinematic model is changed (Fig. 9). The algorithm assigns each bone a capsule-shaped *envelope*. Vertices of the modified skin within these envelopes move with the bones. Where envelopes overlap, vertex motion is a blend between the envelopes. The influence of each bone for vertices within the intersection of two bones' envelopes is controlled by assigning weight values. The ratio of a vertex's weight values, which always total 1.0, determine the relative extent to which each bone's motion affects the vertex. Furthermore, the model gets scaled when the kinematic model is scaled.

As stated before, the model has to simulate and show the grasping of an object in a realistic way. To satisfy this requirement, it is not enough to have a visually realistic model of the surface skin. The model must also be able to predict feasible grasping postures.

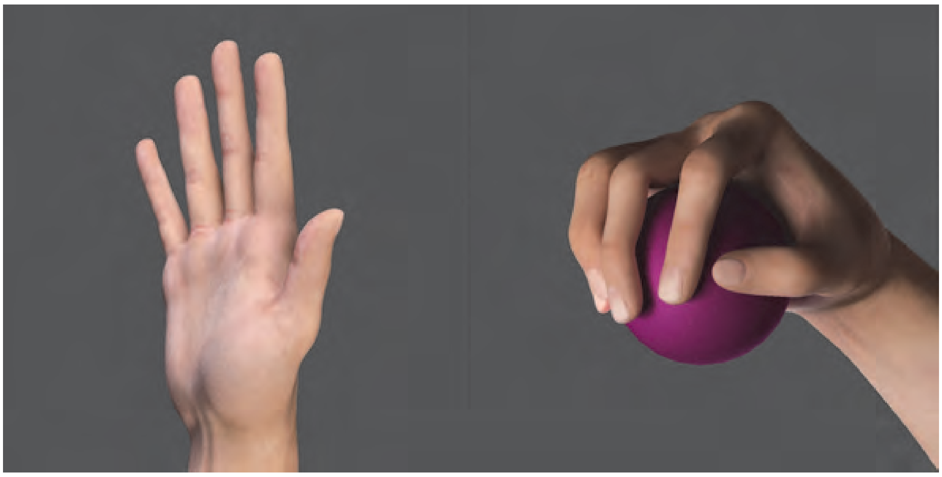

Fig. 9. Surface skin model

In order to generate grasp postures automatically, we propose to use a grasping algorithm based on that of Choi (2008). This algorithm uses a function to automatically generate a natural grasping motion path of the hand model from a fully opened state to a clenched one. The goal is to find contacts between the surface hand skin and the object surface while rotating the joint angles of the fingers. Care has to be taken to properly choose the rotation rate of the finger joints, as it affects the final posture prediction. Based on the results from Choi (2008), we propose to use a variable rotation algorithm, by describing rotations of all joints at observation-based rates. To select the appropriate rotation rate we propose the use of neural networks, similar to those used in Kyota et al. (2005) and Rezzoug & Gorce (2008). This will require intensive experimental work beforehand to record the postures for grasping objects (of different shapes, sizes, weights, etc.) when performing different tasks (power and precision). The experimental data have to be analysed in order to characterise the human grasp and find the parameters affecting the grasping posture. These parameters will be used as input to the neural network to estimate a tentative clenched posture. The rotation rate is defined by the difference between the angles of the fully opened state and the tentative clenched one.

In order to generate the grasp, a contact model is required. We need to check whether the surface skin model makes contact with the surface of the object model. In reality, the surface of a hand is deformed when making contact with the object. Generally, this deformation has a non-linearly elastic property, and it could be simulated using finite element analyses. But this would need a long execution time. This is unacceptable for our model where a large number of different grasp postures have to be generated and tested within a practical time.

Therefore, we propose to consider a simple geometric collision-detection algorithm based on the one used by Endo et al. (2007). The algorithm allows the penetration of the surface skin model and the object model. This penetration is limited by a tolerance that relates to the hand stiffness of each contact region.

The distances between the points on the skin surface and the object are calculated while the joint angles of each joint rotate according to the specific joint rotation algorithm. When the maximum penetration distance between the skin surface points and the object reaches the given tolerance, the contact is achieved and the joint rotation ends. When distal segments of all four fingers make contact with the object, the simulation terminates.

As we have mentioned previously, the model has to provide the contact information required for evaluating the grasp. If a classical robotics quality measure of the grasp is to be performed, the only data needed are the contact points and associated normal vectors at these points, which are easily obtained from the proposed contact model.

When trying to estimate the muscular pattern associated with a grasp, the model needs more contact information. The contact forces between the object and the hand have to be considered in this case. Unlike what happens with robots, real human fingers conform to the grasped object shape. As the contact finger surface is deformable the contact does not occur at just one point but over some finite area that increases as the normal forces increase. Due to this effect, in addition to the normal force and tangential force due to friction, human finger contact may support frictional torsional moments with respect to the normal at the contact point. This clearly shows that the consideration of rigid contact commonly used in robotics is not appropriate for use in studying the human grasp, and a soft contact has to be modelled. Most objects manipulated by human hands are much stiffer than human hands, and it is reasonable to consider the objects to be grasped as rigid bodies, and the hand as a deformable body.

Different soft contact models have been investigated and proposed in order to better account for this deformation effect in the context of soft finger contacts (Ciocarlie et al., 2005, 2007; Gonthier, 2007). In Ciocarlie et al. (2007) friction constraints are derived based on general expressions for non-planar contacts of elastic bodies, taking into account the local geometry and structure of the objects in contact. The following approximation can be used to express the constraint relating the magnitudes of frictional force (f_t) and moment (τ_n):

$$f_t^2 + \frac{\tau_n^2}{e_n^2} \leq \mu^2 \cdot P^2 , \tag{11}$$

where P is the total load applied in the direction of the contact normal, μ is the friction coefficient and e_n is called the eccentricity parameter (height of the ellipsoid described by Eq. 11). Considering a Winkler elastic foundation (Johnson, 1985) of depth h and elastic modulus K, the eccentricity parameter is given by:

$$e_n = \frac{8}{15} \cdot \sqrt{a \cdot b} , \tag{12}$$

where a and b can be calculated from the relative radii of curvature R' and R'' of the objects in contact and the compression δ of the elastic layer:

$$a = \sqrt{2 \cdot \delta \cdot R'} ;\ b = \sqrt{2 \cdot \delta \cdot R''} ;\ \delta = \sqrt{\frac{P \cdot h}{K \cdot \pi \cdot (R' \cdot R'')^{1/2}}} , \tag{13}$$

The actual grasping forces for a given posture will be obtained by considering that they have to satisfy the dynamic equilibrium of the grasped object. There is not a unique set of forces that ensures the equilibrium but we have to take into account the biomechanical limitations (maximal muscle forces) and the control performed by the central nervous system. In an effort to minimise the computational cost, we propose to uncouple the computation of the contact forces from the neuromuscular control model. This can be done by considering that the central nervous system is trying to attempt performing the grasp with minimal contact forces, as implemented for robots in the work of Liu et al. (2004a).

3.5 Neuromuscular control

The movement of the skeletal chains, together with the contact forces and the corresponding application points are input to the model. The problem to be solved is the derivation of the muscle activation levels required to produce the given motion under the external loads. It is, therefore, an inverse dynamics problem.

The dynamics equations of the open chain of rigid bodies have been derived using the Lagrange method (García de Jalón & Bayo, 1994). For a system with m generalised co-ordinates q_k, this equation is expressed as:

$$\frac{d}{dt}\frac{\partial L}{\partial \dot{q}_k} - \frac{\partial L}{\partial q_k} = Q_k^{nc} \quad k = 1,\ldots,m , \tag{14}$$

where L is the Lagrangian function and Q_k^{nc} are the generalised non-conservative forces. The generalised coordinates have been considered coincident with the system DOF (m=23).

Eqs. 14 together with the force balances of the tendon nets lead to an indeterminate problem. For example, in the case of the index finger, there are 12 equations (four corresponding to the DOF considered and eight to force balances in the tendon net) and 18 unknowns (six muscle forces and 12 branch forces of the tendon net). There is not a unique combination of muscular efforts that satisfy the dynamic equilibrium constraints. To solve the problem, a criterion chosen by the central nervous system to determine the muscle action control must be introduced. Our proposal is to maximise the endurance. According to Crowninshield and Brand (1981), this is achieved by minimising the non-linear objective function

$$OBJ = \sum \left(\frac{F_i}{PCSA_i} \right)^n , \tag{15}$$

with n between 2.0 and 4.0, and where F_i represents the force exerted by muscle i, and $PCSA_i$ its physiological cross-sectional area. In this case, n = 2 will be used. This function is minimised when subjected to Eq. 13 together with the force balances of the tendon nets. Additional constraints are that tendon forces must be non-negative, and the limits of muscle forces obtained from Eqs. 2 and 3 varying the muscle activation level from 0 to 1

$$F_{PEE} \cdot F_{\max} \leq F \leq (F_l \cdot F_v + F_{PEE}) \cdot F_{\max} . \tag{16}$$

3.6 Grasp evaluation

A global grasp evaluation can be performed through the use of the proposed model, merging the knowledge from ergonomics, robotics and biomechanics. The classical ergonomics evaluation of grasp posture and reachability is possible, for different percentiles of the population represented by the corresponding anthropometric parameters. Furthermore, CHTD evaluation can be performed by using the predicted postures and muscle forces.

It is advisable to use force closure from robotics as a part of the proposed model; once a grasping posture is estimated by the grasping algorithm, force closure should be assured before consuming time in determining the contact forces. Any of the robotics quality measures could be used for evaluating the grasp. Depending on the task to be performed, it would be better to use a grasp quality measure to evaluate the disturbance resistance or a grasp quality measure to evaluate the manipulability.

But the most relevant contribution to grasp evaluation has to come from biomechanics analysis. Grasp measures related to the muscle and articular forces have to be investigated. Just to provide insight into this sense, and to ensure coherence with our model formulation, we propose the use of Eq. 15 as a quality measure related to fatigue that we can call *fatigue index*: the smaller the fatigue index the better will be the grasp. For power grasps, an alternative measure can be the difference between the maximal force the hand can exert on the grasped object for the posture being analysed and the real contact forces estimated by the contact model; this alternative measure can be seen as a safety margin for the muscle forces, that we can call *muscle safety margin index*. Additional measures can be investigated, such as the maximal contact pressure, etc.

4. Conclusion

A realistic and self-contained biomechanical model of the hand has been proposed by merging the current knowledge of biomechanics, ergonomics and robotics. The model simulates the complete hand and can easily be scaled to study different percentiles of populations. It has a realistic representation that allows the ergonomic evaluation of products. The model is dynamic and can be used to study the muscular patterns associated with a specific grasp. It allows predicting feasible grasping postures and provides the contact information required for evaluating the grasp. Finally, the model incorporates original quality grasping measures such as the fatigue index and the muscle safety margin index, in addition to the usual robotics and ergonomics metrics and evaluations. All the abovementioned features are performed in a virtual environment, without external experimental data.

5. Acknowledgment

We are grateful for the financial support of the Fundació Caixa-Castelló and the Universitat Jaume I throughout the project P1-1B2009-40; of the Spanish Research and Innovation Ministry, and the EU (FEDER funds) throughout the project DPI2010-18177; and of European Community's Seventh Framework Programme through the project GRASP, IST-FP7-IP-215821. This research is related to these three projects.

6. Nomenclature

3D	Three-dimensional	FP	Flexor profundus
ADD	Adductor pollicis	FPB	Flexor pollicis brevis
ADQ	Abductor digiti quinti	FPL	Flexor pollicis longus
APB	Abductor pollicis brevis	FS	Flexor superficialis
APL	Abductor pollicis longus	GWS	Grasp wrench space
CE	Contractile element	HB	Hand breadth
CHT	Cumulative hand trauma		
D	disorders	HL	Hand length
CMC	Carpometacarpal	IP	Interphalangeal
DI	Dorsal interosseous	LU	Lumbrical
DIP	Distal interphalangeal	MCP	Metacarpophalangeal
DOF	Degrees of freedom	OPP	Opponens pollicis
EDC	Extensor digitorum communis	OWS	Object wrench space
		PCS	Physiological cross-sectional
EDQ	Extensor digiti quinti	A	area
EFM	Elastic foundation model	PEE	Parallel elastic element
EI	Extensor indicis	PIP	Proximal interphalangeal
EPB	Extensor pollicis brevis	SEE	Series elastic element
EPL	Extensor pollicis longus	TWS	Task wrench space
FDQ	Flexor digiti quinti	VI	Volar interosseous

7. References

An, K.N., Chao, E.Y., Cooney, W.P. & Linscheid, R.L. (1979). Normative model of human hand for biomechanical analysis. J*ournal of Biomechanics*, 12, 10, pp. (775-788), ISSN 0021-9290

An, K.N., Chao, E.Y.S. and Kaufman, K.R., 1991. Analysis of muscle and joint loads. In: Mow, V.C and Hayes, W.C. (Eds.), *Basic Orthopaedics Biomechanics*. Raven Press. Ltd., New York, pp. 1-50.

Armstrong, T.J., Best, C., Bae, S., Choi, J., Grieshaber, D.C., Park, D., Woolley, C. & Zhou, W. Development of a Kinematic Hand Model for Study and Design of Hose Installation. *Digital Human Modeling*, HCII 2009, LNCS 5620, pp. 85–94, 2009.

Bernabeu, J. & Tornero, J. (2002). Hough Transform for Distance Computation and Collision Avoidance, *IEEE Transactions on Robotics and Automation*, 18, 3, (June 2002), pp. (393-398), ISSN 1042-296X

Biagiotti, L., Lotti, F., Melchiorri, C. & Vassura, G. (2002). Design Aspects for Advanced Robot Hands, IEEE/RSJ *International Conference on Intelligent Robots and Systems.* Towards Intelligent Robotic Manipulation., pp. (1–16)

Bicchi, A. (1994). On the Problem of Decomposing Grasp and Manipulation Forces in Multiple Whole-limb Manipulation, *Int. Journal of Robotics and Autonomous Systems,* 13, 2, (July 1994), pp. (127-147), ISSN 0921-8890

Bicchi, A. (1995). On the Closure Properties of Robotic Grasping. *International Journal of Robotics Research*, 14, 4, (August 1995), pp. (319–334), ISSN 0278-3649

Bicchi, A. & Kumar, V. (2000). Robotic grasping and contact: a review, *Robotics and Automation, 2000. Proceedings. ICRA '00. IEEE International Conference on*, IEEE, pp. 348–353.

Biryukova, E.V., Yourovskaya, V.Z. (1994). A model of human hand dynamics. *Advances in the Biomechanics of the Hand and Wrist*, Eds. F. Schuind, pp. (107-122), Plenum Press, ISBN: 0-306-44580-8, New York.

Borst, C., Fischer, M. & Hirzinger, G. (2003). Grasping the dice by dicing the grasp, *Proc. IEEE/RSJ IROS, ISBN 0-7803-7860-1, Las Vegas, NV, USA, Octuber 2003*Borst, C., Fischer, M. & Hirzinger, G. (2004). Grasp planning: how to choose a suitable task wrench space, *Proc. IEEE ICRA, ISBN 0-7803-8232-3, New Orleans, LA, USA, April-May 2004*

Brand, P.W. & Hollister, A.M. (1992). *Clinical Mechanics of the Hand*, Elsevier Science Health Science div, third edition, ISBN13 9780815127864, St. Louis

Buchholz, B., T.J. Armstrong, &S.A. Goldstein. Anthropometric data for describing the kinematics of the human hand. *Ergonomics* 35, 3, (March 1992), pp.(261-273), ISSN 0014-0139

Buchner, H.J., Hines, M.J., Hemami, H (1988). A dynamic model for finger interphalangeal coordination. *Journal of Biomechanics*, 21, 6,pp. (459-468), ISSN 0021-9290

Case, K., Porter, J.M. and Bonney, M.C., SAMMIE: a man and workplace modelling system. *Computer Aided Ergonomics*, 1990, 31–56 (Taylor & Francis: London).

Casolo, F., Lorenzi, V. (1994). Finger mathematical modelling and rehabilitation. En Advances in the Biomechanics of the Hand and Wrist, Eds. F. Schuind, pp. 197-223, New York. Plenum Press.

Chao, E.Y., Opgrande, J.D., Axmear, F.E. (1976). Three dimensional force analysis of finger joints in selected isometric hand functions. *Journal of Biomechanics*, 9: 387-395.

Chao, E.Y., An, K.N. (1978). Internal forces in human hand. *Journal of the Engineering Mechanics Division*, ASCE, 104 (EM1): 255-272.

Chiu, S.L. (1988). Task compatibility of manipulator pustures. *Int. J. Robotics Research*, 7, 5) pp. (13-21)

Choi, J. (2008). Doctoral dissertation, University of Michigan.

Ciocarlie, M., Miller, A. & Allen, P. (2005). Grasp Analysis Using Deformable Fingers, 2005 IEEE/RSJ International Conference on Intelligent Robots and Systems (IROS 2005)

Ciocarlie, M., Lackner, C. & Allen, P. (2007). Soft Finger Model with Adaptive Contact Geometry for Grasping and Manipulation Tasks, *Second Joint EuroHaptics Conference* *and Symposium on Haptic Interfaces for Virtual Environment and Teleoperator Systems (WHC'07),* ISBN 978-0-7695-2738-3, Tsukuba, Japan, March 2007

Colombo and Cugini, 2005; Virtual humans and prototypes to evaluate ergonomics and safety. *Journal of Engineering Design,* 16, 2, (April 2005), pp. (195–207), ISSN 0954-4828

Craig, S.M., 1992. Anatomy of the joints of the fingers. *Hand Clinics,* 8, 4, (November 1992), pp. (693-700), ISSN 0749-0712

Crowninshield, R.D. & Brand, R.A. (1981). A physiologically based criterion of muscle force prediction in locomotion. *Journal of Biomechanics*. 14: 793-801.

Cutkosky, M. (1989). On grasp choice, grasp models, and the design of hands for manufacturing tasks, IEEE Transactions on Robotics and Automation **5**(3): 269–279.

Davidoff and Freivalds, 1993) Davidoff N.A., Freivalds A. A graphic model of the human hand using CATIA. *International Journal of Industrial Ergonomics*, 1993, 12 (4) 255-264

Denavit, J. and Hartenberg, R.S. (1955) 'A kinematic notation for lower-pair mechanisms based on matrices', *Journal of Applied Mechanics*, Vol. 77, pp.215–221.

Diankov, R. (2010). Automated Construction of Robotic Manipulation Programs, PhD thesis, Carnegie Mellon University, Robotics Institute.

Ding, D., Lee, Y.-H. & Wang, S. (2001). Computation of 3-d form-closure grasps, IEEE Transactions on Robotics and Automation **17**(4): 515 –522.

Dubousset, J.F., 1981. The digital joints. In: Tubiana, R. (Ed.), The Hand. Saunders Company, Philadelphia, pp. 191-201.

Endo, Y., Kanai, S., Kishinami, T., Miyata, N., Kouchi, M., Mochimaru, M. (2007). Virtual grasping assessment using 3D digital hand model. 10th Annual Applied Ergonomics Conference: Celebrating the Past - Shaping the Future.

Endo, Y., Kanai, S., Miyata, N., Kouchi, M., Mochimaru, M., Konno, J., Ogasawara, M., Shimokawa, M. (2009). Optimization-Based Grasp Posture Generation Method of Digital Hand for Virtual Ergonomics Assessment. SAE Int. J. Passeng. Cars - Electron. Electr. Syst. Volume 1, Issue 1, 590-598.

Erdmann, M.A. (1994). On the representation of firction in configuration space. *Int. Journal of Robotics Research,* 13(3),pp. 240-271.

Esteki, A., Mansour, J.M. (1997). A dynamic model of the hand with application in functional neuromuscular stimulation. *Annals of Biomedical Enginnering*, 25: 440-451.

Eyler, D.L. and Markee, J.E., 1954, "The anatomy and function of the intrinsic musculature of the fingers", *The Journal of Bone and Joint Surgery,* Vol. 36-A, pp. 1-18.

Ferrari, C. & Canny, J. (1992). Planning optimal grasps, *Proceedings 1992 IEEE International Conference on Robotics and Automation* pp. 2290–2295.

Fok KS, Chou SM. Development of a finger biomechanical model and its considerations. *Journal of Biomechanics*. 2010 Mar 3;43(4):701-13.

García de Jalón, J. and Bayo, E., 1994. Kinematic and dynamic simulation of multibody systems. Springer-Verlag, New York.

Giurintano, D.J. & Hollister, A.M. (1991). Force analysis of the thumb for a five-link system. ASME Biomechanics Symposium, 120:213-217.

Giurintano, D.J., Hollister, A.M., Buford, W.L., Thompson, D.E. & Myers, L.M. (1995). A virtual 5-link model of the thumb. *Medical Engineering & Physics,* 17, 4, (June 1995), pp. (297-303), ISSN 1350-4533

Goldstein, S.A., Armstrong, T.J., Chaffin, D.B. & Matthews, L.S. (1987). Analysis of cumulative strain in tendons and tendon sheaths. *Journal of Biomechanics*, 20 (1), pp. 1-6.

Gonthier, Y. (2007). Contact Dynamics Modelling for Robotic Task Simulation. Ph. d. thesis. University of Waterloo.

Goussous, F.A. Grasp planning for digital humans. PhD dissertation. Iowa University. 2007

Harada, K., Kaneko, M. & Tsuji, T. (2000). Rolling Based Manipulation for Multiple Objects. *Proc. IEEE Int. Conf. on Robotics and Automation (ICRA),* pp. 3887-3894.

Haschke, R. Steil, J.J., Steuwer, I. & Ritter, H. (2005). Task-oriented quality measures for dextrous grasping. In: *Proc. 6th IEEE Int. Conf. Computational Intelligence in Robotics and Automation*, pp. 689-694.

Hatze, H., 1981. Myocibernetic control models of skeletal Muscle. University of South Africa, Pretoria.

Hertz, H. (1882). On the Contact of Rigid Elastic Solids and on Hardness, Ch 6: Assorted Papers by H. Hertz . MacMillan, New York, 1882.

Hill, A.V., 1938, “The of shortening and dynamic constants of muscle”, Proc R Soc London B, Vol 126, pp. 136-195.

Hollister, A.M., Giurintano, D.J., Buford, W.L., Myers, L.M. & Novich, A. (1995). The axes of rotation of the thumb interphalangeal and metacarpophalangeal joints. *Clinical Orthopaedics*, (320), pp. 188-193.

Howe, R. Kao, I. & Cutkosky, M. (1988). Sliding of robot fingers under combined tornsion and shear loading. Proceedings *IEEE Int. Conf. on Robotics and Automation*, pp. 103-105.

Howe, R. & Cutkosky, M. (1996). Practical force-motion models for sliding manipulation *Int. Journal of Robotics Research* 15(6), pp. 555-572.

Jacobson, M.D., Raab, R., Faxelo. B.M., Abrams, R.A., Botte, M.J. & Lieber, R.L. (1996). Architectutural design of the human intrinsic hand muscles. *The Journal of Hand Surgery*, 17A (5), pp. 804-811.

Johnson, K. L., (1985). Contact Mechanics. Cambridge University Press.

Kamper DG, Fischer HC, Cruz EG. (2006). Impact of finger posture on mapping from muscle activation to joint torque. Clinical Biomechanics. 21(4):361-9.

Kao, I. & Cutkosky, M (1992). Dexterous manipulation with compliance and sliding. *Int. Journal of Robotics Research* 11(1), pp. 20-40.

Kao, I. & Yang, F. (2004). Stiffness and Contact Mechanics for Soft Fingers in Grasping and Manipulation. *IEEE Transactions on Robotics and Automation*, 20(1), pp. 132-135.

Kao, I., Linch, K. & Burdick, J. W. (2008). Contact Modeling and Manipulation. *Handbook of Robotics, chapter 27*, pp. 647-668.

Kapandji, A.I., 1998. *Fisiologie articulaire. Membre Supérieur*. Editions Maloine, Paris.

Kaufman, K.R., An, K.N., Litchy, W.J. and Chao, E.Y.S., 1991. Physiological prediction of muscle forces I. Theoretical formulation. J. Neuroscience 40 (3), 781-792.

Kawaguchi, K., Endo, Y., Kanai, S. (2009). Database-Driven Grasp Synthesis and Ergonomic Assessment for Handheld Product Design. Lecture Notes in Computer Science, Volume 5620/2009, 642-652.

Keyserling, W.M. 2000; Workplace risk factors and occupational musculoskeletal disorders, part 2: A review of biomechanical and Psychophysical research on risk factors associated with upper extremity disorders. AIHA Journal; Mar/Apr 2000; 61 (2) pg. 231-243

Kong, Y., Jang, H. & Freivalds, A. (2006) Wrist and Tendon Dynamics as Contributory Risk Factors in Work-Related Musculoskeletal Disorders. *Human Factors and Ergonomics in Manufacturing*, 16, 1, pp. (83–105), ISSN 1090-8471

Kumar S. 2001. Theories of musculoskeletal injury causation. Ergonomics, 2001, VOL. 44, NO. 1, 17 ± 47

Kurita Y, Onoue T, Ikeda A, Ogasawara T. Biomechanical analysis of subjective pinching effort based on tendon-skeletal model. Conf Proc IEEE Eng Med Biol Soc. 2009;2009:5231-4.

Kyota, F., Watabe, T., Saito, S. & Nakajima, M. (2005). Detection and Evaluation of Grasping Positions for Autonomous Agents. Proceedings of the 2005 International Conference on Cyberworlds (CW'05).

Lee, J.W., Rim, K. (1990). Maximum finger force prediction using a planar simulation of the middle finger. Proc. Instn. Mech. Engnrs. Part H: *Journal of Engineering in Medicine*, 204: 169-178.

Lee SW, Chen H, Towles JD, Kamper DG. (2008a) Effect of finger posture on the tendon force distribution within the finger extensor mechanism. *Journal of Biomechanical Engineering*. 130(5):051014.

Lee SW, Chen H, Towles JD, Kamper DG. (2008b). Estimation of the effective static moment arms of the tendons in the index finger extensor mechanism. *Journal of Biomechanics*. 41(7):1567-73.

Leijnse, J.N.A.L., Bonte, J.E., Landsmeer, J.M.F., Kalker, J.J., Van Der Meulen, J.C., Snijders, C.J. (1992). *Journal of Biomechanics*, 25 (11):1 253-1264.

Leijnse, J.N.A.L., Kalker, J.J. (1995). A two-dimensional kinematic model of the lumbrical in the human finger. *Journal of Biomechanics,* 28 (3): 237-249.

Lemay, M.A. & Crago, P.E. (1996). A dynamic model for simulating movements of the elbow, forearm and wrist. *Journal of Biomechanics*, 29 (19, pp. 1319-1330.

Li, Z & Sastry S. (1988). Task-oriented optimal grasping by multifingered robotic hands. *IEEE Journal of Robotics and Automation*, 4 (1), pp. 32-44.

Li Z., Chang C.-C., Dempsey P. G., Ouyang L., Duan J.. Validation of a three-dimensional hand scanning and dimension extraction method with dimension data. Ergonomics, Vol. 51, No. 11, November 2008, 1672–1692

Liegeois, A. (1977). Automatic supervisory control for the configuration and behavior of multibody mechanisms. *IEEE Trans. System, Man and Cybernetics*, 7 (12), pp. 842-868.

Lin, Q., Burdick, J. M. & Rimon, E. (2000). A stiffness-based quality measure for compliant grasps and fixtures. *IEEE Transactions on Robotics and Automation*, 16(6), pp. 675-688.

Liu, G., Xu, J., & Li, Z. (2004a). On geometric algorithms for real-time grasping force optimization. *IEEE Transactions on Control Systems* Technology, 12 (6): 843–859.

Liu, G., Xu, J., Wang, X. & Li, Z. (2004b). On Quality Functions for Grasp Synthesis, Fixture Planning, and Coordinated Manipulation, *IEEE Transactions on Automation Science and Engineering* **1**(2): 146–162.

Mansour, J.M., Rouvas, C., Sarangapani, J. (1994). Quantitative functional anatomy of finger muscles: Appliction to controlled grasp. *En Advances in the Biomechanics of the Hand and Wrist*, Eds. F. Schuind, pp. 177-188, New York. Plenum Press.

Mason, M. T. (2001). *Mechanics of robotic manipulation*, The MIT Press, Cambridge, MA, USA.
Miller, A. T. & Allen, P. K. (1999). Examples of 3D grasp quality computations, *Robotics and Automation, 1999. Proceedings. 1999 IEEE International Conference on*, Vol. 2, IEEE, pp. 1240–1246.
Miller, A. T., Knoop, S., Christensen, H. & Allen, P. K. (2003). Automatic grasp planning using shape primitives, Robotics and Automation, 2003. Proceedings. ICRA'03. IEEE International Conference on, Vol. 2, IEEE, pp. 1824–1829.
Miller, A., Allen, P.K. (2004). "Graspit!: A Versatile Simulator for Robotic Grasping". *IEEE Robotics and Automation Magazine*, V. 11, No.4, pp. 110-122.
Minami, A., An, K.N., Cooney, W.P. and Linscheid, R.L., 1985. Ligament stability of the MCP joint: A biomechanical study. *J. Hand Surgery* 10A (2), 255-260.
Mirthich, B. & Canny, J. (1994). Easily computable optimum grasps in 2D and 3D. In: *Proc. IEEE ICRA 1994*, pp. 739-747.
Mishra, B., Schwartz, J. T. & Sharir, M. (1987). On the existence and synthesis of multifinger positive grips, *Algorithmica* **2**(1-4): 541–558.
Mital, A. and Kilbom, A., 1992, Design, selection and use of hand tools to alleviate trauma of the upper extremities: Part II- The scientific basis (knowledge base) for the guide, *International Journal of Industrial Ergonomics*, Vol. 10, pp. 7-21
Mommersteeg, T.J.A., Blankevoort, L., Huiskes, R., Kooloos, J.G.M. and Kauer, J.M.G., 1996. Characterization of the mechanical behavior of human knee ligaments: a numerical-experimental approach. J. Biomechanics 29 (2), 151-160.
Morales, A., Sanz, P., Del Poblil, A. & Fagg, A. (2006). Vision-based three-finger grasp synthesis constrained by hand geometry. *Robotics and Autonomous Systems,* 54, 6, (June 2006), pp. (496–512), ISSN 0921-8890
Muggleton, J.M., Allen, R. & Chappell, P.H. Hand and arm injuries associated with repetitive manual work in industry: a review of disorders, risk factors and preventive measures. *Ergonomics*, 1999, VOL. 42, NO. 5, 714 - 739
Napier, J. (1956). The prehensile movements of the human hand, Surger **38**(4): 902–913.
Nguyen, V.-D. (1988). *Constructing force-closure grasps*, Institute of Electrical and Electronics Engineers.
Parada, J. E., Nava, N. E. & Ceccarelli, M. (2008). A Methodology for the Design of Robotic Hands with Multiple Fingers, *International Journal of Advanced Robotic Systems* **5**(2): 177–184.
Park, Y.C. & Starr, G.P. (1992). Grasp synthesis of polygonal objects using a three-fingered robotic hand. *International Journal of Robotics Research,* 11 (3), pp. 163-184.
Peña-Pitarch, E. Virtual human hand. PhD dissertation. Universitat Politècnica de Catalunya. 2007.
Pollard, S.S. (2004). Closure and quality equivalence for efficient synthesis of grasps from examples. *Int. J. Robotics Research*, 23 (6), pp. 595-614.
Ponce, J., Sullivan, S., Sudsang, A., Boissonat, J.D. & Merlet, J.P. (1997). On computing for-finger equilibrium and force-closure grasps of polyhedral objects. *International Journal of Robotics Research*, 16 (1), pp. 11-35.
Qiu D, Fischer HC, Kamper DG. Muscle activation patterns during force generation of the index finger. Conf Proc IEEE Eng Med Biol Soc. 2009;2009:3987-90.
Rezzoug, N. & Gorce, P. (2008). Prediction of fingers posture using artificial neural networks. *Journal of Biomechanics*. 41, pp. 2743-2749.

Rhee T., Neumann U., Lewis J.P. 2006, Human Hand Modeling from Surface Anatomy. I3D '06 Proceedings of the 2006 symposium on Interactive 3D graphics and games, ACM New York

Roa Garzón, M. (2009). *Grasp Planning Methodology for 3D Arbitrary Shaped Objects*, Ph. d. thesis, Universidad Politécnica de Cataluña.

Rogers M. S., Barr A. B., Kasemsontitum B.; Rempel D. M.. A three-dimensional anthropometric solid model of the hand based on landmark measurements. *Ergonomics*, Vol. 51, No. 4, April 2008, 511–526

Roloff I, Schöffl VR, Vigouroux L, Quaine F. Biomechanical model for the determination of the forces acting on the finger pulley system. *Journal of Biomechanics.* 2006;39(5):915-23.

Salisbury, J. (1982). *Kinematics and Force analysis of Articulated Hands*, Ph.d. thesis, Standford University.

Sancho-Bru, J.L., 2000, "Model Biomecànic de la mà orientat al disseny d'eines manuals", Ph.D. thesis, Universitat Jaume I, Castelló.

Sancho-Bru, J.L., Perez-Gonzalez, A., Vergara-Monedero, M., Giurintano,D.J., (2001). A 3-D dynamic model of human finger for studying free movements. *Journal of Biomechanics*, 34, 11, (November 2001), pp. (1491–1500), ISSN 0021-9290

Sancho-Bru, J.L., Perez-Gonzalez, A., Vergara, M., Giurintan, D.J., (2003a). A 3D biomechanical model of the hand for power grip. *Journal of Biomechanical Engineering* 125, 78–83.

Sancho-Bru, J.L., Giurintano, D.J., Pérez-González, A., and Vergara, M., (2003b), "Optimum tool handle diameter for a cylinder grip", *J. Hand. Ther.*, 16(4), pp. 337-342.

Sancho-Bru, J.L, Vergara, M., Rodríguez-Cervantes, P.J., Giurintano, D., Pérez-González, A. (2008). Scalability of the Muscular Action in a Parametric 3D Model of the Index Finger. *Annals of Biomedical Engineering,* 36, 1, (January 2008, pp. (102-107), ISSN 0090-6964

Schoenmarklin R.W., Marras W.S., Leurgans S.E. industrial wrist motions and incidence of hand/wrist cumulative trauma disorders. *Ergonomics*, 1994; 37: 1449-1459

Siciliano, B. & Khatib, O. (eds) (2008). *Springer Handbook of Robotics*, Vol. 15, Springer, Berlin, Heidelberg.

Smith, E.M., Juvinall, R.C., Bender, L.F. Pearson, J.R. (1964). Role of the finger flexors in rheumatoid deformities of the metacarpophalangeal joints. *Arth. Rheum*., 7: 467-480.

Spielholz et al., 2001; P. Spielholz, B. Silverstein, M. Morgan, H. Checkoway And J. Kaufman. Comparison of self-report, video observation and direct measurement methods for upper extremity musculoskeletal disorder physical risk factors. Ergonomics, 2001, VOL. 44, NO. 6, 588 - 613

Spoor, C.W., Landsmeer, J.M.F. (1976). Analysis of the zigzag movement of the human finger under influence of the extensor digitorum tendon and the deep flexor tendon. *Journal of Biomechanics*, 9: 561-566.

Spoor, C.W. (1983). Balancing a force on the fingertip of a two-dimensional finger model without intrinsic muscles. *Journal of Biomechanics*, 16: 497-504.

Stansfield, S. (1991). Robotic grasping of unknown objects: A knowledge-based approach, *The International Journal of Robotics Research* **10**(4): 314–326.

Storace, A., Wolf, B. (1979). Functional role of the finger tendons. *Journal of Biomechanics,* 12: 575-578.

Storace, A., Wolf, B. (1982). Kinematic analysis of the role of the finger tendons. *Journal of Biomechanics*, 15, 5, pp. (391-393), ISSN 0021-9290

Thomas, D.H., Long, C., Landsmeer, J.M.F. (1968). Biomechanical consideration of lumbricalis behaviour in the human finger. *Journal of Biomechanics*, 1: 107-115.

Tubiana, R (1981), 'The hand', Vol. 1, W.B. Sanders Company, 1981.

Tubiana, R., Thomine, J. and Mackin, E. (1996), 'Examination of the hand and wrist', Second Edition, Martin Dunitz, 1996.

Valero-Cuevas, F.J., Zajac, F.E., Burgar, C.G. (1998). Large index-fingertip forces are produced by subject-independent patterns of muscle excitation. *Journal of Biomechanics*, 31: 693:703.

Valero-Cuevas, F.J. (2000). Predictive modulation of muscle coordinatin pattern magnitude scales fingertip force magnitude over the voluntary range. *Journal of Neurophysiology*, 83 (3): 1469-1479.

Valero-Cuevas, F.J. Towles, JD, Hentz, VR. (2000). Quantification of fingertip force reduction in the forefinger following simulated paralysis of extensor and intrinsic muscles. *Journal of Biomechanics*, 33(12):1601-1609.

Valero-Cuevas, F.J. (2005). An integrative approach to the biomechanical function and neuromuscular control of the fingers. *Journal of Biomechanics*, 38(4): p.673-84.

van Nierop O.A., van der Helm A., Overbeeke K.J., Djajadiningrat T.J.P. A natural human hand model. Visual Comput (2008) 24: 31–44

Vigouroux L, Quaine F, Labarre-Vila A, Moutet F. (2006) Estimation of finger muscle tendon tensions and pulley forces during specific sport-climbing grip techniques. *Journal of Biomechanics*, 39, 14, pp. (2583-2592), ISSN 0021-9290

Vigouroux L, Ferry M, Colloud F, Paclet F, Cahouet V, Quaine F. Is the principle of minimization of secondary moments validated during various fingertip force production conditions? *Hum Mov Sci*. 2008 Jun;27(3):396-407.

Weightman, B. & Amis, A.A. (1982). Finger joint force predictions related to design of joint replacements. *Journal of Biomedical Engineering*. 4:197-205.

Wren, D. & Fisher, R. (1995). Dextrous hand grasping strategies using preshapes and digit trajectories, IEEE International Conference on Systems, Man and Cybernetics, Vol. 1, pp. 910 –915 vol.1.

Wu JZ, An KN, Cutlip RG, Dong RG. A practical biomechanical model of the index finger simulating the kinematics of the muscle/tendon excursions. *Biomed Mater Eng*. 2010;20(2):89-97.

Xydas, N. & Kao, I. (1999). Modeling of contact mechanics and friction limit surface for soft fingers with experimental results, *Int. Journal of Robotics Research*, 18(9), pp. 947-950.

Xydas, N., Bhagavat, M. & Kao, I. (2000). Study of soft-finger contact mechanics using finite elements analysis and experiments, *Proceedings 2000 ICRA. Millennium Conference. IEEE International Conference on Robotics and Automation. Symposia Proceedings (Cat. No.00CH37065)* (April): 2179–2184

Yang, J., Kim, J.H., Abdel-Malek, K., Marler, T., Beck, S. & Kopp, G.R. A new digital human environment and assessment of vehicle interior design. Computer-Aided Design 39 (2007) 548–558

Yoshikawa, T. (1985). Manipulability of robotics mechanisms. *Int. J. Robotics Research*, 4, 2, pp. (735-747)

Youm, Y., Gillespie, T.T., Flatt, A.E. & Sprague, B.L. (1978). Kinematic investigation of normal MCP joint. *Journal of Biomechanics*, 11, 3,pp. (109-118), ISSN 0021-9290

Zajac, F.E., 1989. Muscle and tendon: properties, models, scaling, and application to biomechanics and motor control. *Critical Reviews in Biomedical Engineering* 17 (4), 359-411.

Zhu, X., Ding, H. & Li, H. (2001). A quantitative measure for multifingered grasps. In: *Proc. IEEE/ASME Int. Conf. Advanced Intelligent Mechatronics 2001*, pp. 213-219.

Computer Methods in Biomechanics and Biomedical Engineering

Grasp modelling with a biomechanical model of the hand

Journal:	*Computer Methods in Biomechanics and Biomedical Engineering*
Manuscript ID:	GCMB-2011-0253
Manuscript Type:	Original Article
Date Submitted by the Author:	02-Sep-2011
Complete List of Authors:	Sancho-Bru, Joaquin; Universitat Jaume I, Enginyeria Mecànica i Construcció Mora, Marta; Universitat Jaume I, Enginyeria Mecànica i Construcció Leon, Beatriz; Universitat Jaume I, Enginyeria i Ciència dels Computadors Perez, Antonio; Universitat Jaume I, Enginyeria Mecànica i Construcció Iserte, José; Universitat Jaume I, Enginyeria Mecànica i Construcció Morales, Antonio; Universitat Jaume I, Enginyeria i Ciència dels Computadors
Keywords:	grasp, biomechanical model, finger force estimation

Grasp modelling with a biomechanical model of the hand

Joaquín L. Sancho-Bru

Department d'Enginyeria Mecànica i Construcció, Universitat Jaume I, Castelló de la Plana, Spain

Campus de Riu Sec. Avinguda Vicent Sos Baynat s/n. 12071 Castelló de la Plana (Spain). E-mail: sancho@emc.uji.es

Marta C. Mora

Department d'Enginyeria Mecànica i Construcció, Universitat Jaume I, Castelló de la Plana, Spain

Beatriz E. León

Department d'Enginyeria i Ciència dels Computadors, Universitat Jaume I, Castelló de la Plana, Spain

Antonio Pérez-González

Department d'Enginyeria Mecànica i Construcció, Universitat Jaume I, Castelló de la Plana, Spain

José L. Iserte

Department d'Enginyeria Mecànica i Construcció, Universitat Jaume I, Castelló de la Plana, Spain

Antonio Morales

Department d'Enginyeria i Ciència dels Computadors, Universitat Jaume I, Castelló de la Plana, Spain

Grasp modelling with a biomechanical model of the hand

A first approximation to human grasp modelling is presented. A previously validated biomechanical model of the hand has been used. The equilibrium of the grasped object has been added to the model through the consideration of a soft contact model. A grasping posture generation algorithm has been also incorporated to the model. All the geometry has been represented using a spherical extension of polytopes (s-topes) for efficient collision detection. The model has been used to simulate an experiment in which a subject was asked to grasp two cylinders of different diameter and weight. Different objective functions have been checked to solve the indeterminate problem. The normal finger forces estimated by the model have been compared to the ones experimentally registered. The popular objective function sum of the squared muscle stresses has been shown not suitable for the grasping simulation, requiring at least being complemented by task dependent grasp quality measures.

Keywords: grasp; biomechanical model; finger force estimation

1. Introduction

To date, many biomechanical models of the hand have been developed with the aim of providing a tool for studying problems that cannot be directly analysed on humans or that have an experimental cost that is too high; e.g., the study of new alternatives for restoring hand pathologies. Biomechanical models are descriptions of the hand as a mechanical device: the different elements of the hand are defined in terms of rigid bodies, joints and actuators, and the mechanical laws are applied.

First models were very simplified two-dimensional models of a single finger, allowing only flexion-extension movements. They were used to explain the function of different anatomical elements (Leijnse et al. 1992; Leijnse and Kalker 1995; Spoor and Landsmeer 1976; Spoor 1983; Storace and Wolf 1979, 1982; Thomas et al. 1968), the movement coordination of the interphalangeal joints (Buchner et al. 1988; Lee and Rim 1990), to study the causes and effects of hand pathologies (Smith et al. 1964; Storace and Wolf 1979, 1982) or even to obtain approximate values for the articular forces for testing prosthetic designs (Weightman and Amis 1982). By the year 2000, few attempts of developing a three-dimensional model were performed (Biryukova and Yourovskaya 1994; Casolo and Lorenzi 1994; Chao and An 1978; Chao et al. 1976; Esteki and Giurintano et al. 1995; Mansour 1997; Mansour et al. 1994; Valero-Cuevas et al. 1998). These models allowed the study of more complex movements, but still none of them modelled the complete hand.

Recent models are more complete but do not differ much from the ones developed before 2000 (Fok and Chou 2010; Kamper et al. 2006; Kurita et al. 2009; Lee et al. 2008a, 2008b; Qiu et al. 2009; Roloff et al. 2006; Sancho-Bru et al. 2001, 2003a, 2003b, 2008; Valero-Cuevas 2000, 2005; Valero-Cuevas et al. 2000; Vigouroux et al. 2006; Wu et al. 2010). Briefly, the hand kinematics is modelled using the concept of the instantaneous centre of rotation. Thus, all these works use fixed axes of rotation; depending on the joint, one or two axes of rotation are considered. Tendons, operated by muscles, control the kinematics of the hand skeletal chains. To model the action of tendons crossing a joint, the models consider the ideal case of a non-friction belt around a pulley. The muscle behaviour is modelled in most of the works in the literature by using a simple Hill's model that allows the consideration of the three main parameters, i.e., the muscle activation level, and the variation of the maximum deliverable muscle force with the muscle length and the muscle contraction velocity. Finally, the dynamic equilibrium equations on the skeletal chains are obtained, leading to an indeterminate system of equations, with more unknowns (muscle and tendon forces) than available equations. Inequality constraints taking into account the maximal forces that may be delivered by each muscle and that tendons cannot support compressive forces are considered as well. The problem is solved by minimising some cost function. Different cost functions have been investigated, being the most popular the sum of the squared muscle stresses, which has been related to the maximisation of fatigue resistance (Crowninshield and Brand 1981).

Such models have been used in the literature to estimate the muscle forces required to counteract given external forces on the hand while performing given movements. To do that, they consider movements and contact zones and forces that had to be experimentally registered. However, current models do not allow the estimation of the external forces on the hand surface required to perform a given task.

One of the main features of the human hand is the grasping ability. In this sense, the study of the muscular forces needed for grasping daily objects is of great importance. It could be very useful, for example, to study different restoration alternatives of a pathologic hand in order to restore its grasping basic functionality. However, most of the effort in hand biomechanics until now has been focused on appropriately modelling the different hand components (kinematics, muscles, tendons, etc.). Little effort has been spent on the formulation of the grasping problem when using a biomechanical model. In this sense, many limitations persist. Current models do not allow the estimation of the contact information required to use biomechanical models for simulating the grasping of objects.

On the other hand, robot hand grasps have been extensively studied for years. Although the human hand is obviously more complex than robot hands, the methods used in robotics might be raised up to study the human grasp by considering the hand as the human end-effector.

A robot should be able to locate the object and then grasp it, often with the purpose of transporting it to other locations, among other manipulation tasks. The purpose of a grasp is to constrain the potential movements of the object in the event of external disturbances. For a specific robotic hand, different grasp types are planned and analysed in order to decide which one to execute by considering different grasp quality measures. A contact model has to be defined to determine the forces or torques that the robot manipulator must exert on the contact areas. The more common contact models used in robotic grasping are the point contacts with and without friction and the soft-finger contacts (Roa Garzón 2009). Point contact models, also named rigid-body contact models, assume rigid-body models for the hand and the grasped object while the soft-finger contact models, also called compliant or regularised models, assume that the hand is a deformable element grasping a rigid body (Kao et al. 2008). The soft contact model allows the finger to apply an additional torsional moment with respect to the normal at the contact point (Ciocarlie et al. 2005, 2007; Howe et al. 1988; Howe and Cutkosky 1996; Kao and Cutkosky 1992; Kao and Yang 2004). Unlike what happens with robots, human fingers conform to the grasped object shape, then only the soft-finger contact might be applied to the study of the human grasp.

In this work we present a first approximation to the human grasping problem by taking into account the equilibrium not only of the grasping hand but also of the grasped object, through the consideration of a soft contact model.

2. Materials and methods

2.1 Model description

A previously validated 3D scalable biomechanical model of the complete hand (Sancho-Bru et al. 2001, 2003a, 2003b, 2008) was used to incorporate the grasping capabilities. The original model allowed the estimation of the muscle forces required to counteract given external forces on the hand while performing given movements. In this section, this model is modified to tackle the grasping problem. This is done by incorporating a grasping posture generation model that uses a geometrical representation of the different segments of the hand as a spherical extension of polytopes (s-topes) and a soft contact model between the grasping hand and the grasped object.

2.1.1 Musculoskeletal model

The biomechanical model uses the anthropometric parameters hand length (HL) and hand breadth (HB) to scale all its components (Fig. 1).

---- Insert Fig. 1 ----

Kinematic model. The hand model considers 23 degrees of freedom (DOF) selected to realistically simulate the hand movements. The hand has been modelled as five skeletal open chains of rigid bodies (the bones) connected to the carpus through different joints.

Proximal and distal interphalangeal joints (PIP and DIP) of the fingers and the interphalangeal joint (IP) of the thumb are of trochlear type, allowing only flexion-extension movements (Brand and Hollister 1992). They have been modelled as hinge joints.

All metacarpophalangeal joints (MCP) are of condilar type, allowing both flexion-extension and abduction-adduction movements (Brand and Hollister 1992). The carpometacarpal joint (CMC) of the thumb is a saddle joint, also allowing flexion-extension and abduction-adduction movements (Brand and Hollister 1992). All these joints have been modelled as universal joints.

Finally, the model considers the palm arching (very important for grasping) through the model of the little and ring CMC joints. These joints are of arthrodial type, with a very limited movement range (Kapandji 1998). They have been modelled as hinge joints.

Data for the axes location and orientation were obtained from (An et al. 1979; Buchholz et al. 1992; Hollister et al. 1995). These data along with the segment lengths' data were appropriately scaled with respect to the parameters HB and HL (Sancho-Bru et al. 2003b).

Musculotendinous model. Muscles have been modelled using a simple Hill's three-component model (Hill 1938) that takes into account the muscle activation level (α) and the force-length and force-velocity relationships, as well as the different index of architecture of muscles. The model considers a contractile element (CE), which is the basic component that generates force, a parallel elastic element (PEE), which is responsible for the passive force generated by the muscle when it is stretched, and a series elastic element (SEE), the muscle tendon unit, which has been considered to be inextensible (Fig. 2).

---- Insert Fig. 2 ----

The maximum force a muscle can exert in optimal conditions is proportional to its physiological cross-sectional area (PCSA):

$$F_{\max} = PCSA \cdot S_{\max} , \tag{1}$$

where S_{max} is the maximum stress the muscle can bear (An et al. 1991).

As the strain of tendons is insignificant for the magnitude of the forces developed by the muscles (Goldstein et al. 1987), the SEE has been considered to be inextensible. Then, the force the muscle exerts (F) can be written as:

$$F = F_{\max}(F_{CE} + F_{PEE}) , \tag{2}$$

where F_{CE} and F_{PEE} are the normalised forces delivered by the CE and PEE, respectively. The force exerted by the muscle can be decomposed into an active force corresponding to the CE and a passive force corresponding to the PEE. The force delivered by the CE is related to the muscle architecture and is a function of the muscle length l_{CE}, the contraction velocity v_{CE}, and the muscle activation level α (from 0 to 1), which is controlled by the central nervous system (Kaufman et al. 1991):

$$F_{CE} = \alpha \cdot F_l(l_{CE}) \cdot F_v(v_{CE}), \quad (3)$$

where F_l and F_v are the non-dimensional force-length and force-velocity relationships, that have been modelled using the expressions proposed by Kaufman et al. (1991) and Hatze (1981), respectively.

The force generated by the PEE is a function only of its length, and has been modelled considering an exponential relationship (Kaufman et al. 1991; Lee and Rim 1990).

The scalability of the muscular action is achieved by scaling the PCSA of the muscles with respect to the product of the hand length and hand breadth parameters (Sancho-Bru et al. 2008) from its value for a reference hand size:

$$\frac{PCSA(HL, HB)}{PCSA(\overline{HL}, \overline{HB})} = 1 + 0.013 \cdot (HL \cdot HB - \overline{HL} \cdot \overline{HB}) \quad (4)$$

The muscles considered on each skeletal chain are listed in Table 1. PCSA data for index finger muscles have been taken from Valero-Cuevas et al. (1998); data for the remaining muscles have been obtained from Brand and Hollister (1992). The muscle stress limit (S_{max}) has been obtained from Zajac (1989). The remaining required parameters to establish the force-length and force-velocity relationships have been obtained from Lee and Rim (1990), Lemay and Crago (1996), Jacobson et al. (1992) and Kaufman et al. (1991).

---- Insert Table 1----

Most of the muscles do not act directly on the bones, but through the force transmitted to the tendons. To model the tendon action crossing the joints, straight lines connecting 2 points have been considered, one fixed with respect to the proximal bone and the other one with respect to the distal bone (Fig. 3a). This approximation has been found to be close enough to the behaviour of all tendons with the exception of extensors (An et al. 1979), for which Landsmeer's model I has been considered (Fig. 3b).

---- Insert Fig. 3 ----

The extensor hood mechanisms of the fingers are modelled as a deformable tendon net (Sancho-Bru et al. 2003b), in which the appropriate force balances have been considered.

The data for the points defining the tendon paths have been obtained from An et al. (1979), and have been also scaled with respect to HB and HL (Sancho-Bru et al. 2003b).

2.1.2 Grasping posture generation

In order to generate grasp postures automatically, we used a grasping algorithm based on that of Choi (2008). This algorithm uses a function to automatically generate a natural grasping motion path of the hand model from a fully opened state to a clenched one. The goal is to find contacts between the surface hand skin and the object surface while rotating the joint angles of the fingers. Care has to be taken to properly choose the rotation rate of the finger joints, as it affects the final posture prediction. Based on the results from Choi (2008), we have used a variable rotation algorithm, by describing the rotations of all joints at observation-based rates. The rotation rate is defined by the difference between the measured angles of the most fully opened state and the tentative clenched one.

In order to generate the grasp, a contact model is required. We need to check whether the surface skin model makes contact with the surface of the object model. In reality, the surface of a hand is deformed when making contact with the object. Generally, this deformation has a non-linear elastic behaviour, and it could be simulated using finite element analyses. Nonetheless, this would need a long execution time that we considered unacceptable. Therefore, we considered a simple geometric collision-detection algorithm based on the one used by Endo et al. (2007). The algorithm allows the penetration of the surface skin model and the object model. This penetration is limited by a tolerance that relates to the hand stiffness at each contact region. At this first approximation to the grasp problem, we considered only grasps involving contact at the fingertips. A maximum penetration of 3 mm has been considered for all fingertips.

The distances between the points on the skin surface and the object are calculated while each joint rotate according to the specific joint rotation algorithm. When the distance between the skin surface points and the object reaches the given maximum penetration tolerance, the contact is achieved and the joint rotation ends. When the distal segments of all four fingers make contact with the object, the grasping simulation terminates.

In order to perform these calculations in an efficient way, the geometry of the hand surface and the grasped object have been modelled using the spherical extension of polytopes (s-topes). This graphical representation has been successfully used previously in robotics (Bernabeu and Tornero 2002), allowing a fast and efficient collision detection between the grasping hand and the grasped object while showing a sufficient level of realism (Fig. 4). The collision detection is performed by calculating the minimum distance between s-topes, based on the Gilbert-Johnson-Keerthi algorithm

(Gilbert et al. 1988). The algorithm also calculates the minimum distance points that define the normal direction to the contact surface.

---- Insert Fig. 4 ----

2.1.3 Soft contact model

The contact forces between the object and the hand have to be considered when dealing with the estimation of the muscle forces required for grasping an object. Unlike what happens with robots, real human fingers conform to the grasped object shape. As the contact finger surface is deformable, the contact does not occur at just one point but over some finite area that increases as the normal forces increase. Due to this effect, in addition to the normal force and tangential force due to friction, human finger contact may support frictional torsional moments with respect to the normal at the contact point. This clearly shows that the consideration of rigid contacts, commonly used in robotics, is not appropriate for its use in studying the human grasp, and a soft contact model has to be used. Most objects manipulated by human hands are much stiffer than human hands and, therefore, it is reasonable for those cases to consider the grasped objects as rigid bodies and the hand as a deformable body.

In this case, a soft contact model based on that of (Ciocarlie et al. 2005) has been used. Friction constraints are derived based on general expressions for non-planar contacts of elastic bodies, taking into account the local geometry and structure of the objects in contact. The following approximation has been used to express the constraint relating the magnitudes of frictional force (f_t) and moment (τ_n):

$$f_t^2 + \frac{\tau_n^{\ 2}}{e_n^{\ 2}} \le \mu^2 \cdot P^2 , \tag{8}$$

where P is the total load applied in the direction of the contact normal, μ is the friction coefficient and e_n is called the eccentricity parameter (height of the ellipsoid described by Eq. 8). Considering a Winkler elastic foundation (Johnson 1985) of depth h and elastic modulus K, the eccentricity parameter is given by:

$$e_n = \frac{8}{15} \cdot \sqrt{a \cdot b}\,, \qquad (9)$$

where a and b can be calculated from the relative radii of curvature R' and R'' of the objects in contact and the compression δ of the elastic layer:

$$a = \sqrt{2 \cdot \delta \cdot R'};\, b = \sqrt{2 \cdot \delta \cdot R''};\, \delta = \sqrt{\frac{P \cdot h}{K \cdot \pi \cdot \left(R' \cdot R''\right)^{1/2}}}\,, \qquad (10)$$

The values of μ and K have been obtained from Savescu et al. 2008) and Hajian and Howe (1997), respectively.

2.1.4 Problem solving and neuromuscular control

The problem to be solved is to find the muscle forces required to grasp the object. That entails to account for the equilibrium of the grasping hand and the grasped object. It is an inverse dynamics problem.

The dynamics equations of the open chain of rigid bodies have been derived using the Lagrange method (García de Jalón and Bayo 1994). For a system with m generalised co-ordinates q_k, this equation is expressed as:

$$\frac{d}{dt}\frac{\partial L}{\partial \dot{q}_k} - \frac{\partial L}{\partial q_k} = Q_k^{nc} \quad k = 1, \ldots, m\,, \qquad (5)$$

where L is the Lagrangian function and Q_k^{nc} are the generalised non-conservative forces. The generalised coordinates have been considered coincident with the system DOF (m=23).

Eq. 5 together with the force balances of the tendon nets make up the equilibrium equations of the grasping hand (49 equations). The equilibrium of the grasped object is defined by six more equations. A total of 55 equations with 99 unknowns (muscle and tendon forces and contact forces and moments) form the final grasping mathematical problem, along with the inequalities given by the muscle model (lower and upper bounds of muscle forces and lower bounds of tendon forces) and the soft contact model (one inequality by contact point). There is not a unique combination of muscular efforts that satisfy the equilibrium constraints. To solve the problem, a criterion chosen by the central nervous system to determine the muscle action control must be introduced.

The most commonly used criterion in the literature is the maximisation of the endurance (Crowninshield and Brand 1981), through the minimisation of the non-linear objective function

$$OBJ = \sum \left(\frac{F_i}{PCSA_i} \right)^n , \qquad (6)$$

with n between 2.0 and 4.0 (being 2.0 the most used). The validity of this criterion for the grasping simulation will be checked in this work.

The MATLAB system and its optimisation toolbox (version R2008b) have been used to implement the model.

2.2 Validation experiment

The validity of the model was analysed through the simulation of grasping cylindrical objects. An experiment was designed in which a female subject (age 32, height 1.61 m, weight 68 kg, HB 71 mm, HL 163 mm), appropriately instrumented, was asked to grasp alternatively two cylinders of different size and weight and hold them with their axes in vertical orientation (gravity direction).

The subject was seated at a table which height was adjusted so that the subject's elbow coincided with the table height. The subject's arm was lying on the table in a relaxed posture, with the hand placed about 15 cm away from the cylinder to be grasped. The subject was asked to grasp each cylinder with her fingertips and hold it at a fixed height while keeping it in vertical orientation, during two to three seconds approximately, and then return it to its initial location.

First, the subject's hand was instrumented with the Cyberglove ® system (Cyberglove, Immersion Corp.) to register hand posture data. The system was appropriately calibrated (Mora et al. 2011). The subject repeated the action three times for training without data registration, and five more times with posture data registration (Fig. 5, left). Second, subject's hand was instrumented with the Finger TPS ® system (Pressure Profile Systems, Inc) at her fingertips to register finger force data. After the calibration of the system was performed, the subject repeated the action three times for training without data registration, and five more times with force data registration (Fig. 5, right).

---- Insert Fig. 5 ----

This procedure was performed twice: first for a cylinder of 0.401 kg of weight and 64 mm of diameter (cylinder 1) and second for a cylinder of 0.04 kg of weight and 82 mm of diameter (cylinder 2).

The model was used to simulate the grasping of both cylinders. The simulation only considered the static case of holding the cylinders at a fixed height. To perform the simulation, the subject's hand data (HL and HB) and the object data (weight and diameter) are input to the model, along with the most open posture of the hand and the final grasping posture registered with the Cyberglove ®. These postures are required by the model to generate the rotation angle rates that are used to obtain the predicted final grasping posture (which had to be obviously similar to the one measured, but not identical) from the use of the collision detection algorithm.

The results of the simulation of grasping both cylinders were the grasping postures, the contact points, the contact normal directions, the contact finger forces and moments, and the muscle force distribution. The normal finger forces estimated by the model were compared to the ones registered with the Finger TPS ® system.

3. Results and discussion

The hand movement pattern during the experiment can be observed in figures 6 and 7. These figures show the joint angles registered by the Cyberglove ® system in one of the repetitions for cylinders 1 and 2, respectively. The hand starts from a relaxed posture. Just before grasping the cylinder, the hand gets open, which is seen mainly as an extension and abduction of MCP joints. The grasping is then achieved basically by means of the flexion of the different joints. Once the object is grasped, the joint angles registered during the static hold of the cylinders remain quite constant.

---- Insert Figs. 6 and 7 ----

For each cylinder, the model needs the hand most fully-open posture and the hand grasping posture (as tentative) to calculate the joint rotation rates. The most fully-open postures (Tables 2 and 3) were obtained as the mean of the most open postures identified at each of the repetitions, being the standard deviation of the joint angles lower than 8.5 degrees. For each repetition, the mean postures during the static hold of the cylinder were also obtained. The mean of these values for each cylinder was used to define the tentative grasping posture required to calculate the joint rotation rates (Tables 4 and 5). Again, the standard deviation of the joint angles among repetitions was lower than 8.5 degrees, which indicates that the experiment was repeatable. This makes it possible to interrelate the posture data and the force data registered in different repetitions.

---- Insert Tables. 2, 3, 4 and 5 ----

Tables 6 and 7 present the joint angles calculated by the model (from the use of the collision detection algorithm) for the grasping postures of cylinders 1 and 2, respectively. They are similar to the ones measured, but not identical. In the future, it is the aim of the authors that both input postures required by the model to generate this grasping posture will be obtained by using a neuronal net (Kyota and others 2005; Rezzoug and Gorce 2008). Figure 8 shows the realistic appearance of the estimated grasping posture for cylinder 1.

---- Insert Tables. 6 and 7 ----

---- Insert Fig. 8 ----

The finger force patterns registered during the experiment can be observed in figures 9 and 10. These figures show the forces registered by the Finger TPS ® system in one of the repetitions for cylinders 1 and 2, respectively. Due to the greater weight of cylinder 1, it is observed a peak in the finger forces during the cylinder elevation phase corresponding to inertial effects, which is not observed for the case of cylinder 2. Finger forces registered during the static hold of the cylinders remain quite constant. For each repetition, the mean of the finger force registered during the static hold has been considered. The mean of the finger forces among repetitions for both cylinders are shown in table 8. Contributions of the thumb and fingers to the grasp force are presented in table 9 normalised to thumb force, where it can be observed that the thumb is the major contributor.

---- Insert Figs. 9 and 10 ----

---- Insert Tables 8 and 9 ----

Table 10 present the contact forces and torques estimated by the model when the minimisation of the sum of the squared muscle stresses is considered to solve the indeterminate problem. The disagreement between the experimentally measured normal forces and the estimated ones is evident. On the one hand, the estimated values are lower than the experimental ones. On the other hand, the estimated grasping force distributions among fingers do not match the ones measured experimentally. The model predicts that some fingers do not contribute at all to the grasp, which does not match the real behaviour of the human hand.

---- Insert Table 10 ----

One of the factors that could be responsible for the low level of the forces estimated by the model is the friction coefficient between the hand and the cylinder. A smaller friction coefficient will demand greater normal forces to assure the grasp stability. Using the data reported by Savescu et al. (2008), in this work we have used a friction coefficient of 0.8. The results of changing this coefficient to the very low value of 0.3 are shown in table 11. Although the model estimates greater normal forces, the disagreement in the force contributions of the fingers remains. Furthermore, the level of the estimated normal forces for grasping the lighter cylinder is still far from the registered.

---- Insert Table 11 ----

The results from the simulations seem to indicate that it is mathematically feasible to grasp the cylinders without the contribution of some fingers. And even that this fact could be more efficient in some aspects. But the experimental results indicate that the CNS (central nervous system) chooses a more even distribution of the forces between fingers. Trying to account for this coordination mechanism, we have repeated the simulations but adding to the objective function to be minimised a term accounting for the differences between the finger forces:

$$OBJ = \sum \left(\frac{F_i}{PCSA_i} \right)^n + 100^2 \sum \left(F_{n_i} - F_{n_j} \right)^2 \Big|_{i \neq j}, \qquad (7)$$

where F_{n_i} is the normal component of the contact force developed by finger *i*. The results from these simulations are presented in table 12. The use of this function allows achieving more balanced force estimations, but the magnitudes of the estimated forces are still lower than the experimental ones. The use of this objective function and the reduction of the friction coefficient to 0.3 (results not shown for brevity) provided a quite close estimation of forces for the heaviest cylinder, but the magnitudes of the estimated forces for the lightest cylinder were still too small compared to the experimental results.

---- Insert Table 12 ----

All these results seem to point out that the criterion that the CNS uses to select the grasping force distribution among fingers is not only related to some energetic minimisation, as the experimental forces registered are much bigger than those theoretically required to perform the grasp. The key must lie in any other factor. In robotics, the selection of the grasp to be executed by the robotic hand is performed by calculating different kinds of grasp quality measures. Many different quality measure definitions can be found in the robotics literature. Most of them are related to the capability of handling the object once grasped or the ability of the grasp to resist external disturbances (stability). This knowledge might be used also for studying the human grasp. For the experiment simulated in this work, it might make sense that the CNS would be requiring certain level of stability to the cylinder being grasped, given that the subject was asked to hold it still during some seconds.

Most of the robotic quality measures that evaluate the stability of the grasps are geometrical measures that only take into account the contact points and the directions of the normal contact forces. These measures do not account for the magnitudes of the forces and would not be useful for defining the objective function in the case under study. Obviously, the sum of the components of the applied forces that are normal to the object boundary is indicative of the force efficiency in the grasp. Then, a quality measure can be defined as the inverse of the sum of the magnitudes of the normal components of the applied forces required to balance an expected demanding wrench (Liu and others 2004). The index must be minimised to get an optimum grasp.

The results of minimising that function that looks for a more stable grasp, are shown in table 13. The magnitudes of the forces estimated by the model with this assumption are much closer to the experimental ones than with any other of the previous objective functions, even for the lighter cylinder. These results confirm that, for the experiment being simulated, the CNS is trying to ensure the stability of the grasped cylinder. Although the results do not match exactly the experimental measurements, they adjust better than any other of the previously considered scenarios.

---- Insert Table 13 ----

Anyway, the criterion selected by the CNS in each case should probably be a function of the task to be performed. The objective function that has provided good results in these simulations may not provide so good results under other requirements. For example, if the subject were asked to grasp a cylindrical bottle to pour water. In that case, the grasp should allow certain level of manipulability that will be in conflict with the stability. More research is needed in this matter. Anyway, what seems clear is that the popular objective function sum of the squared muscle stresses, is not suitable for grasping simulation using biomechanical models of the hand, or that it should be at least complemented by task dependent grasp quality measures (manipulability or stability).

4. Conclusions

The extension of a previously validated biomechanical model of the hand to study the human grasp has been presented. The geometrical representation of the hand segments and the grasped object as a spherical extension of polytopes (s-topes) has shown a sufficient level of realism and a fast and efficient collision detection.

Realistic grasping postures have been obtained through the use of the grasping algorithm implemented in the model. However, the generation of the natural grasping motion path of the hand from a fully opened state to a clenched one required the calculation of rotation rates at each joint from two experimentally registered postures (the most fully opened posture and the clenched posture). To avoid these experimental input data, more research is required in the future to develop a neural net able to obtain both input postures required by the model.

Using the contact information provided by the grasping algorithm, the equilibrium of the grasped object has been added to the model through the consideration of a simple soft contact model that considers the frictional moment at each contact zone. That has leaded to an indeterminate problem that has been solved by minimising different objective functions. The model underestimated the normal contact forces when the criterion of minimising the sum of the squared muscle stresses was used. Furthermore, according to the model predictions, it is mathematically feasible to grasp the cylinders without the contribution of some fingers, and this is more efficient in some aspects. But it is not the real behaviour of the human hand that was experimentally observed.

For the simulated experiment, best results were obtained when the indeterminate problem was solved using a robotic grasp quality measure as objective function that tried to ensure the stability of the grasped cylinder. Although this function has provided good results in these simulations, it may fail for others entailing certain level of manipulability, as the criterion selected by the CNS in each case will be probably a function of the task to be performed. Further research on the application of other robotics grasp quality measures for different tasks involving different levels of stability and manipulability is needed.

Finally, the model presented in this work has been used to study only grasps of cylinders with the fingertips. More complex grasps, involving more contact zones and more complex object geometries should be investigated in the future.

5. Aknowledgements

We are grateful for the financial support of the Fundació Caixa-Castelló and the Universitat Jaume I throughout the project P1-1B2009-40; of the Spanish Research and Innovation Ministry, and the EU (FEDER funds) throughout the project DPI2010-18177; and of European Community's Seventh Framework Programme through the project GRASP, IST-FP7-IP-215821. This research is related to these three projects.

6. Nomenclature

3D	Three-dimensional
ADD	Adductor pollicis
ADQ	Abductor digiti quinti
APB	Abductor pollicis brevis
APL	Abductor pollicis longus
CE	Contractile element

CMC	Carpometacarpal
CNS	Central nervous system
DI	Dorsal interosseous
DIP	Distal interphalangeal
DOF	Degrees of freedom
EDC	Extensor digitorum communis
EDQ	Extensor digiti quinti
EI	Extensor indicis
EPB	Extensor pollicis brevis
EPL	Extensor pollicis longus
FDQ	Flexor digiti quinti
FP	Flexor profundus
FPB	Flexor pollicis brevis
FPL	Flexor pollicis longus
FS	Flexor superficialis
HB	Hand breadth
HL	Hand length
IP	Interphalangeal
LU	Lumbrical
MCP	Metacarpophalangeal
OPP	Opponens pollicis
PCSA	Physiological cross-sectional area
PEE	Parallel elastic element
PIP	Proximal interphalangeal
SEE	Series elastic element
VI	Volar interosseous

7. References

An KN, Chao EYS, Kaufman KR. 1991. Basic orthopaedics biomechanics. New York: Raven Press. Ltd. Analysis of muscle and joint loads; p.1-50.

An K, Chao E, Cooney W, Linscheid R. 1979. Normative model of human hand for biomechanical analysis. J Biomech 12(10):775-788.

Bernabeu E, Tornero J. 2002. Hough transform for distance computation and collision avoidance. IEEE Trans Rob Autom 18(3):393-398.

Biryukova EV, Yourovskaya VZ. 1994. Advances in the biomechanics of the hand and wrist. New York: Plenum Press. A model of human hand dynamics; p. 107-122.

Brand PW, Hollister AM. 1992. Clinical mechanics of the hand. Third ed. St. Louis: Elsevier Science Health Science div.

Buchholz B, Armstrong T, Goldstein S. 1992. Anthropometric data for describing the kinematics of the human hand. Ergonomics 35(3):261-273.

Buchner H, Hines M, Hemami H. 1988. A dynamic-model for finger interphalangeal coordination. J Biomech 21(6):459-468.

Casolo F, Lorenzi V. 1994. Advances in the biomechanics of the hand and wrist. New York: Plenum Press. Finger mathematical modelling and rehabilitation; p. 197-223.

Chao EY, An KN. 1978. Determination of internal forces in human hand. ASCE J Eng Mech Div 104(1):255-272.

Chao EY, Opgrande JD, Axmear FE. 1976. Three dimensional force analysis of finger joints in selected isometric hand functions. J Biomech 9(6):387.

Choi J. 2008. Developing a 3-dimensional kinematic model of the hand for ergonomic analyses of hand posture, hand space envelope, and tendon excursion. University of Michigan.

Ciocarlie M, Lackner C, Allen P. 2007. Soft finger model with adaptive contact geometry for grasping and manipulation tasks. Paper presented at: World Haptics 2007. Second Joint EuroHaptics Conference, 2007 and Symposium on Haptic Interfaces for Virtual Environment and Teleoperator Systems.

Ciocarlie M, Miller A, Allen P. 2005. Grasp analysis using deformable fingers. Paper presented at: IEEE/RSJ International Conference on Intelligent Robots and Systems.

Crowninshield R, Brand R. 1981. A physiologically based criterion of muscle force prediction in locomotion. J Biomech 14(11):793-801.

Endo Y, Kanai S, Kishinami T, Miyata N, Kouchi M, Mochimaru M. 2007. Virtual grasping assessment using 3D digital hand model. Presented at: 10th Annual Applied Ergonomics Conference: Celebrating the Past - Shaping the Future.

Esteki A, Mansour JM. 1997. A dynamic model of the hand with application in functional neuromuscular stimulation. Ann Biomed Eng 25(3):440-51.

Fok KS, Chou SM. 2010. Development of a finger biomechanical model and its considerations. J Biomech 43(4):701-13.

García de Jalón J, Bayo E. 1994. Kinematic and dynamic simulation of multibody systems. New York: Springer-Verlag.

Gilbert E, Johnson D, Keerthi S. 1988. A fast procedure for computing the distance between complex objects in 3-dimensional space. IEEE J Robotic Autom 4(2):193-203.

Giurintano D, Hollister A, Buford W, Thompson D, Myers L. 1995. A virtual 5-link model of the thumb. Med Eng Phys 17(4):297-303.

Goldstein S, Armstrong T, Chaffin D, Matthews L. 1987. Analysis of cumulative strain in tendons and tendon sheaths. J Biomech 20(1):1-6.

Hajian A, Howe R. 1997. Identification of the mechanical impedance at the human finger tip. J Biomech Eng-T ASME 119(1):109-114.

Hatze H. 1981. Myocibernetic control models of skeletal muscle. Pretoria: University of South Africa.

Hill A. 1938. The heat of shortening and the dynamic constants of muscle. Proceedings of the Royal Society of London Series B-Biological Sciences 126(843):136-95.

Hollister A, Giurintano D, Buford W, Myers L, Novick A. 1995. The axes of rotation of the thumb interphalangeal and metacarpophalangeal joints. Clin Orthop (320):188-93.

Howe R, Kao I, Cutkosky M. 1988. Sliding of robot fingers under combined tornsion and shear loading. Presented at: IEEE Int. Conf. on Robotics and Automation.

Howe R, Cutkosky M. 1996. Practical force-motion models for sliding manipulation. Int J Robotics Res 15(6):557-72.

Jacobson M, Raab R, Fazeli B, Abrams R, Botte M, Lieber R. 1992. Architectural design of the human intrinsic hand muscles. J Hand Surg-Am Volume 17A(5):804-9.

Johnson KL. 1985. Contact mechanics. Cambridge University Press.

Kamper D, Fischer H, Cruz E. 2006. Impact of finger posture on mapping from muscle activation to joint torque. Clin Biomech 21(4):361-9.

Kao I, Linch K, Burdick JW. 2008. Springer-Verlag. Handbook of robotics. Chapter 27, Contact modeling and manipulation; p. 647-668

Kao I, Yang F. 2004. Stiffness and contact mechanics for soft fingers in grasping and manipulation. IEEE Trans Rob Autom 20(1):132-5.

Kao I, Cutkosky M. 1992. Quasi-static manipulation with compliance and sliding. Int J Robotics Res 11(1):20-40.

Kapandji AI. 1998. Fisiologie articulaire. membre supérieur. Paris: Editions Maloine.

Kaufman K, An K, Litchy W, Chao E. 1991. Physiological prediction of muscle forces .1. theoretical formulation. Neuroscience 40(3):781-92.

Kurita Y, Onoue T, Ikeda A, Ogasawara T. 2009. Biomechanical analysis of subjective pinching effort based on tendon-skeletal model. Conf Proc IEEE Eng Med Biol Soc. 2009; p. 5231-5234.

Kyota F, Watabe T, Saito S, Nakajima M. 2005. Detection and evaluation of grasping positions for autonomous agents. Presented at: International Conference on Cyberworlds, 2005; Singapore.

Lee JW, Rim K. 1990. Maximum finger force prediction using a planar simulation of the middle finger. Proc Inst Mech Eng Part H J Eng Med 204:169-78.

Lee SW, Chen H, Towles JD, Kamper DG. 2008a. Effect of finger posture on the tendon force distribution within the finger extensor mechanism. J Biomech Eng-T ASME 130(5):051014.

Lee SW, Chen H, Towles JD, Kamper DG. 2008b. Estimation of the effective static moment arms of the tendons in the index finger extensor mechanism. J Biomech 41(7):1567-73.

Leijnse J And Kalker J. 1995. A 2-dimensional kinematic model of the lumbrical in the human finger. J Biomech 28(3):237-49.

Leijnse J, Bonte J, Landsmeer J, Kalker J, Vandermeulen J, Snijders C. 1992. Biomechanics of the finger with anatomical restrictions - the significance for the exercising hand of the musician. J Biomech 25(11):1253-64.

Lemay M, Crago P. 1996. A dynamic model for simulating movements of the elbow, forearm, and wrist. J Biomech 29(10):1319-30.

Liu G, Xu J, Wang X, Li Z. 2004. On quality functions for grasp synthesis, fixture planning, and coordinated manipulation. IEEE Trans. Autom. Sci. Eng. 1(2):146-62.

Mansour JM, Rouvas C, Sarangapani J, Hendrix L, Crago PE. 1994. Advances in the biomechanics of the hand and wrist. New York: Plenum Press. Quantitative functional anatomy of finger muscles: Application to controlled grasp; p. 177-188.

Mora MC., Sancho-Bru JL, Iserte JL, Pérez-González A, Porcar-Bonet B. 2011. Protocolo de calibración para guante instrumentado en la caracterización cinemática del agarre humano. Presented at: X Congreso Iberoamericano de Ingeniería Mecánica; Porto, Portugal.

Qiu D, Fischer HC, Kamper DG. 2009. Muscle activation patterns during force generation of the index finger. Conf Proc IEEE Eng Med Biol Soc. 2009; p. 3987-3990.

Rezzoug N, Gorce P. 2008. Prediction of fingers posture using artificial neural networks. J Biomech 41(12):2743-9.

Roa Garzón M. 2009. Grasp planning methodology for 3D arbitrary shaped objects. Universitat Politècnica de Catalunya.

Roloff I, Schoffl V, Vigouroux L, Quaine F. 2006. Biomechanical model for the determination of the forces acting on the finger pulley system. J Biomech 39(5):915-23.

Sancho-Bru JL, Giurintano DJ, Pérez-González A, Vergara M. 2003a. Optimum tool handle diameter for a cylinder grip. J Hand Ther 16(4):337-42.

Sancho-Bru JL, Perez-Gonzalez A, Vergara M, Giurintano DJ. 2003b. A 3D biomechanical model of the hand for power grip. J Biomech Eng 125(1):78-83.

Sancho-Bru JL, Perez-Gonzalez A, Vergara-Monedero M, Giurintano D. 2001. A 3-D dynamic model of human finger for studying free movements. J Biomech 34(11):1491-500.

Sancho-Bru JL, Vergara M, Rodriguez-Cervantes P, Giurintano DJ, Perez-Gonzalez A. 2008. Scalability of the muscular action in a parametric 3D model of the index finger RID E-6162-2010 RID C-8708-2011. Ann Biomed Eng 36(1):102-7.

Savescu AV, Latash ML, Zatsiorsky VM. 2008. A technique to determine friction at the fingertips. J Appl Biomech 24(1):43-50.

Smith E, Pearson J, Juvinall R, Bender L. 1964. Role of finger flexors in rheumatoid deformities of metacarpophalangeal joints. Arthritis Rheum 7(5P1):467-480.

Spoor C. 1983. Balancing a force on the fingertip of a two-dimensional finger model without intrinsic muscles. J Biomech 16(7):497-504.

Spoor C, Landsmeer J. 1976. Analysis of zigzag movement of human finger under influence of extensor digitorum tendon and deep flexor tendon. J Biomech 9(9):561-6.

Storace A, Wolf B. 1982. Kinematic analysis of the role of the finger tendons. J Biomech 15(5):391-3.

Storace A, Wolf B. 1979. Functional-analysis of the role of the finger tendons. J Biomech 12(8):575-8.

Thomas DH, Long C, Landsmeer JMF. 1968. Biomechanical consideration of lumbricalis behaviour in the human finger. J Biomech 1:107-15.

Valero-Cuevas FJ, Zajac FE, Burgar CG. 1998. Large index-fingertip forces are produced by subject-independent patterns of muscle excitation. J Biomech 31(8):693-703.

Valero-Cuevas F. 2005. An integrative approach to the biomechanical function and neuromuscular control of the fingers. J Biomech 38(4):673-84.

Valero-Cuevas F. 2000. Predictive modulation of muscle coordination pattern magnitude scales fingertip force magnitude over the voluntary range. J Neurophysiol 83(3):1469-79.

Valero-Cuevas F, Towles J, Hentz V. 2000. Quantification of fingertip force reduction in the forefinger following simulated paralysis of extensor and intrinsic muscles. J Biomech 33(12):1601-9.

Vigouroux L, Quaine F, Labarre-Vila A, Moutet F. 2006. Estimation of finger muscle tendon tensions and pulley forces during specific sport-climbing grip techniques. J Biomech 39(14):2583-92.

Weightman B, Amis A. 1982. Finger joint force predictions related to design of joint replacements. J Biomed Eng 4(3):197-205.

Wu JZ, An K, Cutlip RG, Dong RG. 2010. A practical biomechanical model of the index finger simulating the kinematics of the muscle/tendon excursions. Biomed Mater Eng 20(2):89-97.

Zajac F. 1989. Muscle and tendon - properties, models, scaling, and application to biomechanics and motor control. Crit Rev Biomed Eng 17(4):359-411.

Table 1. Muscles modelled on each skeletal chain (acronyms in the nomenclature section)

Index	Medial	Ring	Little	Thumb
1^{st} FP	2^{nd} FP	3^{rd} FP	4^{th} FP	APB
1^{st} FS	2^{nd} FS	3^{rd} FS	4^{th} FS	FPB
1^{st} EDC+EI	2^{nd} EDC	3^{rd} EDC	EDQ	OPP
1^{st} LU	2^{nd} LU	3^{rd} LU	4^{th} LU	ADD
1^{st} DI	2^{nd} DI	4^{th} DI	3^{rd} VI	1^{st} DI
1^{st} VI	3^{rd} DI	2^{nd} VI	FDQ	APL
			ADQ	EPB
				FPL
				EPL

Table 2. Joint angles defining the most open posture for grasping cylinder 1

	MCC		MCP		PIP	DIP
	Flexion (º)	Abduction (º)	Flexion (º)	Abduction (º)	Flexion (º)	Flexion (º)
Thumb	-8.0	49.0	25.1	0.0	19.1	-
Index	-	-	10.2	8.9	37.6	18.8
Medial	-	-	10.2	0.0	37.6	18.8
Ring	0.0	-	6.2	9.8	22.8	11.4
Little	0.0	-	2.1	17.7	9.4	4.7

Table 3. Joint angles defining the most open posture for grasping cylinder 2

	MCC		MCP		PIP	DIP
	Flexion (º)	Abduction (º)	Flexion (º)	Abduction (º)	Flexion (º)	Flexion (º)
Thumb	-10.0	50.0	23.9	0.0	17.6	-
Index	-	-	2.4	10.0	38.1	19.0
Medial	-	-	2.4	0.0	38.1	19.0
Ring	0.0	-	1.6	11.6	24.2	12.1
Little	0.0	-	0.9	19.5	11.7	5.8

Table 4. Joint angles defining the mean grasping posture for cylinder 1

	MCC		MCP		PIP	DIP
	Flexion (º)	Abduction (º)	Flexion (º)	Abduction (º)	Flexion (º)	Flexion (º)
Thumb	1.0	47.5	20.9	0.0	49.7	-
Index	-	-	26.2	-2.1	48.3	24.1
Medial	-	-	26.2	0.0	48.3	24.1
Ring	4.0	-	19.5	7.1	35.6	17.8
Little	8.0	-	12.8	13.6	31.4	15.7

Table 5. Joint angles defining the mean grasping posture for cylinder 2

	MCC		MCP		PIP	DIP
	Flexion (º)	Abduction (º)	Flexion (º)	Abduction (º)	Flexion (º)	Flexion (º)
Thumb	0.0	50.8	20.9	0.0	35.5	-
Index	-	-	9.4	9.7	46.7	23.4
Medial	-	-	9.4	0.0	46.7	23.4
Ring	4.0	-	7.6	9.1	33.6	16.8
Little	8.0	-	5.8	19.2	28.0	14.0

Table 6. Grasping posture estimated by the model for cylinder 1

	MCC		MCP		PIP	DIP
	Flexion (º)	Abduction (º)	Flexion (º)	Abduction (º)	Flexion (º)	Flexion (º)
Thumb	0.3	47.7	21.2	0.0	47.3	-
Index	-	-	20.4	1.9	44.4	18.8
Medial	-	-	23.0	0.0	46.1	27.4
Ring	4.2	-	20.0	7.0	36.2	43.9
Little	8.5	-	13.5	13.4	32.8	7.8

Table 7. Grasping posture estimated by the model for cylinder 2

	MCC		MCP		PIP	DIP
	Flexion (º)	Abduction (º)	Flexion (º)	Abduction (º)	Flexion (º)	Flexion (º)
Thumb	-3.0	50.5	21.8	0.0	30.2	-
Index	-	-	9.7	9.7	47.1	23.5
Medial	-	-	12.9	0.0	51.1	25.5
Ring	6.7	-	11.6	7.4	40.0	20.0
Little	7.8	-	5.7	19.2	27.6	13.8

Table 8. Mean finger forces (N) registered for the grasping of both cylinders

	Thumb (N)	Index (N)	Medial (N)	Ring (N)	Little (N)
Cylinder 1	10.7	3.4	4.6	5.8	4.1
Cylinder 2	11.0	9.3	3.0	2.9	1.7

Table 9. Mean finger force contribution (%) observed during the grasping of both cylinders

	Thumb (%)	Index (%)	Medial (%)	Ring (%)	Little (%)
Cylinder 1	100	32	44	55	38
Cylinder 2	100	85	27	26	15

Table 10. Contact finger forces and moments estimated by the model minimising the sum of the squared muscle forces ($\mu = 0.8$)

		Thumb	Index	Medial	Ring	Little
Cylinder 1	Normal (N)	4.05	0.01	1.97	0.96	0.60
	Tangential (N)	3.23	0.01	1.57	0.76	0.48
	Torque (N·mm)	-4.70	0.00	-1.40	-0.60	-0.30
Cylinder 2	Normal (N)	0.41	0.00	0.24	0.11	0.01
	Tangential (N)	0.30	0.01	0.19	0.09	0.01
	Torque (N·mm)	1.00	0.00	-0.10	0.00	0.00

Table 11. Contact finger forces and moments estimated by the model minimising the sum of the squared muscle forces, and reducing the friction coefficient ($\mu = 0.3$)

		Thumb	Index	Medial	Ring	Little
Cylinder 1	Normal (N)	10.59	2.96	1.98	2.54	3.12
	Tangential (N)	3.18	0.89	0.59	0.76	0.94
	Torque (N·mm)	0.00	0.10	-0.30	-0.50	-0.70
Cylinder 2	Normal (N)	0.98	0.18	0.53	0.00	0.26
	Tangential (N)	0.29	0.05	0.16	0.00	0.08
	Torque (N·mm)	-0.10	0.00	0.00	0.00	0.00

Table 12. Contact finger forces and moments estimated by the model when adding a term to the objective function related to the differences among finger forces ($\mu = 0.8$)

		Thumb	Index	Medial	Ring	Little
Cylinder 1	Normal (N)	3.81	0.91	0.92	0.92	0.92
	Tangential (N)	3.02	0.73	0.72	0.71	0.73
	Torque (N·mm)	-5.80	0.10	-1.10	-1.70	0.00
Cylinder 2	Normal (N)	0.45	0.12	0.11	0.11	0.11
	Tangential (N)	0.35	0.09	0.09	0.07	0.09
	Torque (N·mm)	-0.60	0.00	0.10	0.30	0.00

Table 13. Contact finger forces and moments estimated by the model when using the robotics stability optimisation ($\mu = 0.8$)

		Thumb	Index	Medial	Ring	Little
Cylinder 1	Normal (N)	6.62	2.12	1.64	1.47	2.12
	Tangential (N)	3.15	1.68	1.27	0.95	1.69
	Torque (N·mm)	-25.20	3.00	-3.80	-7.60	1.20
Cylinder 2	Normal (N)	4.98	1.79	1.32	0.48	1.56
	Tangential (N)	0.36	0.20	0.30	0.38	0.70
	Torque (N·mm)	-36.50	16.20	-10.90	0.90	-8.70

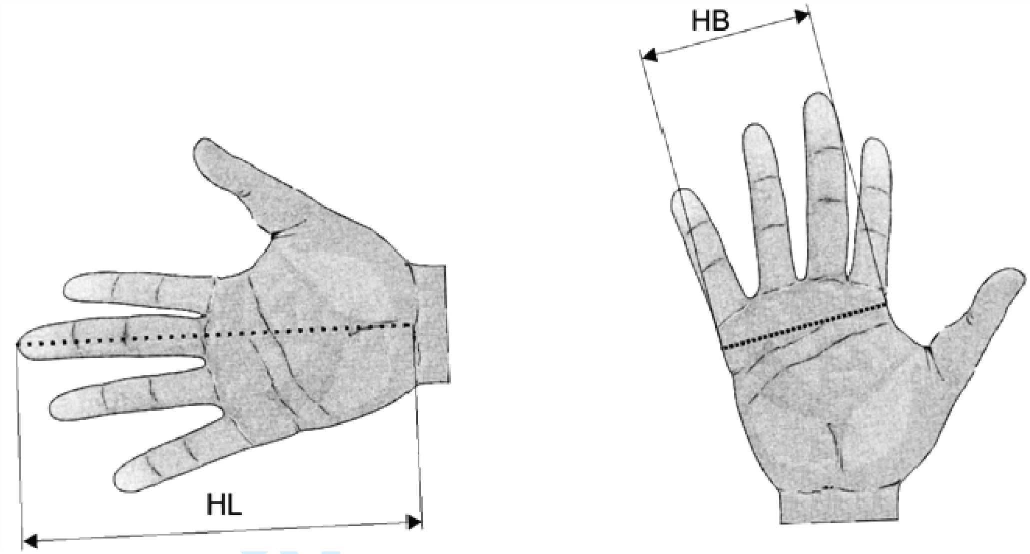

Figure 1: Parameters used to scale the model: HL (hand length) and HB (hand breadth)

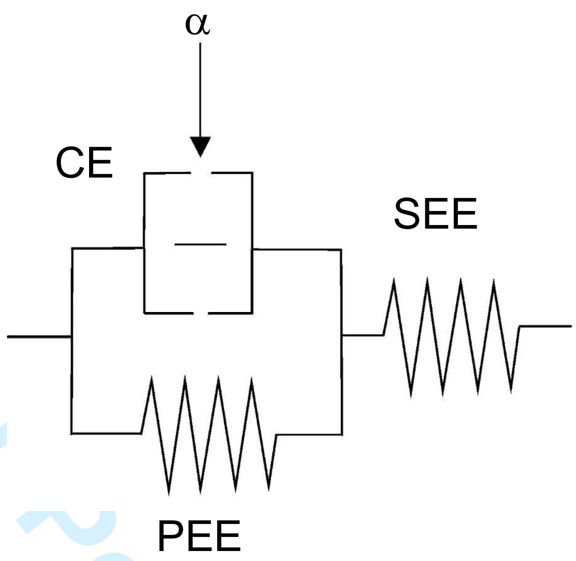

Figure 2. Hill's muscle model

a)

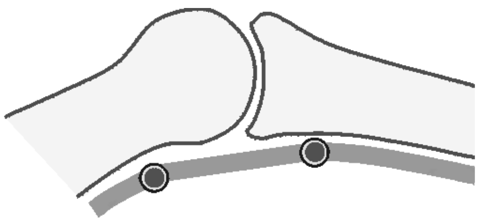

b)

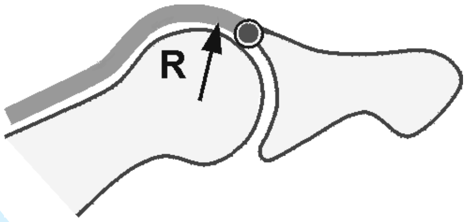

Figure 3. Models for the tendons crossing the joints: a) Straight lines; b) Landsmeer's model I.

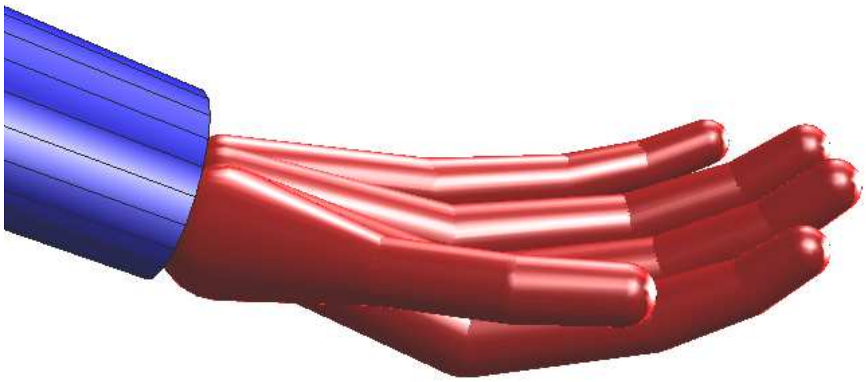

Figure 4. External geometrical representation of the hand with s-topes

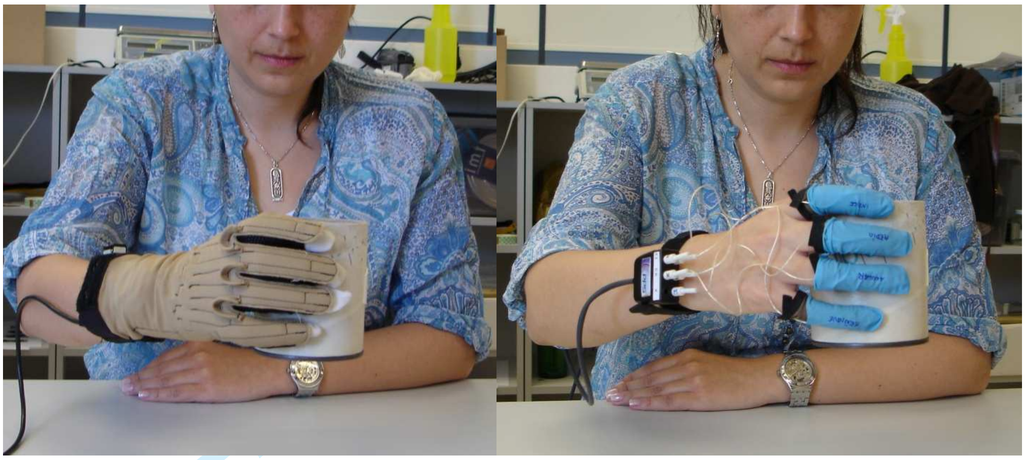

Figure 5. The subject is holding the lighter cylinder (cylinder 1) of the experiment. Left, hand instrumented for posture data registration. Right, hand instrumented for finger force data registration.

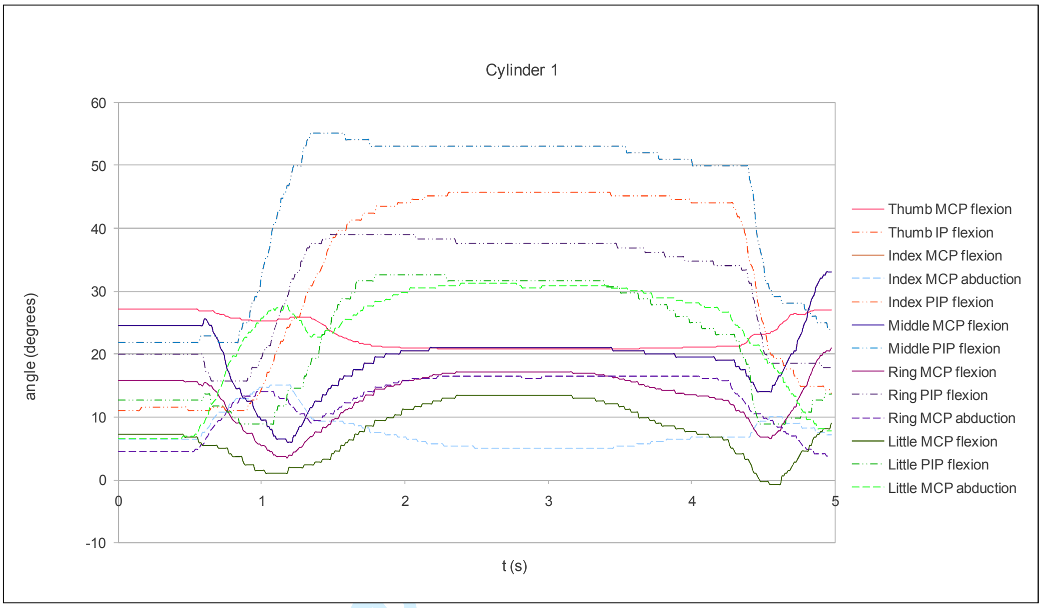

Figure 6. Joint angles (in degrees) registered during one of the repetitions of the cylinder 1 grasping.

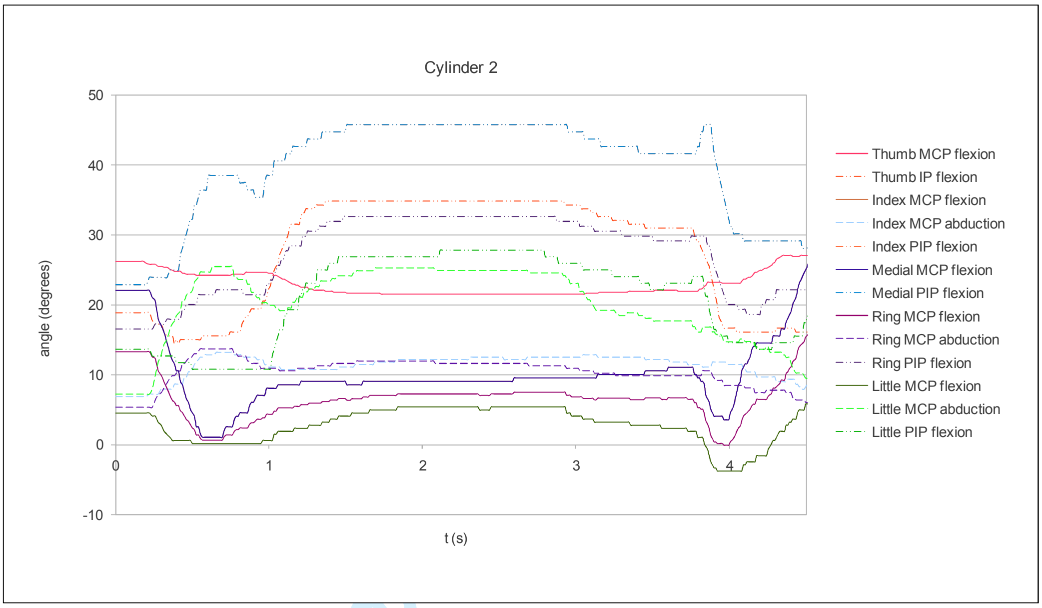

Figure 7. Joint angles (in degrees) registered during one of the repetitions of the cylinder 2 grasping.

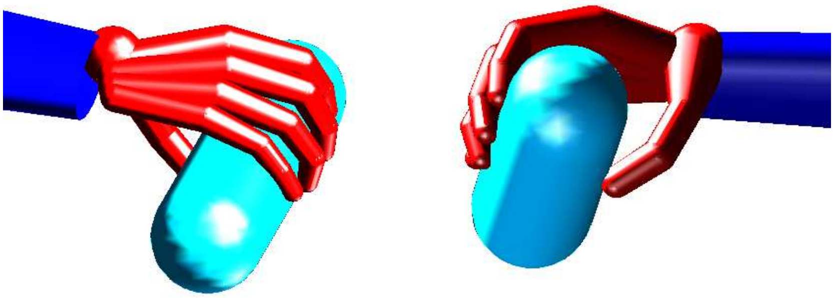

Figure 8. Grasping posture estimated by the model for cylinder 1.

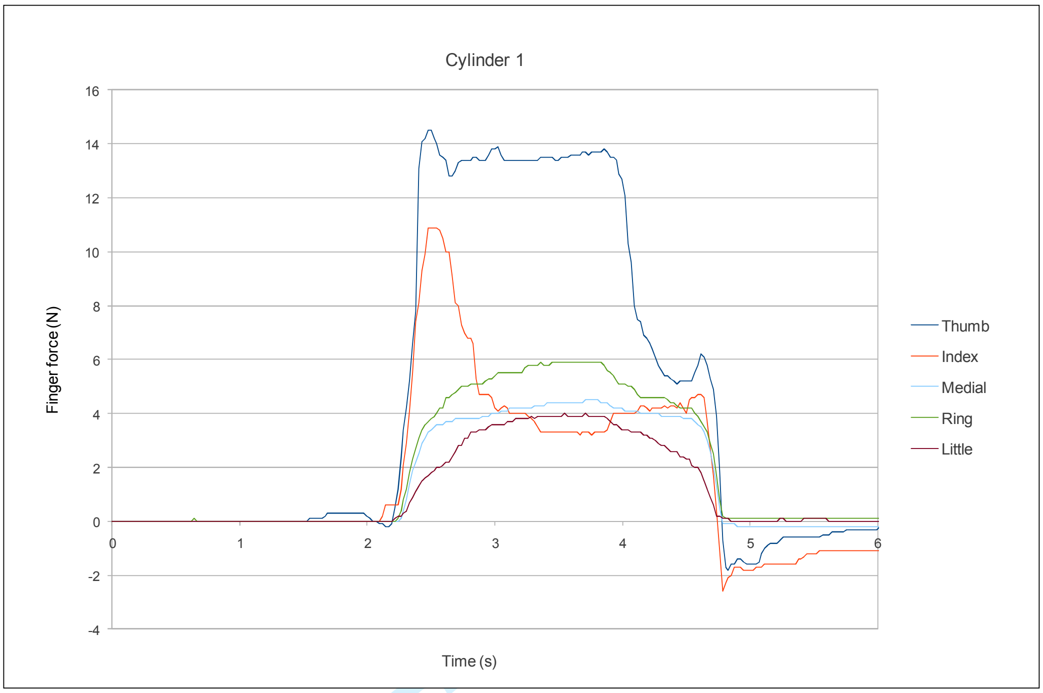

Figure 9. Finger forces (N) registered during one of the repetitions of the cylinder 1 grasping.

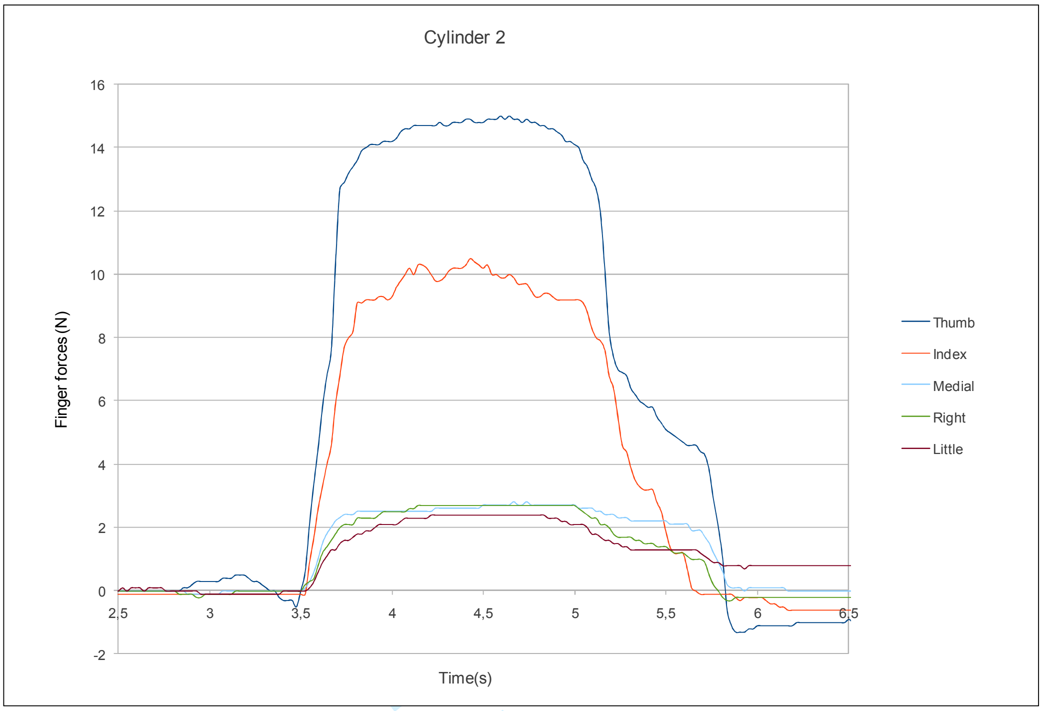

Figure 10. Finger forces (N) registered during one of the repetitions of the cylinder 2 grasping.

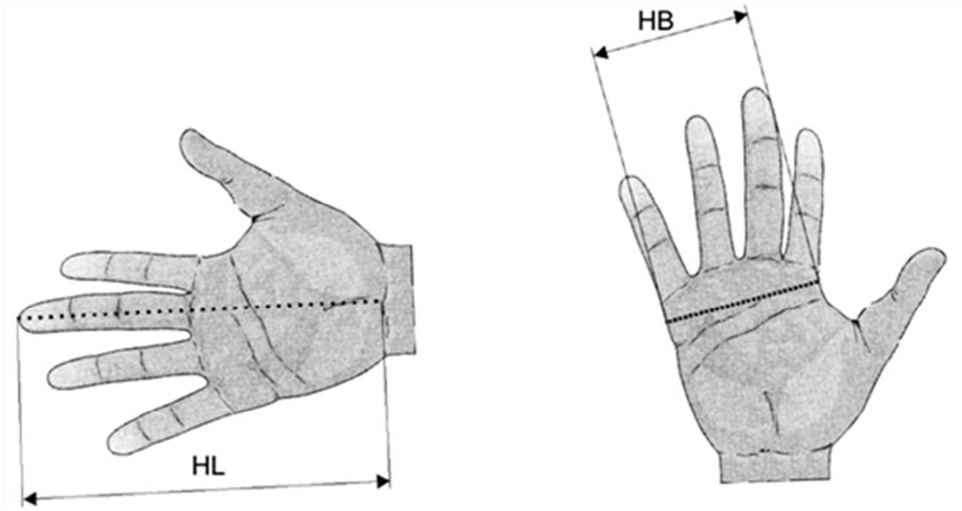

Parameters used to scale the model: HL (hand length) and HB (hand breadth)
152x81mm (96 x 96 DPI)

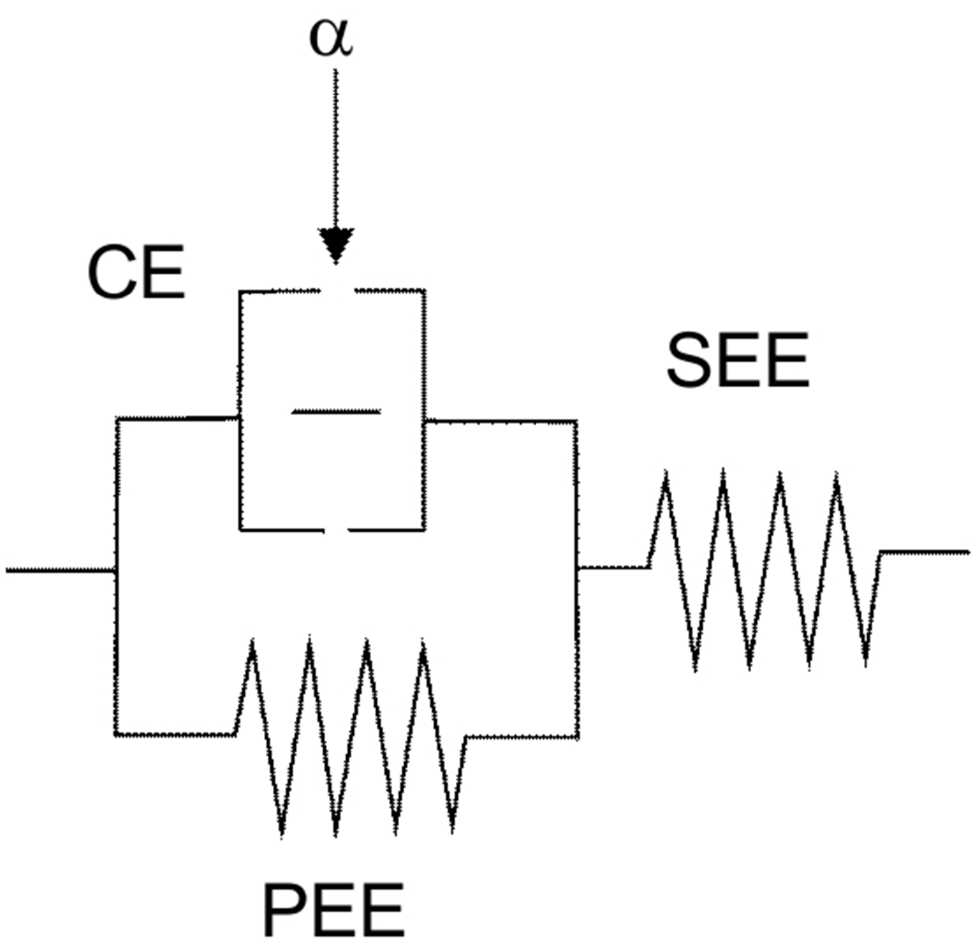

Hill's muscle model
195x200mm (72 x 72 DPI)

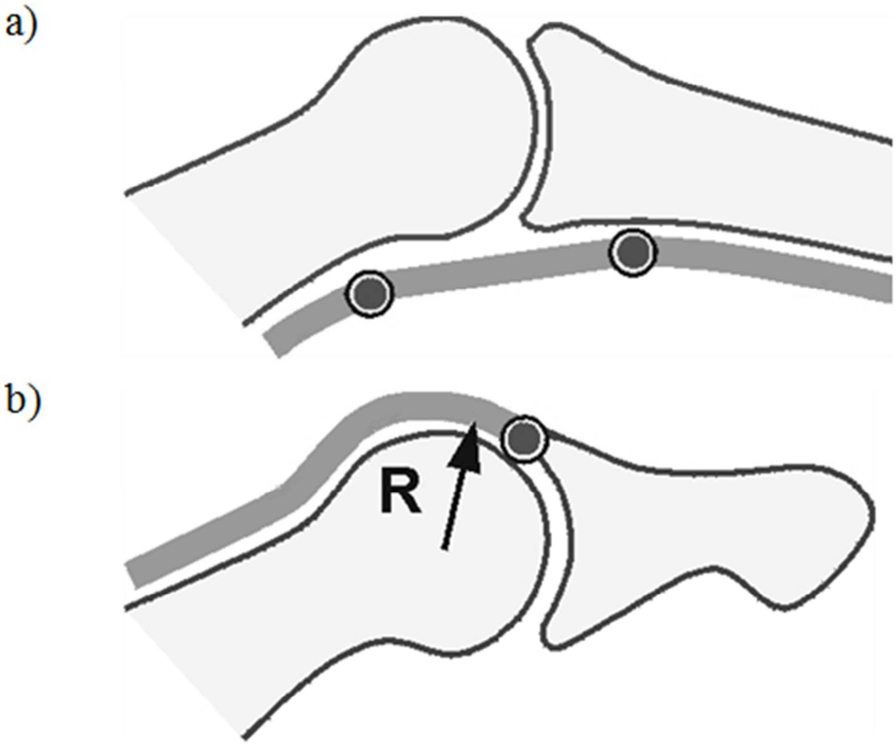

Models for the tendons crossing the joints: a) Straight lines; b) Landsmeer's model I.
136x114mm (96 x 96 DPI)

External geometrical representation of the hand with s-topes
128x73mm (96 x 96 DPI)

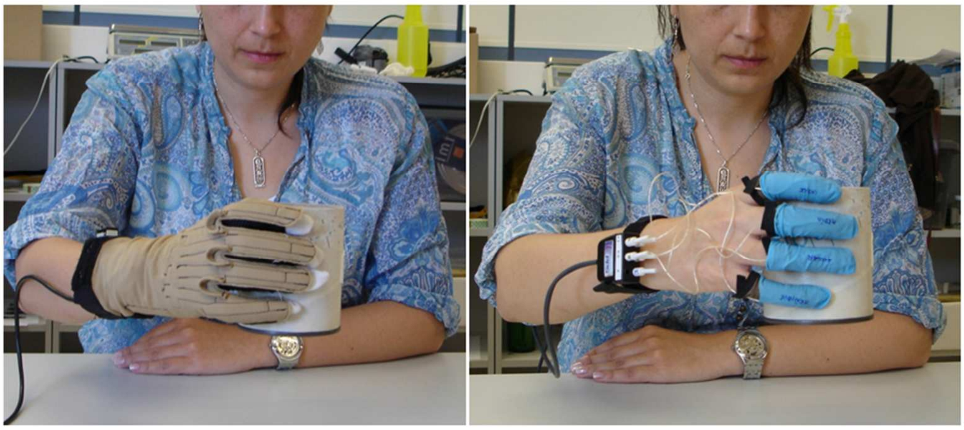

The subject is holding the lighter cylinder (cylinder 1) of the experiment. Left, hand instrumented for posture data registration. Right, hand instrumented for finger force data registration.
239x108mm (96 x 96 DPI)

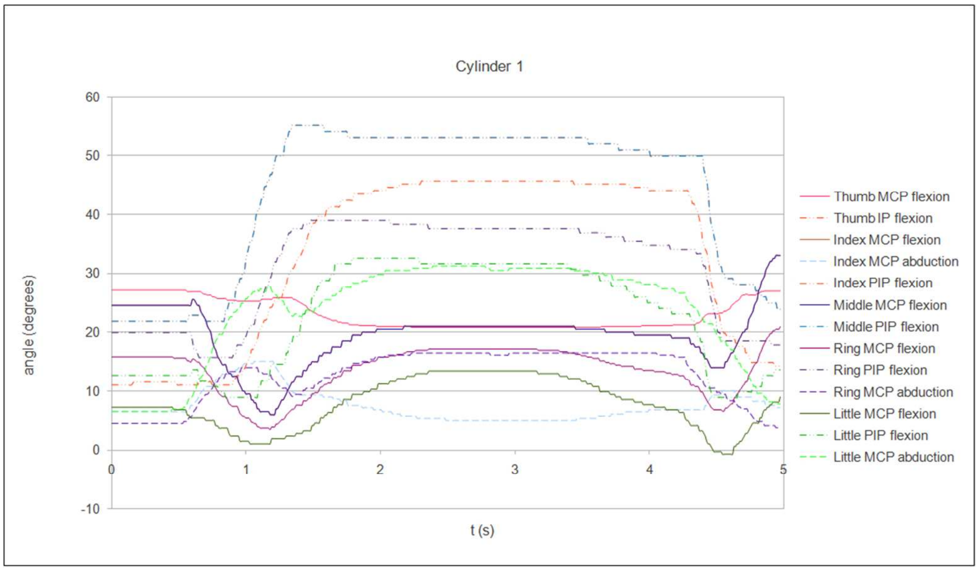

Joint angles (in degrees) registered during one of the repetitions of the cylinder 1 grasping.
286x165mm (96 x 96 DPI)

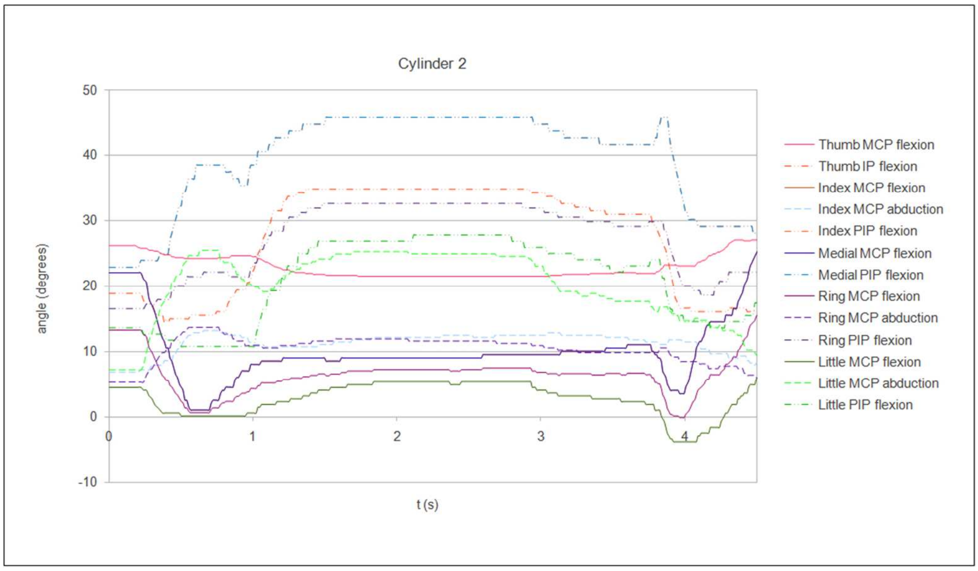

Joint angles (in degrees) registered during one of the repetitions of the cylinder 2 grasping.
286x165mm (96 x 96 DPI)

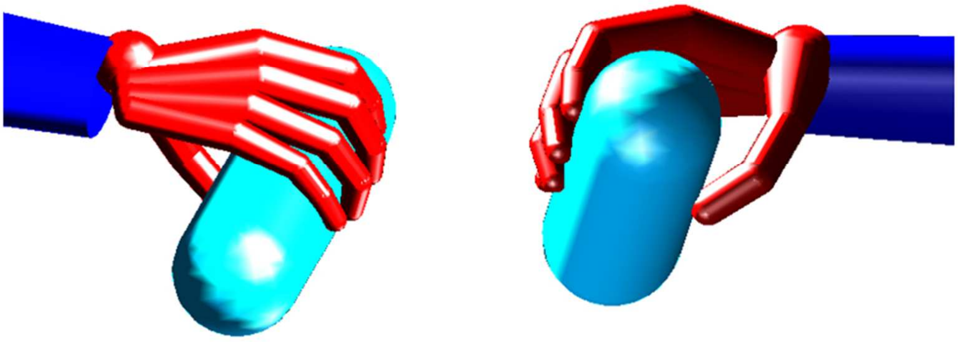

Grasping posture estimated by the model for cylinder 1.
222x88mm (96 x 96 DPI)

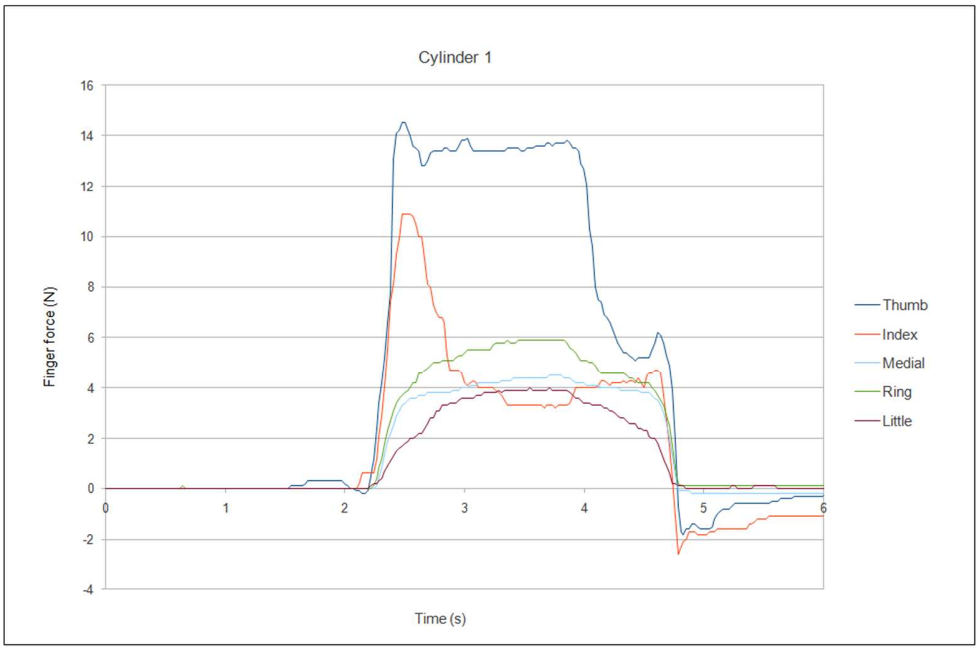

Finger forces (N) registered during one of the repetitions of the cylinder 1 grasping.
264x174mm (96 x 96 DPI)

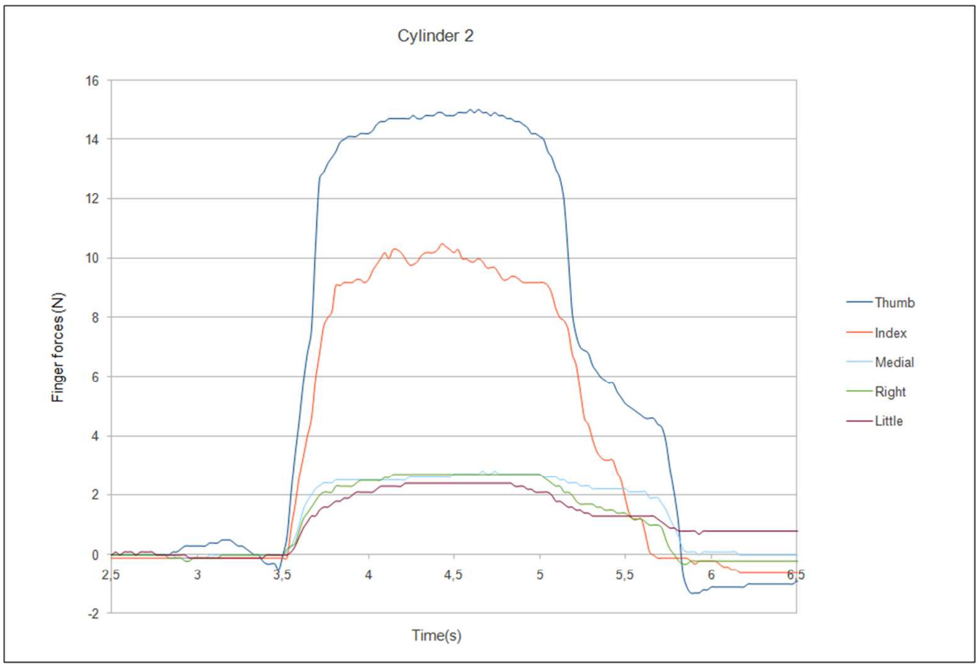

Finger forces (N) registered during one of the repetitions of the cylinder 2 grasping.
257x174mm (96 x 96 DPI)

Table 1. Muscles modelled on each skeletal chain (acronyms in the nomenclature section)

Index	Medial	Ring	Little	Thumb
1^{st} FP	2^{nd} FP	3^{rd} FP	4^{th} FP	APB
1^{st} FS	2^{nd} FS	3^{rd} FS	4^{th} FS	FPB
1^{st} EDC+EI	2^{nd} EDC	3^{rd} EDC	EDQ	OPP
1^{st} LU	2^{nd} LU	3^{rd} LU	4^{th} LU	ADD
1^{st} DI	2^{nd} DI	4^{th} DI	3^{rd} VI	1^{st} DI
1^{st} VI	3^{rd} DI	2^{nd} VI	FDQ	APL
			ADQ	EPB
				FPL
				EPL

Table 2. Joint angles defining the most open posture for grasping cylinder 1

	MCC		MCP		PIP	DIP
	Flexion (º)	Abduction (º)	Flexion (º)	Abduction (º)	Flexion (º)	Flexion (º)
Thumb	-8.0	49.0	25.1	0.0	19.1	-
Index	-	-	10.2	8.9	37.6	18.8
Medial	-	-	10.2	0.0	37.6	18.8
Ring	0.0	-	6.2	9.8	22.8	11.4
Little	0.0	-	2.1	17.7	9.4	4.7

Table 3. Joint angles defining the most open posture for grasping cylinder 2

	MCC		MCP		PIP	DIP
	Flexion (º)	Abduction (º)	Flexion (º)	Abduction (º)	Flexion (º)	Flexion (º)
Thumb	-10.0	50.0	23.9	0.0	17.6	-
Index	-	-	2.4	10.0	38.1	19.0
Medial	-	-	2.4	0.0	38.1	19.0
Ring	0.0	-	1.6	11.6	24.2	12.1
Little	0.0	-	0.9	19.5	11.7	5.8

Table 4. Joint angles defining the mean grasping posture for cylinder 1

	MCC		MCP		PIP	DIP
	Flexion (º)	Abduction (º)	Flexion (º)	Abduction (º)	Flexion (º)	Flexion (º)
Thumb	1.0	47.5	20.9	0.0	49.7	-
Index	-	-	26.2	-2.1	48.3	24.1
Medial	-	-	26.2	0.0	48.3	24.1
Ring	4.0	-	19.5	7.1	35.6	17.8
Little	8.0	-	12.8	13.6	31.4	15.7

Table 5. Joint angles defining the mean grasping posture for cylinder 2

	MCC		MCP		PIP	DIP
	Flexion (º)	Abduction (º)	Flexion (º)	Abduction (º)	Flexion (º)	Flexion (º)
Thumb	0.0	50.8	20.9	0.0	35.5	-
Index	-	-	9.4	9.7	46.7	23.4
Medial	-	-	9.4	0.0	46.7	23.4
Ring	4.0	-	7.6	9.1	33.6	16.8
Little	8.0	-	5.8	19.2	28.0	14.0

Table 6. Grasping posture estimated by the model for cylinder 1

	MCC		MCP		PIP	DIP
	Flexion (º)	Abduction (º)	Flexion (º)	Abduction (º)	Flexion (º)	Flexion (º)
Thumb	0.3	47.7	21.2	0.0	47.3	-
Index	-	-	20.4	1.9	44.4	18.8
Medial	-	-	23.0	0.0	46.1	27.4
Ring	4.2	-	20.0	7.0	36.2	43.9
Little	8.5	-	13.5	13.4	32.8	7.8

Table 7. Grasping posture estimated by the model for cylinder 2

	MCC		MCP		PIP	DIP
	Flexion (º)	Abduction (º)	Flexion (º)	Abduction (º)	Flexion (º)	Flexion (º)
Thumb	-3.0	50.5	21.8	0.0	30.2	-
Index	-	-	9.7	9.7	47.1	23.5
Medial	-	-	12.9	0.0	51.1	25.5
Ring	6.7	-	11.6	7.4	40.0	20.0
Little	7.8	-	5.7	19.2	27.6	13.8

Table 8. Mean finger forces (N) registered for the grasping of both cylinders

	Thumb (N)	Index (N)	Medial (N)	Ring (N)	Little (N)
Cylinder 1	10.7	3.4	4.6	5.8	4.1
Cylinder 2	11.0	9.3	3.0	2.9	1.7

Table 9. Mean finger force contribution (%) observed during the grasping of both cylinders

	Thumb (%)	Index (%)	Medial (%)	Ring (%)	Little (%)
Cylinder 1	100	32	44	55	38
Cylinder 2	100	85	27	26	15

Table 10. Contact finger forces and moments estimated by the model minimising the sum of the squared muscle forces ($\mu = 0.8$)

		Thumb	Index	Medial	Ring	Little
Cylinder 1	Normal (N)	4.05	0.01	1.97	0.96	0.60
	Tangential (N)	3.23	0.01	1.57	0.76	0.48
	Torque (N·mm)	-4.70	0.00	-1.40	-0.60	-0.30
Cylinder 2	Normal (N)	0.41	0.00	0.24	0.11	0.01
	Tangential (N)	0.30	0.01	0.19	0.09	0.01
	Torque (N·mm)	1.00	0.00	-0.10	0.00	0.00

Table 11. Contact finger forces and moments estimated by the model minimising the sum of the squared muscle forces, and reducing the friction coefficient ($\mu = 0.3$)

		Thumb	Index	Medial	Ring	Little
Cylinder 1	Normal (N)	10.59	2.96	1.98	2.54	3.12
	Tangential (N)	3.18	0.89	0.59	0.76	0.94
	Torque (N·mm)	0.00	0.10	-0.30	-0.50	-0.70
Cylinder 2	Normal (N)	0.98	0.18	0.53	0.00	0.26
	Tangential (N)	0.29	0.05	0.16	0.00	0.08
	Torque (N·mm)	-0.10	0.00	0.00	0.00	0.00

Table 12. Contact finger forces and moments estimated by the model when adding a term to the objective function related to the differences among finger forces ($\mu = 0.8$)

		Thumb	Index	Medial	Ring	Little
Cylinder 1	Normal (N)	3.81	0.91	0.92	0.92	0.92
	Tangential (N)	3.02	0.73	0.72	0.71	0.73
	Torque (N·mm)	-5.80	0.10	-1.10	-1.70	0.00
Cylinder 2	Normal (N)	0.45	0.12	0.11	0.11	0.11
	Tangential (N)	0.35	0.09	0.09	0.07	0.09
	Torque (N·mm)	-0.60	0.00	0.10	0.30	0.00

Table 13. Contact finger forces and moments estimated by the model when using the robotics stability optimisation ($\mu = 0.8$)

		Thumb	Index	Medial	Ring	Little
Cylinder 1	Normal (N)	6.62	2.12	1.64	1.47	2.12
	Tangential (N)	3.15	1.68	1.27	0.95	1.69
	Torque (N·mm)	-25.20	3.00	-3.80	-7.60	1.20
Cylinder 2	Normal (N)	4.98	1.79	1.32	0.48	1.56
	Tangential (N)	0.36	0.20	0.30	0.38	0.70
	Torque (N·mm)	-36.50	16.20	-10.90	0.90	-8.70

Evaluation of Human Prehension Using Grasp Quality Measures

Beatriz León, Joaquín Sancho-Bru, Sergio Rodríguez, Máximo A. Roa and Antonio Morales

Abstract— **One of the main features of the human hand is its grasping ability. Robot grasping has been studied for years, and different quality measures have been proposed to evaluate the grasp's ability to resist disturbances and its dexterity properties. Although the human hand is obviously more complex than robot hands, the methods used in robotics might be adopted to study the human grasp. The purpose of this work is to apply some of the most common robotic grasp quality measures to the human hand and to assess their use in the evaluation of the quality of human grasps. As robotic measures do not consider biological and neurological aspects of the human hand, a biomechanical quality measure, the fatigue index, is proposed to introduce the muscle stresses into the evaluation. A first approximation of finding the minimum set of indices that allows the evaluation of the different aspects of the grasp is presented and its validity is checked by reproducing a human prehension experiment.**

I. INTRODUCTION

Many biomechanical human hand models have been developed so far, with the aim of providing a tool for studying problems that cannot be directly analysed on humans or that have too high a cost. One of the main features of the human hand is its grasping capability. However, the current models have a limited ability to predict feasible grasping postures or to evaluate the quality of a grasp.

Evaluating the quality of a human grasp could have several applications. First of all, it can be used in biomechanical human hand models as a criterion to solve the problem of finding the contact forces to grasp an object in a given posture. Second, it can be applied in the ergonomic design of hand-held products. Additionally, the design of hand prosthesis can also be improved if the quality of grasp performed by a given mechanical hand can be measured and compared to the physiological hand. Therefore, having a model that incorporates grasp quality measures can significantly increase their use by the biomechanics, medical and ergonomics communities.

For many years the robotics community has been studying the autonomous handling of objects by robots. Many grasp quality measures have been developed that allow comparing different aspects of the robotic grasp (see [1] for a thorough review). There have been some attempts in robotics to combine some of these measures to create global quality indices [1]. A simple method uses the algebraic sum of the quality measures in a single global index, considering that all of them have to be either maximized or minimized [2]. A variation of this approach normalizes the outcome of each criterion dividing it by the difference between the measures of the best and the worst grasp [3]. Different global measures can be obtained by adding different basic criteria [4], specifically adapted for different practical applications. Kim et al. [5] used five normalized quality measures to create a global quality index defined as the minimum value out of five normalized ones. Cheraghpour et al. [6] created a weighted grasp performance index for cooperative manipulators.

There are few studies evaluating the quality of a human grasp [7], [8]. Both works use the robotic measure proposed by [9] without assessing its validity. To the best of our knowledge, there has not been any study adapting other robotic quality measures to the human hand or proposing a global human grasp quality index.

Although the human hand is obviously more complex than robot hands, the methods used in robotics might be adopted to study the human grasp. The purposes of this work are:

- to adapt the most common robotic grasp quality measures to the human hand grasp
- to find the minimum set of robotic indices that allows evaluating the different aspects of the grasp
- to propose complementary quality indices that may consider biomechanical human hand aspects
- to assess their use in providing an overall assessment of the grasp quality

II. BACKGROUND

The purpose of a grasp is to constrain the potential movements of the object in the event of external disturbances. In this context, a grasp is commonly defined as a set of contacts on the surface of the object.

The force applied by a finger at a contact point generates a wrench on the object with force and torque components. A wrench is the representation of a generalized force acting on a body represented by vector $w \in \mathbb{R}^6$:

$$w = \begin{pmatrix} f \\ \tau/\rho \end{pmatrix}$$

where $f \in \mathbb{R}^3$ and $\tau \in \mathbb{R}^3$ are the force and torque, respectively, and ρ is a parameter with units of length that allows all the components of w to have units of force [10].

The contact model maps the wrench at some reference point of the object, usually the centre of mass. The more common contact models used in robotic grasping are the

B. León, S. Rodríguez and A. Morales are with the Robotic Intelligence Laboratory at the Department of Computer Science and Engineering, Universitat Jaume I, 12006 Castellón, Spain {len,serodrig,morales}@uji.es

J. Sancho-Bru is with the Group of Biomechanics and Ergonomics at the Department of Mechanical Engineering and Construction, Universitat Jaume I, 12006 Castellón, Spain sancho@uji.es

M. A. Roa is with the Institute of Robotics and Mechatronics, German Aerospace Center (DLR), 82234 Wessling, Germany. maximo.roagarzon@dlr.de

point contacts with and *without friction* and the *soft-finger contacts* [1].

The Grasp Matrix and Hand Jacobian define the relevant velocity kinematics and force transmission properties of the contacts. They are used for some of the quality measures so we introduce them here, but a complete explanation can be found in [11]. Each contact should be considered as two coincident points: one on the hand and one on the object.

The transpose of the Grasp Matrix (G) maps the object wrench to the contact frames. G is the combination of the grasp matrices for each of the n contact points. The hand Jacobian (J_h) maps the joint velocities to hand wrenches expressed in the contact frames. The hand-object Jacobian is the matrix H given by:

$$H = (G^{+})^{T} J_h \tag{1}$$

with G^{+} being the generalized inverse of G.

III. GRASP QUALITY MEASURES

This section presents a description of the measures implemented in the study. We have classified the measures into five groups. Groups A, B, C and D correspond to the adaptation of existing robotic measures. Some of them focus on evaluating the ability to resist external disturbances, others on evaluating the dexterity, while group E corresponds to the biomechanical quality measure that we are proposing.

- Group A: stability indicators that consider the algebraic properties of the grasp matrix G to measure the grasp capability of withstanding external wrenches; they use the contact points and normal directions and assume no limitation for the contact force values.
- Group B: stability indicators that use the location of the contact points. Better stability of the grasps is assumed when contact points are distributed in a uniform way on the object surface. This can be done by measuring either the angles or the area of the polygon whose vertices are the contact points. Another measure considers the distance between the centroid of the contact points polygon and the object center of mass aiming to minimize the effect of gravitational and inertia forces.
- Group C: stability indicators that take into account the magnitude of forces applied at the contact points. The previous indicators do not consider any limitation on the finger forces, so that in some cases the fingers have to apply very large forces to resist small perturbations.
- Group D: measures that take into account the configuration of the end-effector, requiring the hand-object Jacobian for their calculation, measuring its manipulability. They calculate the hand-object jacobian or penalize the hand joints that are at their maximum limits.
- Group E: considers the muscle stresses using the biomechanical measure proposed, the fatigue index.

A. Measures

1) Smallest singular value of G (A1): This quality measure indicates how far the grasp configuration is from falling into a single configuration, losing the capability of withstanding external wrenches [12]. When a grasp is in a singular configuration, at least one of the singular values of G is zero.

$$Q_{A1} = \sigma_{min}(G) \tag{2}$$

where $\sigma_{min}(G)$ is the smallest singular value of the matrix G.

2) Volume of the ellipsoid in the wrench space (A2): The volume of the set of generalized forces [12] that can be exerted on the rigid body at a nominal configuration (wrench space) can be calculated as:

$$Q_{A2} = \beta\sqrt{det(GG^{T})} = \beta(\sigma_1\sigma_2\ldots\sigma_6) \tag{3}$$

where $\beta > 0$ is a constant and $(\sigma_1\sigma_2\ldots\sigma_6)$ denote the singular values of the G matrix. This measure should be maximized to obtain an optimum grasp.

3) Grasp Isotropy Index (A3): The precise position or force control may not be guaranteed in part if any finger lies near a singular position. This quality measure tries to obtain an isotropic grasp where the magnitude of internal forces are similar [13], and is calculated as:

$$Q_{A3} = \frac{\sigma_{min}}{\sigma_{max}} \tag{4}$$

where σ_{min} and σ_{max} denote the minimum and maximum singular values of G. This measure approaches to one at a desirable configuration (isotropic) and is equal to zero at the singular configuration.

4) Distance between the centroid of the contact polygon and the object's center of mass (B1): This index aims to minimize the effect of gravitational and inertia forces during the motion of the robot, measuring the distance between the center of mass g_o of the grasped object and the centroid of the contact points g_c [14]. The centroid of the contact points is calculated as:

$$g_c = \frac{1}{n}\sum_{i=1}^{n} g_i \tag{5}$$

where n is the number of contact points and g_i is the location of each contact point. Then the measure is calculated as:

$$Q_{B1} = distance(g_o, g_c) \tag{6}$$

where g_o can be calculated as the centroid of the object when it can be assumed that the object has a uniform mass distribution.

5) Area of the grasp polygon (B2): This measure is defined as the area of the polygon formed by the contact points. The optimum grasp is the one that best resists forces and torques about the grip plane, which has the largest polygon area [15]. It has been used in robotics for three finger hands, where all finger points lie in a plane. For the five fingers of the human hand, it can be extended using the method proposed by [16]. The contact plane is generated by selecting three fingers and the remaining contacts such as they are perpendicularly projected onto that plane. In the case of the human hand, the thumb and index fingers are selected given their leading role in grasping, and the third finger can be selected either the middle or ring finger. The little finger is not chosen given his minor role in grasp formation. In our work, the middle finger was selected as the third finger.

$$Q_{B2} = Area(Polygon(p1, p2, p3, p4_P, p5_P)) \quad (7)$$

where $p1, p2, p3$ are the contact points for the thumb, index and middle fingers, and $p4_P, p5_P$ are the projected points of the ring and little fingers onto the plane.

This measure makes sense for a robot hand, however for the human hand it may not work, because the thumb, index and middle fingers are stronger and play a more important role than the other two fingers, which creates a non uniform distribution of forces or contact points.

6) Shape of the grasp polygon (B3): This measure compares how far the internal angles of the grasp polygon are, from those of the corresponding regular polygon [13]. It is assumed that the quality of a grasp is improved if the contact points are distributed in a uniform way on the object surface, generating a regular polygon. As explained for the previous index, given the different roles of the human hand fingers it is likely that an optimum grasp does not require a uniform finger distribution. This index is calculated as:

$$Q_{B3} = \frac{1}{\theta_{max}} \sum_{i=1}^{n_f} |\theta_i - \bar{\theta}| \quad (8)$$

where n_f denotes the number of fingers, θ_i is the inner angle at the i^{th} grasp point, $\bar{\theta}$ denotes the average angle of all inner angles of the grasp polygon, given by:

$$\bar{\theta} = \frac{180(n_f - 2)}{n_f} \quad (9)$$

and θ_{max} is the sum of the internal angles when the polygon has the most ill-conditioned shape (such as a line):

$$\theta_{max} = (n_f - 2)(180 - \bar{\theta}) + 2\bar{\theta} \quad (10)$$

7) Smallest maximum wrench to be resisted (C1): The grasp quality is equal to the magnitude of the minimum, over all wrench directions, of the maximum wrench we can exert in that direction [9]. Only the direction of forces is used and their magnitudes are upper-bounded to 1. Defining $B\zeta$ as the set of all possible wrenches acting on the object, the maximum of $w \in B\zeta$ lies on the boundary of $B\zeta$. Then the quality metric is the radius of the largest sphere center at the origin which is contained in $B\zeta$.

$$Q_{C1} = min_{w \in Boundary(B\zeta)} \|w\| \quad (11)$$

where $B\zeta$ is calculated as:

$$B\zeta = ConvexHull(\bigcup_{i=1}^{n} \{w_{i,1}, \ldots, w_{i,m}\}) \quad (12)$$

This measure depends on the choice of the origin of the reference system used to compute torques. In this work, the center of mass of the object is used.

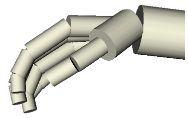

Fig. 1. Natural posture for the human hand

8) Volume of the convex hull (C2): This measure calculates the volume of the boundary of the set of all possible wrenches acting on the object [17]:

$$Q_{C2} = Volume(B\zeta) \quad (13)$$

where $B\zeta$ is defined by Eq. 12.

9) Normal Grasping Force (C3): This measure takes into account the magnitudes of the applied forces as indicative of the force efficiency in the grasp. It indicates how much passive forces the grasp can produce on the object to resist external disturbances [18]. The normal grasping force is defined by:

$$f_n = \sum_{i=1}^{k} f_{i,n} \quad (14)$$

where $f_{i,n}$ is the normal component of the finger force and k is the number of fingers in the hand. Then, for a given grasp and applied finger forces that resist a given external wrench w_o, the quality of the grasp is given by:

$$Q_{C3} = \frac{1}{f_n} \quad (15)$$

This measure should be minimized to obtain an optimum grasp.

10) Posture of hand finger joints (D1): This index assesses the manipulation ability of the hand at the grasp position, measuring how far each joint is from its maximum limits [19]. It is given as:

$$Q_{D1} = 1/n \sum_{i=1}^{n} \left(\frac{y_i - a_i}{R_i} \right)^2 \quad (16)$$

where n is the number of joints and a_i is the middle-range position. In the case of the human hand, the joint angles defininig the natural or relaxed hand posture [20] can be used to define a_i (see Fig. 1). R_i is the joint angle range, used to normalize the index, defined as:

$$R_i = \begin{cases} a_i - y_{im} & \text{if } y_i < a_i \\ y_{iM} - a_i & \text{if } y_i > a_i \end{cases}$$

where y_{iM} and y_{im} are the maximum and minimum angle limits of the joint i. The grasp is optimal when all hand joints are at the natural posture, having a quality measure of zero, and it goes to one when all its joints are at their maximum angle limits.

11) The condition number of the hand-object jacobian (D2): This measure considers the capability of the hand to move an object in any direction with the same gain, which implies a good manipulation ability [1]. When the contribution of each joint velocity is the same in all components of the object velocity, the transformation between the velocity domain in the finger joints and the velocity domain of the object is uniform. The condition number of the hand-object Jacobian is a measure of such ability [21], [22] and can be calculated as:

$$Q_{D2} = \frac{\sigma_{max}}{\sigma_{min}} \tag{17}$$

where σ_{max} and σ_{min} are the largest and smallest singular values of the hand-object Jacobian matrix H.

When the condition number is equal to one, the columns of H are vectors orthogonal to each other and with the same module, indicating a uniform transformation and a grasp with the maximum quality.

12) Fatigue Index (E1): In addition to the adaptation of robotic quality measures, we propose the use of a new biomechanical quality indicator. This quality measure uses the common definition of fatigue proposed by [23] widely used in biomechanics, to measure the fatigue caused to the muscles when performing a grasp:

$$Q_{E1} = \sum_{i=1}^{m} \left(\frac{F_i}{PCSA_i} \right)^2 \tag{18}$$

where m represents the number of muscles, F_i the force exerted by each muscle and $PCSA_i$ its physiological cross-sectional area. The smaller the fatigue index the better will be the grasp. This has to be calculated using the biomechanical model.

IV. IMPLEMENTATION

The calculation of the different measures described in the previous section requires different input data. A kinematic model of the hand with a planning algorithm capable of estimating feasible grasping postures would be enough for estimating the input data required for measures from groups A, B and D: contact points and normals. Measures from group C and the biomechanical measure proposed are more demanding as they need the contact and the muscle forces required for the grasp, respectively. In this case, a dynamic model of the hand with an appropriate contact model is required for obtaining these data. The implementation of such a model is described in this section. The MATLAB system and its optimization toolbox have been used to implement the biomechanical model and the calculation of all quality measures.

A. Biomechanical Model

A previously-validated 3D, scalable, biomechanical model of the complete hand [24] was implemented in the robotic simulation environment OpenRAVE [25].

The model has been developed in a scalable way, choosing two very well known anthropometric parameters of the hand: the hand length (HL) and hand breadth (HB) that are easy to measure and representative of the hand size.

The hand model considers 25 degrees of freedom selected to realistically simulate the hand movements. The hand has been modeled as five skeletal open chains of rigid bodies (the bones) connected to the carpus through different joints. All the interphalangeal joints of the fingers and thumb allow only flexion-extension movements and have been modelled as hinge joints. All metacarpophalangeal joints allow both flexion-extension and abduction-adduction movements and have been modelled as universal joints.

A total of 34 muscles for the hand have been modelled using a simple Hill's three-component model. Most of the muscles do not act directly on the bones, but through the force transmitted to tendons. To model the tendon action crossing the joints, straight lines connecting 2 points have been considered, one fixed with respect to the proximal bone and the other one with respect to the distal bone. This approximation has been used for all tendons with the exception of extensors, for which Landsmeer's model I has been considered.

B. Closure Algorithm

In order to generate grasp postures automatically, we used a grasping algorithm based on that of Choi [26]. This algorithm uses a function to automatically generate a natural grasping motion path of the hand model from a fully opened state to a clenched one. The goal is to find contacts between the surface hand skin and the object surface while rotating the joint angles of the fingers.

In order to do that, we considered a simple geometric collision-detection algorithm based on the one used by [8], which allows the penetration of the surface skin model and the object model. This penetration is limited by a tolerance that relates to the hand stiffness of each contact region. The distances between the points on the skin surface and the object are calculated while the joint angles of each joint rotate according to the specific joint rotation algorithm. When the maximum penetration distance between the skin surface points and the object reaches the given tolerance, the contact is achieved and the joint rotation ends. At this point, OpenRAVE is queried to find each contact point, specified as its position vector and normal direction. These contact points and normals are used to calculate the related quality measures.

C. Soft Contact Model

Unlike what happens with most robots, real human fingers conform to the grasped object shape. As the contact finger surface is deformable, the contact does not occur at just one point but over some finite area that increases as the normal forces increase. Due to this effect, in addition to the normal force and tangential force due to friction, human finger contact may support frictional torsional moments with respect to the normal at the contact point. In this work, a soft contact model based on that of [27] has been used. Friction constraints are derived based on general expressions for non-planar contacts of elastic bodies, taking into account the local geometry and structure of the objects in contact. The values for the human hand skin friction coefficient and the stiffness modulus have been obtained from [28] and [29] respectively.

V. EXPERIMENTAL ASSESSMENT

A. Methods

A series of experiments in which a bottle was grasped using four different postures, was used to assess the validity of the quality measures.

Five human male subjects were selected to grasp a semi-filled bottle (weight 0.401 kg), and hold it for five seconds in a vertical orientation. The subjects were asked to imitate four predefined postures to perform the grasp (see Fig. 2). Each posture was grasped three times. At the end, the subjects were asked to assess the overall quality of the grasp ordering the grasps from best to worst, with no indication on the specific characteristic to be rated.

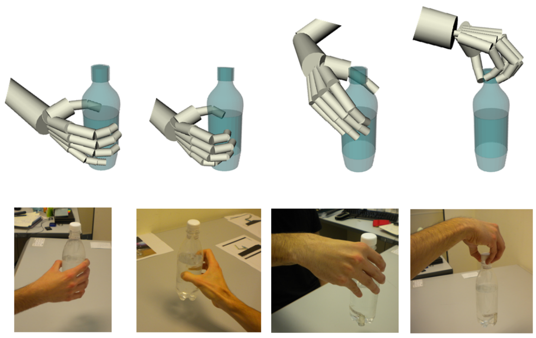

(a) (b) (c) (d)

Fig. 2. Selected postures: (a) cylindrical, (b) claw, (c) diagonal and (d) top grasp.

In order to assess the quality measures, the four grasping postures were simulated using the biomechanical hand model. For each posture, all quality measures were calculated.

- A statistical analysis was performed in order to identify whether some groups of indices were giving the same information. The objective was to find the minimum set of indices required for studying the different aspects of the grasp.
- The results were compared with the assessment of the same grasps performed by human subjects in the experiments.

B. Results

The results of the rankings given by the subjects that participated in the experiment are shown in Table I.

The best grasp was the cylindrical one, followed by the diagonal or top (with the same rating), and the worst was the claw (as was expected).

The results of the quality measures evaluated for the selected postures are shown in Table II. For each measure whether it has to be maximized or minimized to obtain the best grasp is indicated. According to this criteria, the ranking of the four grasps for each measure is shown in Table III.

TABLE I

RESULTS OF RANKING BY SUBJECTS FOR SELECTED POSTURES

Subjects	Best to worst			
Subject 1	cyl	diag	claw	top
Subject 2	cyl	top	diag	claw
Subject 3	cyl	top	diag.	claw
Subject 4	cyl	diag.	top	claw
Subject 5	cyl	top	diag	claw

TABLE II

GRASP QUALITY MEASURES RESULT FOR SELECTED POSTURES

Measures			Postures			
			Cyl.	Claw	Diag.	Top
Q_{A1}	$\sigma_{min}(G)$	max	0.1310	0.0769	0.2036	0.1950
Q_{A2}	Volume ellipsoid	max	2.5506	0.8146	5.1993	5.3130
Q_{A3}	Grasp Isotropy	max	0.0584	0.0341	0.0910	0.0864
Q_{B1}	Distance	min	0.0207	0.0225	0.0657	0.1293
Q_{B2}	Area polygon	max	0.0016	0.0016	0.0012	0.0005
Q_{B3}	Shape polygon	max	0.6667	0.6667	0.5115	0.1761
Q_{C1}	Largest sphere	max	7.37E-3	4.22E-3	1.57E-3	2.89E-3
Q_{C2}	Volume CH	max	5.30E-3	2.89E-3	1.68E-3	4.48E-4
Q_{C3}	Normal force	min	0.1286	0.0813	0.1663	0.1346
Q_{D1}	Finger posture	min	0.1352	0.2694	0.1934	0.1961
Q_{D2}	The cond. num.	min	298.71	318.63	208.64	115.24
Q_{E1}	Fatigue Index	min	4714	2021.8	3307	1059.8

TABLE III

RESULTS OF RANKING BY QUALITY MEASURE FOR SELECTED POSTURES

Measures		Best to worst			
Q_{A1}	$\sigma_{min}(G)$	diag	top	cyl	claw
Q_{A2}	Volume ellipsoid	top	diag	cyl	claw
Q_{A3}	Grasp Isotropy	diag	top	cyl	claw
Q_{B1}	Distance	cyl	claw	diag	top
Q_{B2}	Area polygon	cyl	claw	diag	top
Q_{B3}	Shape polygon	top	diag	cyl	claw
Q_{C1}	Largest sphere	cyl	claw	top	diag
Q_{C2}	Volume CH	cyl	claw	diag	top
Q_{C3}	Normal force	claw	cyl	top	diag
Q_{D1}	Finger posture	cyl	diag	top	claw
Q_{D2}	The cond. num.	top	diag	cyl	claw
Q_{E1}	Fatigue Index	top	claw	diag	cyl

The variety of the ranking results corroborates that the quality indices measure different aspects of the grasp. In fact, in this case only Q_{D1} is able to predict the ranking assessed by the human. This confirms the importance of combining the different criteria to create an overall quality index. The importance of each aspect being measured by the indices will depend on the task to be performed. In this sense, it is important to identify which are the independent aspects that are being measured by all these indices that have been calculated. Even more important is the identification of a physical interpretation of these independent aspects.

1) Statistical Correlation: In order to analyse the relations between the quality measures, a Pearson correlation coefficient is calculated for each combination of measures and the results are shown in Table IV.

Several measures show a correlation greater than 0.8 with each other. Q_{A1}, Q_{A2}, Q_{A3} and Q_{C3} show a very high correlation. Q_{B1}, Q_{B2}, Q_{B3}, Q_{C2} and Q_{D2} are also correlated. Q_{C1} and Q_{C2} are correlated which make sense given that they are in the same group. The biomechanical index Q_{E1} is surprisingly correlated with Q_{C2}, and Q_{D1} is not correlated with any measure.

We have identified five independent sets of measures that are evaluating different aspects of the grasp. Moreover, one measure from each of these groups could be enough to assess these aspects:

- From the first one, Q_{A3} can be chosen giving an idea of *how restricted the grip is*. It is worth noting than to calculate Q_{C3} the biomechanical model needs to be used, therefore it would be a great advantage if the same evaluation can be performed with some measure of the group A which needs only the contact points.
- From the second group, Q_{B1} can be chosen giving an idea of *how distributed the restriction of the grip is*. In our experiment these measures shows high correlations, but it would be interesting to investigate what happens when objects of different shapes and weights are evaluated.
- From Q_{C1} and Q_{C2}, Q_{C1} can be chosen giving an idea of the *ability to resist external wrenches*.
- The proposed index E1 can also be chosen to evaluate the *fatigue associated with the grasp*. However, as it shows a high correlation with Q_{C2} and is not too low with Q_{C1}, it would be interesting to study whether these correlations increase with more experiments. Such an increase would mean that the biomechanical model will not be necessary to evaluate the quality of the grasp.
- Finally, Q_{D1} is also chosen given that is not correlated with any measure showing that is measuring a completely different aspect of the grasp which can be interpreted as *comfort*.

2) Global Quality Index: The measures proposed provide us with an evaluation of the five aspects of the human grasp mentioned above. However, each of the selected measures have their own units and ranges, making it difficult to compare them. To avoid this, the values of the selected measures have been normalized by dividing them by their maximum posible values and setting the best value to "1" and the worst value to "0". The normalized values are presented in Table V. As the subjects were simply asked to rate the overall quality of the grasps, with no indication on the specific characteristic to be rated, it is difficult to compare these values with the human assessment.

We can observe that the measure that has a greater variation between the different postures is Q_{E1_N}, followed, to a lesser extent, by Q_{D1_N}. However, Q_{A3_N} and Q_{E1_N} hardly change, which means that they are less sensitive to the variations between the selected postures. Most likely Q_{E1_N} would have shown greater differences, had we used objects with different weights. In order to verify that these measures are useful to assess the human grasp, a sensitivity analysis has to be performed in order to evaluate the variability of their results.

TABLE V

RESULTS OF NORMALIZED GRASP QUALITY MEASURES

Measures		Postures			
		Cyl.	Claw	Diag.	Top
Q_{A3_N}	Grasp Isotropy	0.0584	0.0341	0.0910	0.0864
Q_{B1_N}	Distance	0.8554	0.8427	0.5411	0.0974
Q_{C1_N}	Largest sphere	0.0511	0.0290	0.0102	0.0162
Q_{D1_N}	Finger posture	0.8648	0.7306	0.8066	0.8039
Q_{E1_N}	Fatigue	0.8901	0.9528	0.9229	0.9753
Q_T	Average	0.5439	0.5179	0.4743	0.3958

These measures can be merged in order to obtain an overall measure that evaluates the quality of a grasp. A first approximation can be obtained by using the mean of the normalised qualities calculated by the different criteria, the best grip is given by the one with the largest score. This average quality index is presented in Table V.

The average quality index predicted the cylindrical grasp as the best one, followed by the claw grasp, the diagonal grasp and ranked the top grasp as the worst one. This ranking does not match the human assessment observed in the experiment giving an indication that we need to change the influence of each criterion on the global quality value. In order to do that, it is necessary to use a more complex implementation such as a weighted sum. However, to obtain reliable values of these weights further experiments have to be performed.

VI. CONCLUSIONS AND FUTURE WORKS

In this paper, we adapted the most common robotic grasp quality measures to evaluate the human grasp. The fatigue index was proposed to consider biomechanical and neurological aspects of the human hand. These measures were implemented and then evaluated using different grasps that were also reproduced by human subjects. Through a correlation analysis, groups of measures that evaluate similar aspects of the grasp were determined, allowing us to find a reduced number of indices to assess the overall quality of the grasp.

The experiments performed in this study are the first steps and do not suffice to draw general conclusions. Therefore, further experiments varying different aspects of the grasp will be performed. These include changing the shape and weight of the objects, specifying a task to perform after the grasp, as well as increasing the number of subjects. In addition, a quantitative assessment instead of a ranking of grasps would allow us to obtain a global measure that can then be more easily compared with the results of the quality indices. The subjects could be also asked to assess the different characteristics of the grasp which are somehow related with the results of the selected measures to have additional information.

TABLE IV

RESULTS OF STATISTICAL CORRELATION BETWEEN DIFFERENT QUALITY MEASURES

	Q_{A1}	Q_{A2}	Q_{A3}	Q_{B1}	Q_{B2}	Q_{B3}	Q_{C1}	Q_{C2}	Q_{C3}	Q_{D1}	Q_{D2}	Q_{E1}
Q_{A1}	1.00											
Q_{A2}	1.00	1.00										
Q_{A3}	1.00	0.99	1.00									
Q_{B1}	0.76	0.82	0.75	1.00								
Q_{B2}	-0.69	-0.76	-0.68	-0.99	1.00							
Q_{B3}	-0.71	-0.77	-0.70	-1.00	1.00	1.00						
Q_{C1}	-0.59	-0.61	-0.59	-0.61	0.54	0.54	1.00					
Q_{C2}	-0.59	-0.65	-0.59	-0.86	0.83	0.83	0.89	1.00				
Q_{C3}	0.92	0.88	0.92	0.45	-0.36	-0.39	-0.42	-0.28	1.00			
Q_{D1}	-0.45	-0.40	-0.45	-0.04	0.03	0.05	-0.45	-0.41	-0.62	1.00		
Q_{D2}	-0.85	-0.90	-0.84	-0.99	0.97	0.97	0.62	0.83	-0.58	0.15	1.00	
Q_{E1}	-0.11	-0.19	-0.10	-0.68	0.71	0.69	0.59	0.83	0.27	-0.67	0.57	1.00

VII. ACKNOWLEDGMENTS

The research leading to these results has received funding from the Spanish Research and Innovation Ministry and the FEDER through the project DPI2010-18177; Fundació Caixa-Castelló and the Universitat Jaume I through the project P1-1B2011-25; and the European Community's Seventh Framework Programme under grant agreement 215821.

REFERENCES

[1] R. Suárez, M. Roa, and J. Cornella, "Grasp quality measures," Technical University of Catalonia, Tech. Rep., 2006.

[2] E. Boivin, I. Sharf, and M. Doyon, "Optimum grasp of planar and revolute objects with gripper geometry constraints," in *Proceedings of the IEEE International Conference on Robotics and Automation*, vol. 1, april-may 2004, pp. 326 – 332.

[3] E. Chinellato, R. Fisher, A. Morales, and A. del Pobil, "Ranking planar grasp configurations for a three-finger hand," in *Proceedings of the IEEE International Conference on Robotics and Automation*, vol. 1, sept. 2003, pp. 1133 – 1138 vol.1.

[4] E. Chinellato, A. Morales, R. Fisher, and A. del Pobil, "Visual quality measures for characterizing planar robot grasps," *Systems, Man, and Cybernetics, Part C: Applications and Reviews, IEEE Transactions on*, vol. 35, no. 1, pp. 30 –41, feb. 2005.

[5] B.-H. Kim, B.-J. Yi, S.-R. Oh, and I. H. Suh, "Non-dimensionalized performance indices based optimal grasping for multi-fingered hands," *Mechatronics*, vol. 14, no. 3, pp. 255 – 280, 2004.

[6] F. Cheraghpour, S. Moosavian, and A. Nahvi, "Multiple aspect grasp performance index for cooperative object manipulation tasks," in *IEEE/ASME International Conference on Advanced Intelligent Mechatronics. AIM 2009.*, july 2009, pp. 386 –391.

[7] F. A. Goussous, "Grasp planning for digital humans," Ph.D. dissertation, Iowa University, July 2007.

[8] Y. Endo, S. Kanai, T. Kishinami, N. Miyata, M. Kouchi, and M. Mochimaru, "A computer-aided ergonomic assessment and product design system using digital hands," in *Proceedings of the 1st international conference on Digital human modeling*. Springer-Verlag, 2007, pp. 833–842.

[9] C. Ferrari and J. Canny, "Planning optimal grasps," *Proceedings 1992 IEEE International Conference on Robotics and Automation*, pp. 2290–2295, 1992.

[10] M. Roa and R. Suarez, "Computation of independent contact regions for grasping 3-d objects," *IEEE Transactions on Robotics*, vol. 25, no. 4, pp. 839 –850, aug. 2009.

[11] I. Kao, K. Lynch, and J. Burdick, "Contact Modeling and Manipulation," *Springer Handbook of Robotics*, pp. 647–668, Sep. 2008.

[12] Z. Li and S. Sastry, "Task-oriented optimal grasping by multifingered robot hands," *IEEE Journal of Robotics and Automation,*, vol. 4, no. 1, pp. 32 –44, Feb. 1987.

[13] B.-H. Kim, S.-R. Oh, B.-J. Yi, and I. H. Suh, "Optimal grasping based on non-dimensionalized performance indices," in *Proceedings of the IEEE International Conference on Intelligent Robots and Systems*, vol. 2, 2001, pp. 949 –956.

[14] D. Ding, Y.-H. Lee, and S. Wang, "Computation of 3-d form-closure grasps," *IEEE Transactions on Robotics and Automation*, vol. 17, no. 4, pp. 515 –522, Aug. 2001.

[15] B. Mirtich and J. Canny, "Easily computable optimum grasps in 2-d and 3-d," in *Proceedings IEEE International Conference on Robotics and Automation*, May 1994, pp. 739–747.

[16] T. Supuk, T. Kodek, and T. Bajd, "Estimation of hand preshaping during human grasping." *Medical engineering & physics*, vol. 27, no. 9, pp. 790–7, Nov. 2005.

[17] A. T. Miller and P. K. Allen, "Examples of 3D grasp quality computations," in *Proceedingsof the IEEE International Conference on Robotics and Automation*, vol. 2, no. May. IEEE, 1999, pp. 1240–1246.

[18] G. Liu, J. Xu, X. Wang, and Z. Li, "On Quality Functions for Grasp Synthesis, Fixture Planning, and Coordinated Manipulation," *IEEE Transactions on Automation Science and Engineering*, vol. 1, no. 2, pp. 146–162, Oct. 2004.

[19] A. Liegeois, "Automatic supervisory control of the configuration and behavior of multibody mechanisms," *IEEE Trans. Systems, Man, and Cybernetics*, vol. 7, no. 12, pp. 842–868, 1977.

[20] J. Sancho-Bru, "Modelo biomecànic de la mà orientat al disseny d'eines manuals," Ph. D. thesis, Universitat Jaume I, 2000.

[21] J. K. Salisbury and J. J. Craig, "Articulated Hands: Force Control and Kinematic Issues," *The International Journal of Robotics Research*, vol. 1, no. 1, pp. 4–17, 1982.

[22] J.-O. Kim and P. Khosla, "Dexterity measures for design and control of manipulators," *Proceedings IROS Workshop on Intelligent Robots and Systems*, no. 91, pp. 758–763, 1991.

[23] R. D. Crowninshield and R. A. Brand, "A physiologically based criterion of muscle force prediction in locomotion," *Journal of Biomechanics*, vol. 14, no. 11, pp. 793 – 801, 1981.

[24] J. Sancho-Bru, M. Vergara, P.-J. Rodrguez-Cervantes, D. Giurintano, and A. Prez-Gonzlez, "Scalability of the muscular action in a parametric 3d model of the index finger," *Annals of Biomedical Engineering*, vol. 36, pp. 102–107, 2008.

[25] R. Diankov, "Automated construction of robotic manipulation programs," Ph.D. dissertation, Carnegie Mellon University, Robotics Institute, August 2010.

[26] J. Choi, "Developing a three-dimensional kinematic model of the hand for ergonomic analyses of hand posture, hand space envelope, and tendon excursion," Ph.D. dissertation, University of Michigan, 2008.

[27] M. Ciocarlie, C. Lackner, and P. Allen, "Soft Finger Model with Adaptive Contact Geometry for Grasping and Manipulation Tasks," *Second Joint EuroHaptics Conference and Symposium on Haptic Interfaces for Virtual Environment and Teleoperator Systems*, pp. 219–224, Mar. 2007.

[28] A. V. Savescu, M. L. Latash, and V. M. Zatsiorsky, "A technique to determine friction at the fingertips." *Journal of Applied Biomechanics*, vol. 24, no. 1, pp. 43–50, 2008.

[29] A. Z. Hajian and R. D. Howe, "Identification of the mechanical impedance at the human finger tip," *Journal of Biomechanical Engineering*, vol. 119, no. 1, pp. 109–114, 1997.

Constrained Model-Driven Grasping Using the Model-Object Overlap Metric (MOOM)

A. Aldoma, J. Felip, B. Leon, W. Wohlkinger, A. Morales and M. Vincze

***Abstract*— Model-driven grasping approaches take advantage of object recognition and pose estimation to execute grasp hypotheses — computed on 3D models — on real objects for robotic manipulation. Because recognition and pose estimation are obtained from partial views of an actual object, the grasping planning assumes that the unseen parts of the object match the recognized model. Even though this assumption is richer than symmetry assumptions taken by other researchers, in some ill-conditioned situations where the exact pose of the object is not unequivocal (i.e, a partial view from a mug where the handle is not seen) , the model assumption will lead to execution of grasp hypotheses with uncertain success. In this paper we introduce the Model-Object Overlap Metric (MOOM) between the recognized model and the actual part of the object that is seen from the camera. The MOOM constrains the grasp hypotheses computed on the full model by giving a lower weight to those hypotheses that use unseen parts of the object. We show as well how the MOOM can be used not only to select better grasp hypotheses but also to constraint approach directions and the path planning space, thus reducing the amount of time needed to find a successful grasp hypotheses without time consuming involving reachability checks and collision free paths. We present grasping results on a set of 15 objects of daily using a simple online grasp planner — with and without MOOM — provided by the opensource simulation platform OpenRAVE.**

I. INTRODUCTION

A key capability for mobile robotic platforms and cognitive robotic systems is grasping. Therefore, in the last decades, robotic grasping is a well researched problem. There exist several techniques to compute stable grasps on complete models of objects, [1], [2] but these techniques are hard to transfer to real environments where the perception of a robot is uncertain and incomplete.

Model-driven grasp approaches [3], [4] assume that a model of the objects exist and the actual objects are grasped using the computed grasps on the models. The models of the objects are normally represented as triangle meshes obtained using high-precission scanners techniques which are normally not available on mobile platforms. The goal is to robustly identify the models and their configurations (position, orientation) in the environment of a robot in order to apply the grasp knowledge from the models on the real objects.

This work was conducted within the EU Cognitive Systems project GRASP (FP7-215821) funded by the European Commission.

Aldoma, Wohlkinger and Vincze are with Vision4Robotics Group, Automation and Control Institute, Vienna University of Technology Vienna, Austria `aa @ acin.tuwien.ac.at`

Leon, Felip and Morales are with Robotic Intelligence Lab - Universitat Jaume I Castellon Spain `len @ uji.es`

The challenge is to match these models with the actual data delivered by image and depth sensors available in mobile platforms. Noise, uncertainty, occlusions, missing parts due to lack of texture and restricted viewpoint make this a very difficult task.

With the advent of the Microsoft Kinect providing dense 3D information, some promising methods have been lately presented dealing with the problem of recognizing objects in the world using 3D synthetic meshes as input for a training stage [5], [6]. The recognition results can be used to guide a grasp planner to perform operations on real objects using the precomputed grasp knowledge.

Still, the grasp planner assumes that the recognized model matches the reality although we have no real evidence of that due to occlusions (hidden parts by the object itself or by other elements in the environment) and moreover, the recognition results could be wrong or undetermined. In order to better deal with these uncertainties, we propose to effectively use the evidence of data to constrain the grasp hypotheses and avoid those with less probability of being correct.

The advantages of the presented method are three-fold:

1) It allows to deal with uncertainties of non-observed data but still makes use of the assumptions taken by object recognition, which is less restrictive than symmetry or similar assumptions [7].
2) For online grasp planners, the MOOM can be used to speed up the computation of successful hypotheses by pruning approachings direction to the object that intersect parts of the model with lower MOOM.
3) Finally, it provides a metric to rank those grasp hypotheses with force-closure according to online observations. Because grasp hypotheses are labeled as successful or unsuccessful depending on force-closure, there is no real criteria to decide which successful hypotheses should be actually executed, apart from reachability and collision checks.

In the remaining of this paper, we review similar model-driven grasping methods and an object recognition technique to provide the pose of the 3D models in the actual scene. In Section IV, we present how the MOOM is computed and how it is integrated in the grasping pipeline. Finally, we present an experimental evaluation to demonstrate how the metric can be used to improve speed and grasp accuracy on an online grasp planner provided by the opensource robotic planning architecture OpenRAVE [8].

II. Related Work

Grasping in general and model-driven grasping is a well-studied problem in the literature. There have been several approaches relying on object recognition or similarity between objects to transfer grasps between objects represented as 3D meshes [9] or from 3D mesh models to real objects [3], [10].

More recently, there have been some interest in combining different strategies for grasping. In [11], the authors use a probabilistic model to decide which is the best object representation that can be used to grasp a real object: fitting primitives to the partial point cloud obtained with the depth sensor, recognizing the object against a database of objects and by estimating their pose applying known grasps or directly computing grasp hypotheses in the mesh reconstructed from the partial view.

Brook et al. [4] present a similar approach to [11]. Instead of deciding which is the best model representation to grasp the actual object, the method tries to reach a consensus between all different model representations and the best grasp is selected. The first object representation is a recognition-based representation obtained using a matching algorithm based on a 2-dimensional matcher that iteratively aligns each model in the database to the segmented cluster of the depth sensor. Because of the simple recognition technique used, only objects rotationally symmetrical or standing in a known orientation can be recognized. The second object representation is based solely on the segmented clusters obtained from the depth sensor and the grasp hypotheses are computed using a set of heuristics.

There are several limitations in both [11] and [4]: (i) the set of heuristics used by the grasp planner are not easy to port to more dexterous hands than the PR2 gripper and (ii) the recognition method is only able to recognize objects with very specific constraints and does not scale with the number of objects. It is as well not trivial to decide which representation should be ultimately used when no consensus is reached between the different representations.

Therefore, we propose to strongly rely on the model representation obtained using more advanced recognition methods but transfer the absence or presence of real observations to the model representation so that the grasp planner can implicitly use it.

III. Recognition

Model-driven grasp approaches rely on object recognition and pose estimation to apply grasps learned on a mesh to a real object. Grasp planners usually work with triangle mesh representations of the objects to compute force closure grasp hypotheses and therefore, we seek an object recognition method that can be trained on triangle meshes and yet recognize the objects obtained with a depth sensor like the Kinect. This eases training as there is no need for several representations of the objects: both grasping and recognition pipeline can use the same models. Fig. 1 show an image of a example scene together with the reconstructed point cloud and the recognition results overlayed. The recognition results are provided to the grasping pipeline.

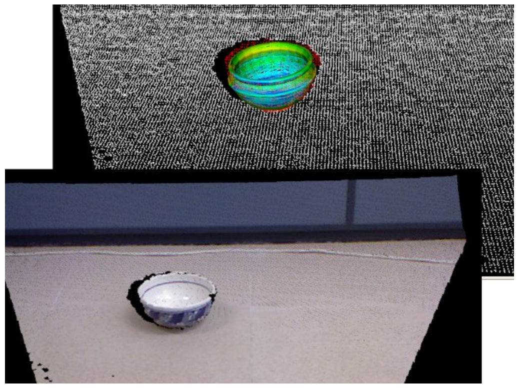

Fig. 1. RGB-D image from the Kinect and recognition results overlayed. The mesh is overlayed on the point cloud and colored according to the overlap between the segmented cluster and the mesh.

We decide to use the Clustered Viewpoint Feature Histogram (CVFH) descriptor and the recognition pipeline presented in [5] which has been shown to perform well in similar scenarios. CVFH is a semi-global, view based descriptor composed by several histograms based on angular normal distributions of the object surface. Because of its multivariate representation, it can deal with occlusions and data defects due to the sensor limitations. Moreover, CVFH is not scale invariant and combined with the Camera's Roll Histogram (CRH) [5] and a post-processing step it is able to deliver accurate object poses efficiently. As scale and pose are key factors for successful manipulation, CVFH is a perfect fit for our specific problem. Even though, we decided for this specific recognition pipeline, the rest of the paper applies to any recognition pipeline able to match mesh representations to the real world.

The mesh representation of the objects used for the experiments have been obtained from different sources: simple objects like boxes or cylinders have been manually modeled, other objects were obtained from the KIT Object Database [12] and others were automatically classified using the Shape Distribution on Voxel Surfaces descriptor (SDVS [6]) and its scale was obtained using the pose alignment method presented in [13]. Models obtained using the automatic method do not match the real object completely, making the recognition and grasping task even more challenging. The decision of using models that do not match real objects completely is motivated by: (i) it eases training as there is no need to the real objects to build a mesh representation of it that can be used by the grasp planner and (ii) it allows to show how the overlap metric can be used to enhance grasping even in these challenging scenarios where the 6DOF pose estimation will never be accurate due to differences between model and real object.

IV. MOOM: Model-Object Overlap Metric

After recognition and pose estimation, the grasping pipeline assumes that the recognized model matches the reality although we have no real evidence of that, apart from the metrics obtained from the recognition module.

Why should the grasping pipeline throw away the valuable information from the depth sensor after recognition? The main idea behind the overlap computation is to encode the real evidence of data in the mesh representation together with the recognized object and pose so that all available information is provided to the grasping pipeline to use it wisely.

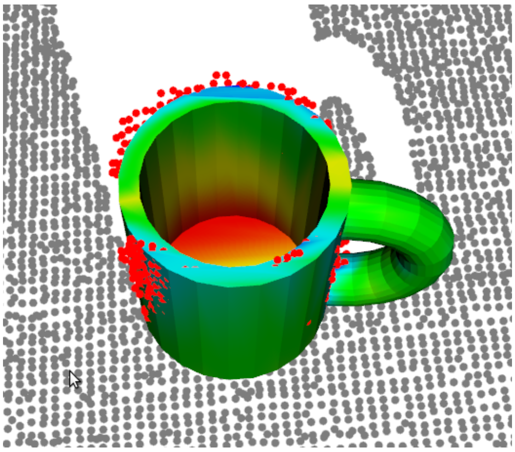

Fig. 2. A closer look to a recognized mug. The colors of the mesh represent the overlap between the segmented cluster (red dots) and the mesh. The color representation of the overlap increasing from red (worse overlap) to blue (best overlap).

A. Computation

The computation of the overlap metric is straightforward. Given a mesh $\mathcal{M}$ aligned to a point cloud $\mathcal{P}$ representing the object — both in camera coordinates — using the recognition pipeline from the previous section, the overlap metric is computed by building an octree from $\mathcal{P}$ and finding the closest neighbour for each vertex v_i of $\mathcal{M}$ in the octree representation. Given p_i is the closest neighbour of v_i, the overlap metric at v_i is computed as follows:

$$O(v_i, p_i) = \frac{1}{1 + \frac{||v_i - p_i||}{M_d}} \quad (1)$$

where M_d represents the maximum distance considered for a point v_i to overlap. We use a value of $2mm$ for M_d in all experiments. The overlap metric inside the mesh triangles is obtained by linear interpolation between the 3 vertices of the triangle although it is not stored and always computed on the fly when needed.

B. MOOM and the grasping pipeline

We use the grasping pipeline from OpenRAVE [8]. It provides an open architecture targeting a simple integration of simulation, visualization, planning, scripting and control of robot systems.

OpenRAVE includes a planner algorithm called fastGrasping which purpose is to find the first feasible grasp for an

Algorithm 1: OpenRAVE's fast grasping with MOOM

input : $\mathcal{O}_{hull}$, $\mathcal{O}_{mesh}$, robot
output: An executable grasp
begin
  AV := get approach vectors for $\mathcal{O}_{hull}$;
  for *each av in AV* **do**
    compute MOOM($\mathcal{O}_{hull}, p$) (see Sec. IV-B.1);
  sort (AV); //in decreasing order;
  for *each approach vector* **do**
    test grasping object in the approach vector direction;
    if *grasp is "force closure"* **then**
      if *grasp is reachable and collision free* **then**
        compute MOOM($\mathcal{O}_{mesh}, P$) for grasp contact points;
        if *MOOM($\mathcal{O}_{mesh}, P$) $\geq$ threshold* **then**
          send grasp for execution;
          break;

object as fast as possible without generating a grasp database. The approach vectors are generated taking the bounding box of the object and sample its surface uniformly. The first intersection of the object and a ray originating from each point going inwards is taken and the normal of the object's surface at the intersection points is taken as the approaching direction of the manipulator.

These approach vectors are used to generate a set of grasps, using a combination of predefined preshapes, standoffs and wrist rolls. Each one of these grasps is tested first for force-closure and second to be reachable by the robot manipulator in a trajectory free of collisions with the environment.

The first grasp to fulfill these conditions is sent for execution to the robot. We have modified this algorithm to include the overlap information at two different levels: (i) to sort the approach directions so that those intersecting at points of the model with high MOOM are preferred and (ii) to check the quality of the force-closure grasps by computing the overal MOOM of the contact points between the manipulator and the object.

Let $\mathcal{M}$ be the mesh aligned with the point cloud $\mathcal{P}$ and $\mathcal{C}_\mathcal{M}$ the convex hull of $\mathcal{M}$. For both, $\mathcal{M}$ and $\mathcal{C}_\mathcal{M}$ the overlap metric with $\mathcal{P}$ is computed applying the procedure from Sec. IV-A obtaining two meshes, $\mathcal{O}_{mesh}$ and $\mathcal{O}_{hull}$ respectively. $\mathcal{O}_{hull}$ is used to filter and sort the approach vectors and $\mathcal{O}_{mesh}$ to check the quality of the grasp (see Algorithm 1).

1) Overlap metric for approach vectors MOOM($\mathcal{O}_{hull}, p$): Using $\mathcal{O}_{hull}$ instead of $\mathcal{O}_{mesh}$ for the approach vectors weighting ensures that the algorithm will not discard those approach vectors coming from the top in non-convex objects like mugs or bowls. For instance, the approach vectors for the mug in Fig. 2 using $\mathcal{O}_{mesh}$ would intersect with the bottom of the mug which has a poor MOOM as it is not seen from the camera viewpoint (see Fig. 3).

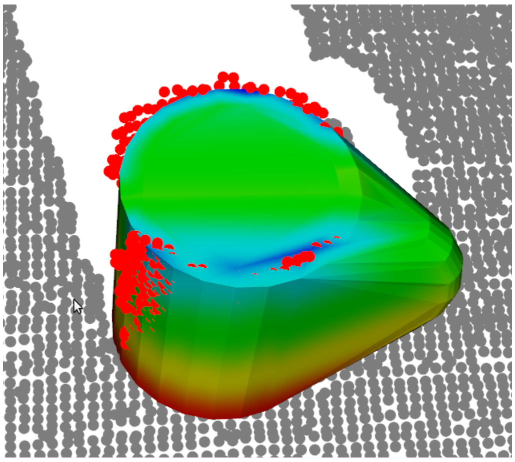

Fig. 3. Using the convex hull of the mesh instead of the mesh itself, allows to deal with non-convex objects to compute feasible approach vectors. The colors of the mesh represent the overlap between the segmented cluster (red dots) and the mesh of the convex hull. The color representation of the overlap increasing from red (worse overlap) to blue (best overlap).

To account for the table plane obstacle, $\mathcal{O}_{hull}$ is reweighted. Each vertex $v_i \in \mathcal{O}_{hull}$ is reweighted according to its distance to the table plane by a factor f_i computed as follows:

$$f_i = \begin{cases} 1 & d(v_i, t_p) \geq min_d \\ \frac{d(v_i, t_p)}{min_d} & \text{otherwise} \end{cases} \quad (2)$$

where t_p represents the table plane, $d(v_i, t_p)$ the point-to-plane distance from point v_i to the plane t_p and min_d the minimal distance to the table needed by the embodiment to approach an object parallel to the table. In our case, we use a value of $10cm$ for objects higher than $10cm$, otherwise the maximum height of the object. Modifying the overlap metric in this way, we enforce the planner algorithm to first test those approach vectors that are more likely to provide a collision free path when trying to reach the object (see Figure 4).

2) Overlap metric for grasp hypotheses MOOM($\mathcal{O}_{mesh}, P$): Once OpenRAVE has found a grasp hypotheses $\mathcal{G}$ with force-closure and with a feasible path, the algorithm computes the overall MOOM of the contact points between the object and the manipulator of $\mathcal{G}$. Let P represent all contact points between $\mathcal{G}$ and the manipulator. The MOOM($\mathcal{O}_{mesh}, P$) is computed by averaging the $\mathcal{O}_{mesh}(p_i)$ where $p_i \in P$ resulting in a metric to rank the overall quality of the grasp in relation to the observed data (see bottom of Fig. 4).

3) Overlap metric with a grasp database: Algorithm 2 presents a variation of the algorithm used along the paper when an off-line generated grasp database is available. It can be seen that this kind of model-driven approaches can also take advantage of MOOM to increase efficiency and robustness.

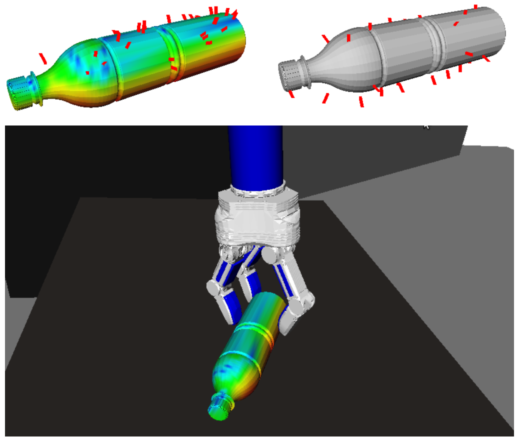

Fig. 4. White bottle lying on the table. Top-row: First 30 approach vectors sorted using MOOM (left) and 30 approach vectors retrieved without MOOM (right). Without MOOM there is no implicit criteria to decide which approach vectors should be tried first. Bottom: First force-closure grasp hypothesis found with a MOOM($\mathcal{O}_{mesh}, P$) higher than 0.5.

Algorithm 2: Grasping with MOOM using a grasp database

input : $\mathcal{O}_{hull}$, $\mathcal{O}_{mesh}$, robot, DB:= Database of force closure grasp for the given object and robot
output: An executable grasp
begin
    for *each grasp in* DB **do**
        compute MOOM($\mathcal{O}_{hull}, p$) for approach vectors (see Sec. IV-B.1);
        compute MOOM($\mathcal{O}_{mesh}, P$) for grasp contact points;
    $DB_{filtered}$:= filter(DB) for which MOOM($\mathcal{O}_{hull}, p$) $\geq$ threshold;
    sort ($DB_{filtered}$) by MOOM($\mathcal{O}_{mesh}, P$); //in decreasing order;
    for *each grasp in* $DB_{filtered}$ **do**
        if *grasp is reachable and collision free* **then**
            send grasp for execution;
            break;

V. Experimental Setup and Evaluation

In order to test and validate the method presented, we have compared the *fast grasping* grasp planner from OpenRAVE [8] with Algorithm 1. The plans have been executed on a real robotic platform to validate whether the planned grasps were successful.

A. Robotic platform

The proposed methods are implemented an validated for a particular embodiment, in our case an anthropomorphic torso, called *Tombatossals* which has 25 DOF (see Fig. 5). It is composed of two 7 DOF Mitsubishi PA10 arms. The right arm has a 4 DOF Barrett Hand and the left arm has a 7DOF Schunk SDH2 Hand. Both hands are endowed with

Weiss Tactile Sensor system on the fingertips. Each arm has a JR3 Force-Torque sensor attached on the wrist between the arm and the hand. The visual system is composed of a TO40 4 DOF pan-tilt-verge head with two Imaging Source DFK 31BF03-Z2 cameras. Attached to the center of the pan-tilt there is a Kinect sensor used throughout the experiments to extract the point cloud needed for the vision system and all the components of the left arm to execute the planned grasps.

B. Object set and assumptions

In the environment where the experiments are performed there is a table in front of the robot that acts as a surface where the objects stand. The object set is composed of several household objects of different shapes: boxes, cups, mugs, bowls, bottles, duct tapes and fruits. See Fig. 6.

Although the grasp pipeline allows more than one object at a time, to perform the grasping experiments, one single object is put on the table in front of the robot in any position and orientation. The object position has to be close enough to allow the robotic arm to reach and grasp the object.

The presence of a dominant plane in the scene is assumed to segment the object of interest [14].

C. Experimental evaluation

The following metrics are captured for the different grasp planners for the evaluation in order to measure improvement in both accuracy and computational efficiency:

- Grasp hypotheses tested: Percentage of grasp hypotheses checked on the simulator until the first valid grasp is sent for execution to the real platform from all possible grasp hypothesis generated by the planner. The total number of grasp hypotheses is a combination of approach vectors, stand-offs, wrist rolls and preshapes.
- Time: Elapsed time by the grasp planner until a grasp hypothesis is sent to the robot.
- Grasp success: Whether the final grasp execution was successful or not on the real robot. This input is given by the operator: a grasp is considered successful if the robot is able to lift the object, failure otherwise.

Fig. 7 presents the percentage of grasp hypotheses tested from all generated grasp hypotheses until a feasible one

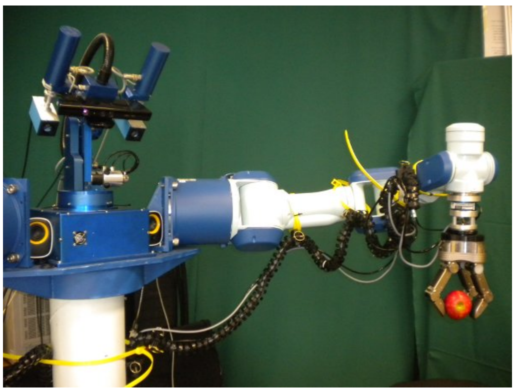

Fig. 5. The experimental robotic platform: Tombatossals, the UJI humanoid torso.

Fig. 6. Object set used for the experiments. The objects are identified with their position in the grid from top to bottom and left to right. This identifier is used on the experiment graphs (starting at 0)

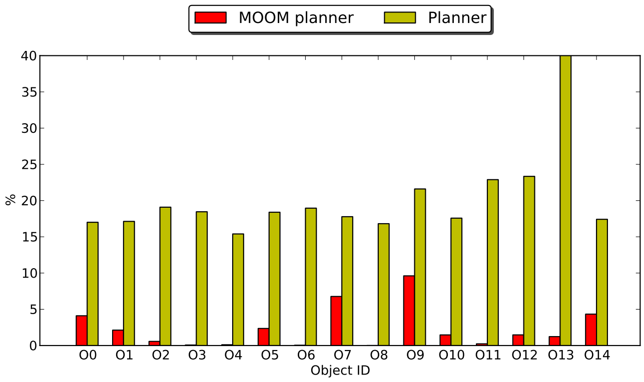

Fig. 7. Percentages of grasp hypotheses tested for the MOOM grasp planner and the standard OpenRAVE fastGrasping planner until the first feasible grasp can be sent for execution.

is found that can be send for execution. It is clear from the figure that the goodness of the grasp hypotheses using MOOM is much higher than those from the standard planner which are randomly selected. Because grasp hypotheses are generated from the set of approach vectors, the approach vectors sorted using MOOM are found on collision free areas (see Fig. 4) and their overlap tends to be high enough to be executed once the a force-closure grasp is found.

Fig. 8 presents the time elapsed on the grasp planning until a feasible one is found that can be send for execution. Results confirm those from Fig. 7 although it can be seen that for some objects (with ids 7 and 9), the MOOM planner needs more time to process less approach vectors. This is due to the fact that very bad grasp hypotheses can be filtered much faster than those with a higher goodness.

Finally, Fig. 9 presents grasp success rates for both planners regarding execution on the real platform. From the figure it can be seen that the planner using MOOM performs better than the standard planner — 42.5% of improvement — and in average needs about 10 times less time to find the first feasible grasp. To obtain a more representative evaluation, the objects are grasped again twice using the grasp planner with

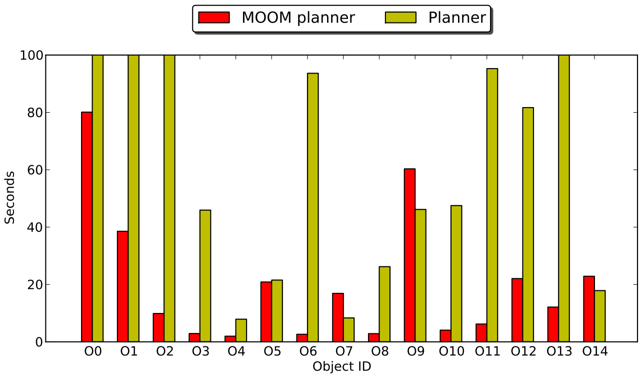

Fig. 8. Average planning time for each object until the frist feasible grasp can be sent for execution for both MOOM grasp planner and the standard OpenRAVE fastGrasping planner. Grasp plans taking more than 100 seconds are cut.

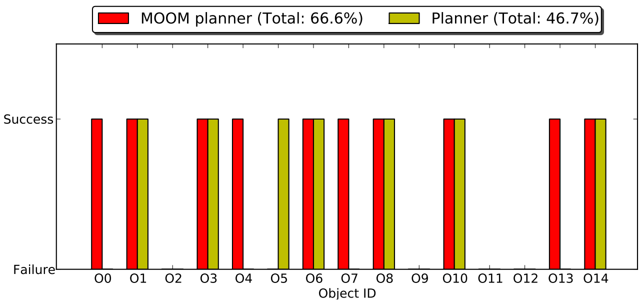

Fig. 9. Grasp success or failure for each object. Both MOOM grasp planner and the standard OpenRAVE fastGrasping planner are used. One trial per object.

MOOM. Fig. 10 presents the results of this evaluation and it can be seen the overall success rate is similar (2% less). It is worth mentioning that even though success rates are rather low in comparison to state-of-the-art grasping techniques, we arguee that there is a lot of room for improvement in our pipeline as: (i) the model of the objects do not match completely the real objects and there are no constraints on the objects or their configuration, (ii) the first grasp found by the planner is sent for execution and (iii) our starting point is a standard planner which very low success rates as seen in Fig. 9.

VI. Conclusions and Future Works

We have presented the Model-Object Overlap Metric (MOOM) to incorporate information obtained from the depth-sensor into the grasp planning. We have shown how MOOM can be incorporated at different stages and in different fashions to conventional grasping pipelines to increase efficiency and robustness to errors from recognition.

To better account for mismatches between simulation and reality, reactive grasp controllers [15] could be activated to boost the grasp success rate. This and the implementation of MOOM in more advanced grasp planners are considered as possible future works.

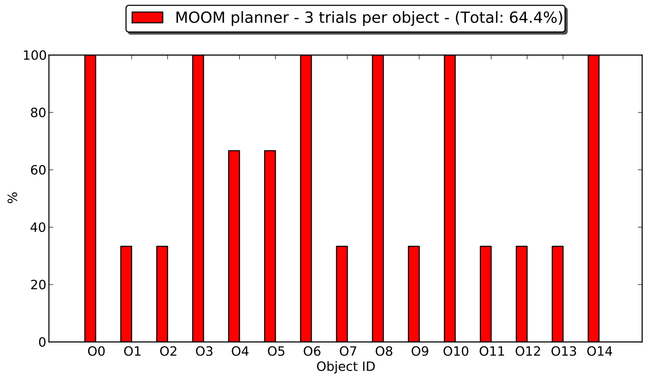

Fig. 10. Grasp success rate for MOOM grasp planner using 3 trials per object.

References

[1] M. Przybylski, T. Asfour, and R. Dillmann, "Planning grasps for robotic hands using a novel object representation based on the medial axis transform," in *IROS*, 2011.

[2] C. Goldfeder, P. K. Allen, C. Lackner, and R. Pelossof, "Grasp planning via decomposition trees," in *in Robotics and Automation, 2007 IEEE International Conference on*, 2007, pp. 10–14.

[3] C. Goldfeder, M. Ciocarlie, J. Peretzman, H. Dang, and P. K. Allen, "Data-driven grasping with partial sensor data," in *IEEE/RSJ International Conference on Intelligent Robots and Systems*, 2009, pp. 1278–1284.

[4] P. Brook, M. Ciocarlie, and K. Hsiao, "Collaborative grasp planning with multiple object representations," in *IEEE Intl. Conf. on Robotics and Automation, ICRA*, 2011.

[5] A. Aldoma, N. Blodow, D. Gossow, S. Gedikli, R. B. Rusu, M. Vincze, and G. Bradski, "CAD-Model Recognition and 6DOF Pose Estimation Using 3D Cues," in *In Workshop: 3rd IEEE Workshop on 3D Representation and Recognition, ICCV Yet to appear, see http://3d-net.org/privatepapers/ICCVWorkshop.pdf*, 2011.

[6] W. Wohlkinger and M. Vincze, "Shape Distributions on Voxel Surfaces for 3D Object Classification From Depth Images," 2011.

[7] J. Bohg, M. Johnson-Roberson, B. León, J. Felip, X. Gratal, N. Bergström, D. Kragic, and A. Morales, "Mind the Gap - Robotic Grasping under Incomplete Observation," in *Proceedings of the IEEE International Conference on Robotics and Automation*, May 2011.

[8] R. Diankov, "Automated construction of robotic manipulation programs," Ph.D. dissertation, Carnegie Mellon University, Robotics Institute, August 2010.

[9] C. Goldfeder, M. Ciocarlie, H. Dang, and P. K. Allen, "The columbia grasp database," in *IEEE Intl. Conf. on Robotics and Automation*, 2009.

[10] P. Azad, T. Asfour, and R. Dillmann, "Stereo-based 6D Object Localization for Grasping with Humanoid Robot Systems," in *IEEE/RSJ International Conference on Intelligent Robots and Systems (IROS)*, 2007, pp. 919–924.

[11] K. Hsiao, M. Ciocarlie, and P. Brook, "Bayesian grasp planning," in *ICRA*, 2011.

[12] Z. Xue, A. Kasper, M. J. Zoellner, and R. Dillmann, "An automatic grasp planning system for service robots," in *Proceedings of the 14th International Conference on Advanced Robotics*, 2009.

[13] A. Aldoma and M. Vincze, "Pose Alignment for 3D Models and Single View Stereo Point Clouds Based on Stable Planes," *International Conference on 3D Imaging, Modeling, Processing, Visualization and Transmission*, 2011.

[14] R. B. Rusu, Z. C. Marton, N. Blodow, M. Dolha, and M. Beetz, "Towards 3D Point Cloud Based Object Maps for Household Environments," *Robotics and Autonomous Systems Journal (Special Issue on Semantic Knowledge)*, 2008.

[15] J. Felip and A. Morales, "Robust sensor-based grasp primitive for a three-finger robot hand," in *Intelligent Robots and Systems, 2009. IROS 2009. IEEE/RSJ International Conference on*, 2009, pp. 1811 –1816.